# LICENCIATURA EN FISICA MEDICA

# BIOFISICA

## CAPITULO 3

## La Cinemática y la Dinámica del Cuerpo Humano.

# BIOFISICA

## CAPITULO 3

Estabilidad, Cinemática,
Dinámica y Musculatura

# DIRECCIONES, ORIENTACIONES Y PLANOS ANATOMICOS I

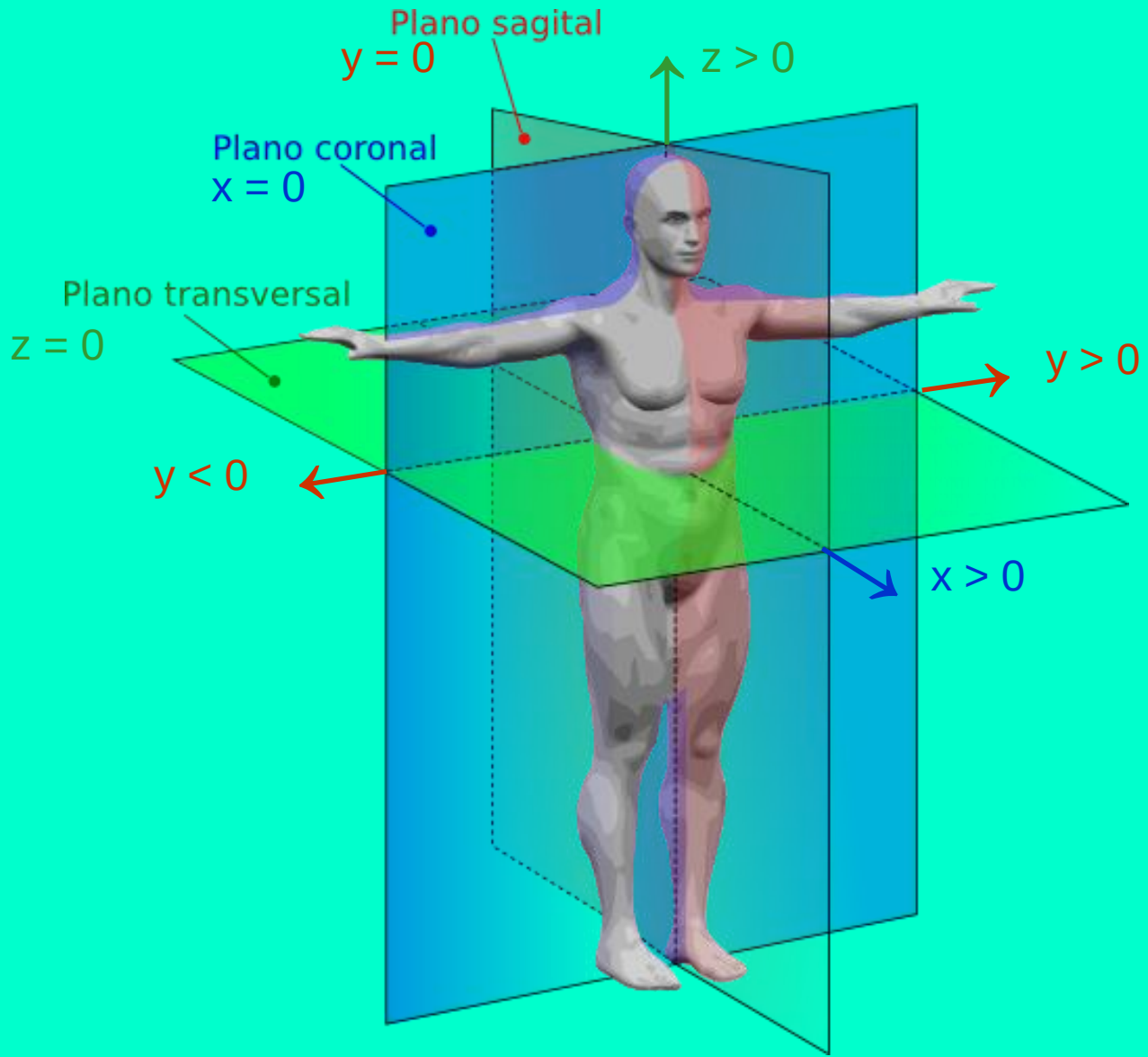

# CONVENCION SOBRE ANGULOS

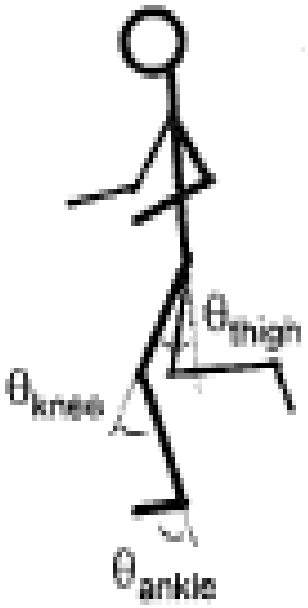


**Fig. 3.1.** One set of conventions for hip (thigh), knee (lower leg), and ankle (foot) angles. Other conventions are also used, such as with the thigh angle being relative to the vertical and the ankle angle defined as 90° less than here. (Based on [150])

# EXTENSIONES Y FLEXIONES REQUERIDAS PARA CAMINAR, CORRER, SALTAR, ETC.

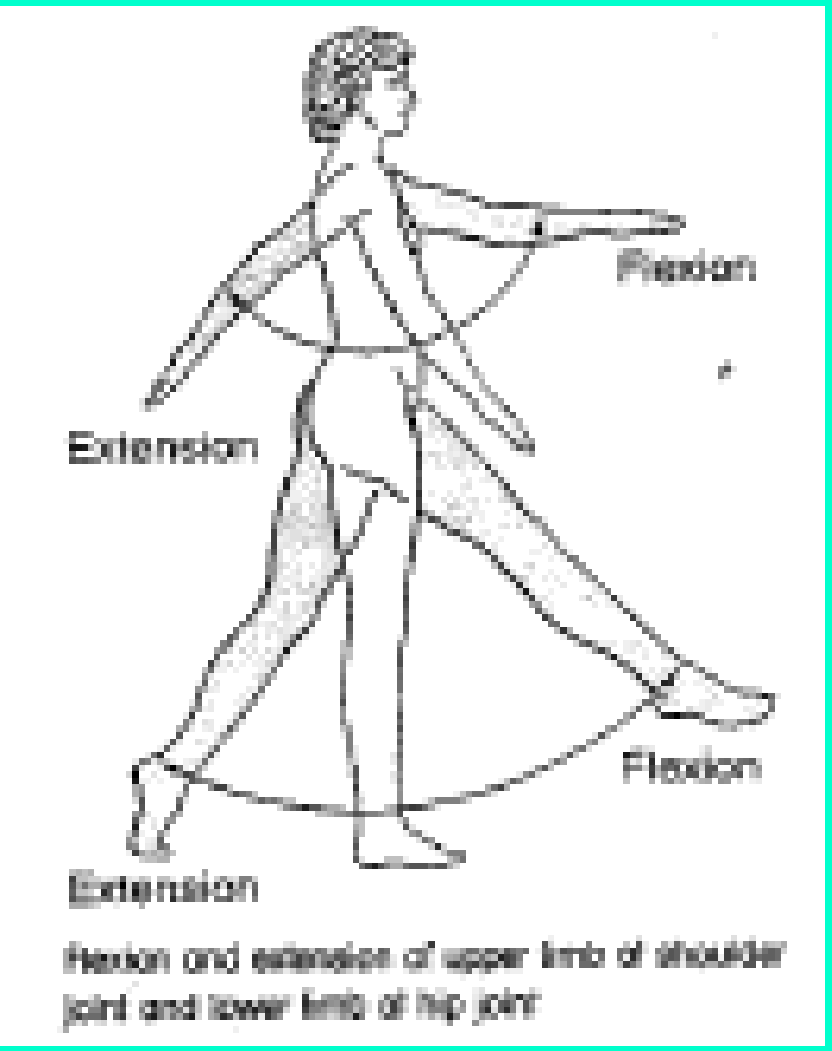


Flexion and extension of upper limb at shoulder joint and lower limb at hip joint

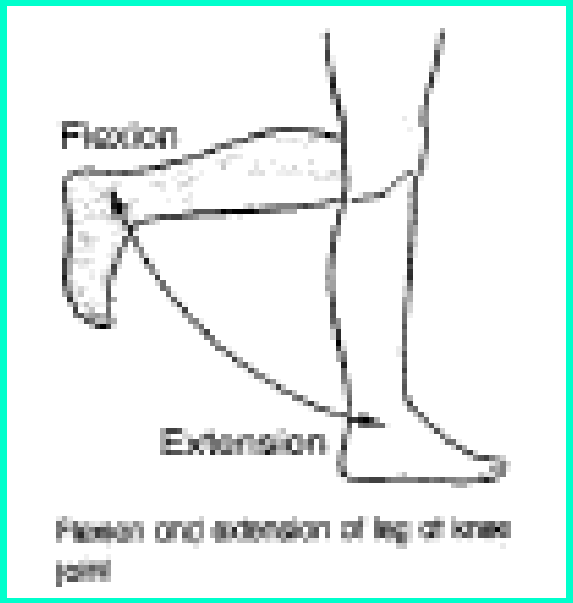


Flexion and extension of leg at knee joint

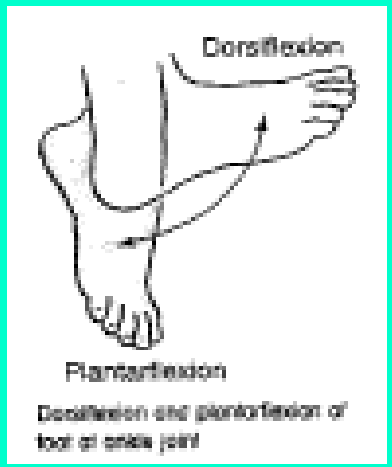


Dorsiflexion and plantarflexion of foot at ankle joint

# ESTABILIDAD ESTANDO PARADO I

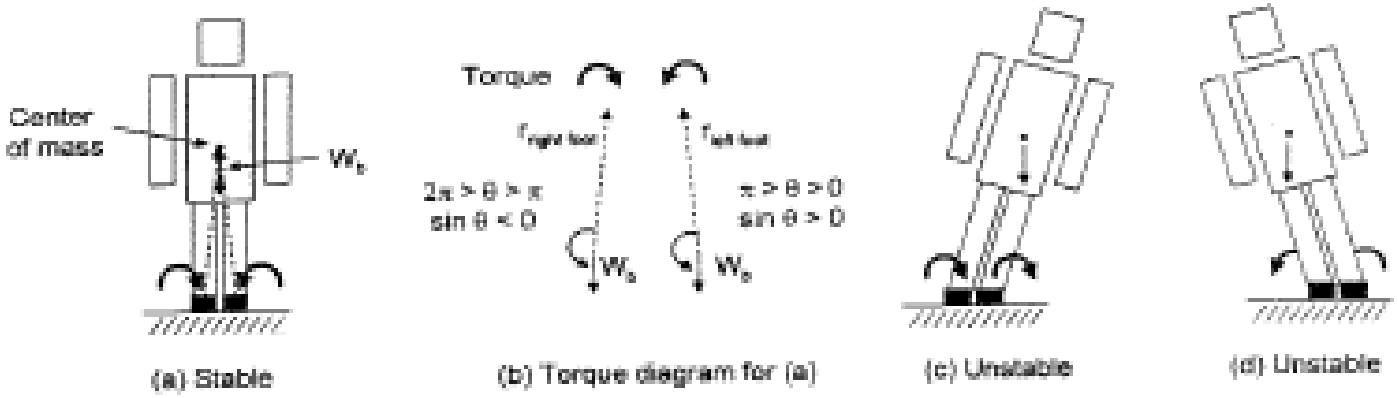


**Fig. 3.5.** Stability during standing for a model person (**a**) standing upright and with (**b**) torque diagrams, (**c**) leaning to her left, and (**d**) leaning to her right


**Fig. 3.6.** A standing person is stable when her center of mass is over the cross-hatched region spanned by her feet, as shown here with her feet (**a**) together, (**b**) apart, (**c**) and apart, with stability also provided by a cane or crutch. (Based on [110])

# ESTABILIDAD ESTANDO PARADO II

Pedigrafía

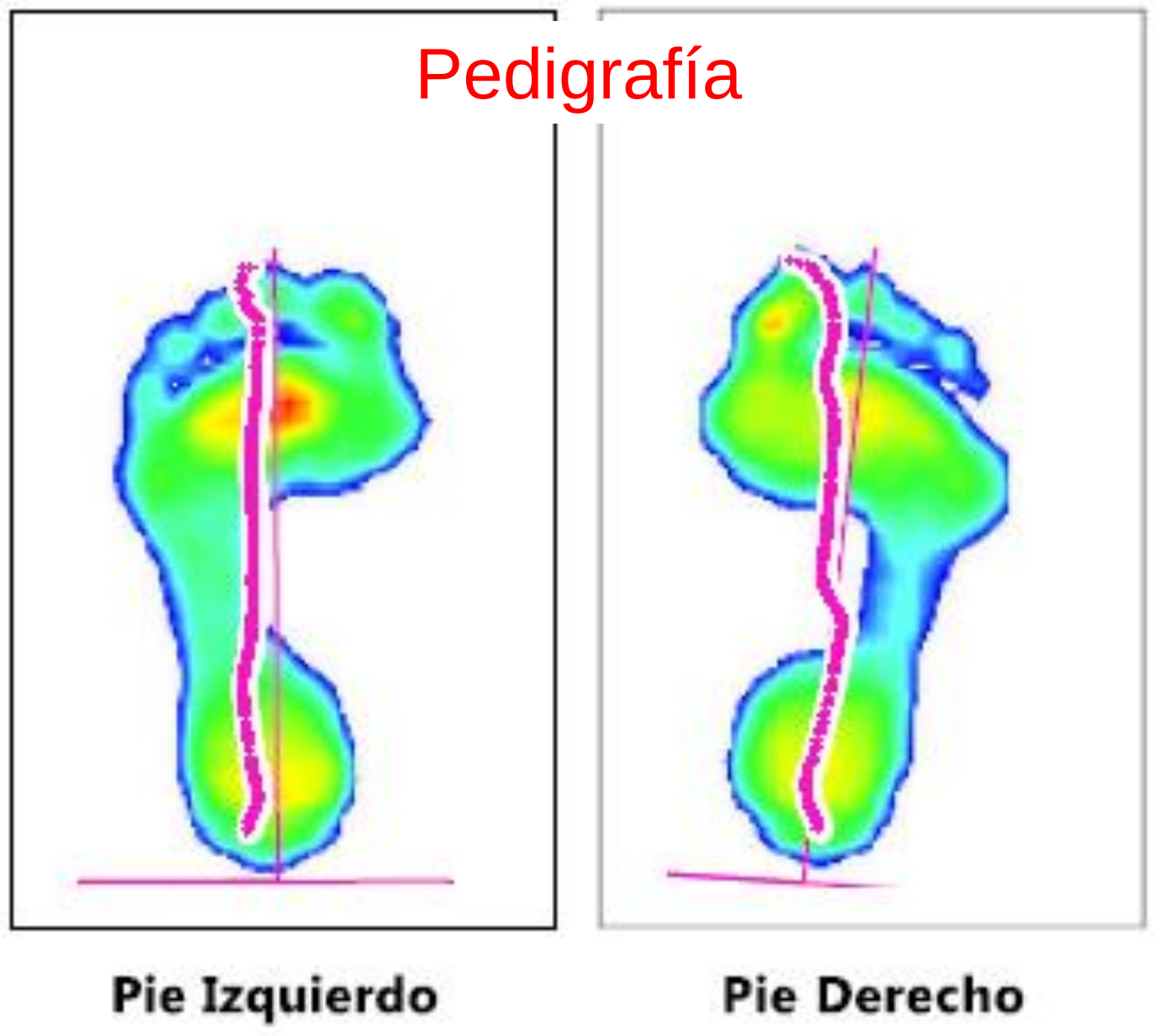

# ESTABILIDAD ESTANDO PARADO III

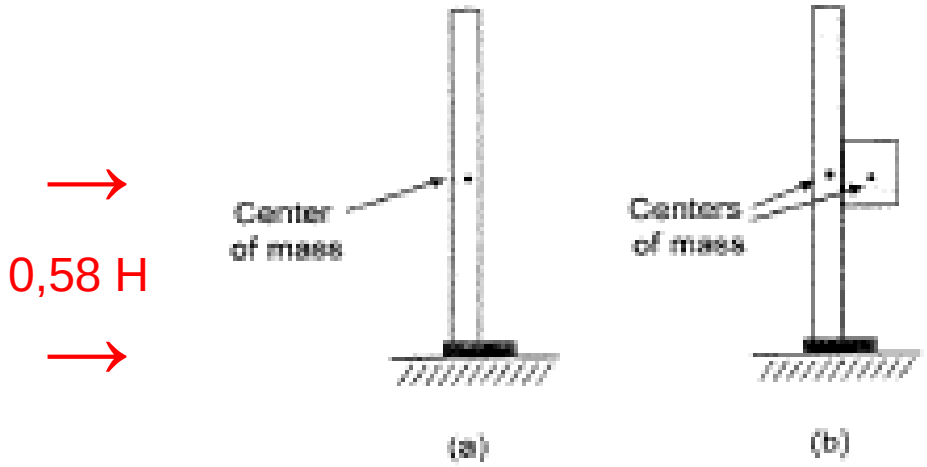


**Fig. 3.7.** Simple models of people facing to the right: (a) an upright person with mass fairly well balanced in front and back, with the person's center of mass shown – which is normally 58% of the person's height over the soles of his feet, and (b) one with unbalanced mass, such as a person with a beer belly or a woman who is pregnant, with separate centers of mass shown for the main body and the additional mass (which are approximately, but not exactly, at the same height). Clearly, the overall center of mass of the person in (b) is displaced to the right relative to that in (a). To prevent this being in front of the balls of the feet, the person often contorts his position, which can lead to muscle strain and a bad back. (See [110] for more details)

# PEDIGRAFÍA DEL CAMINAR

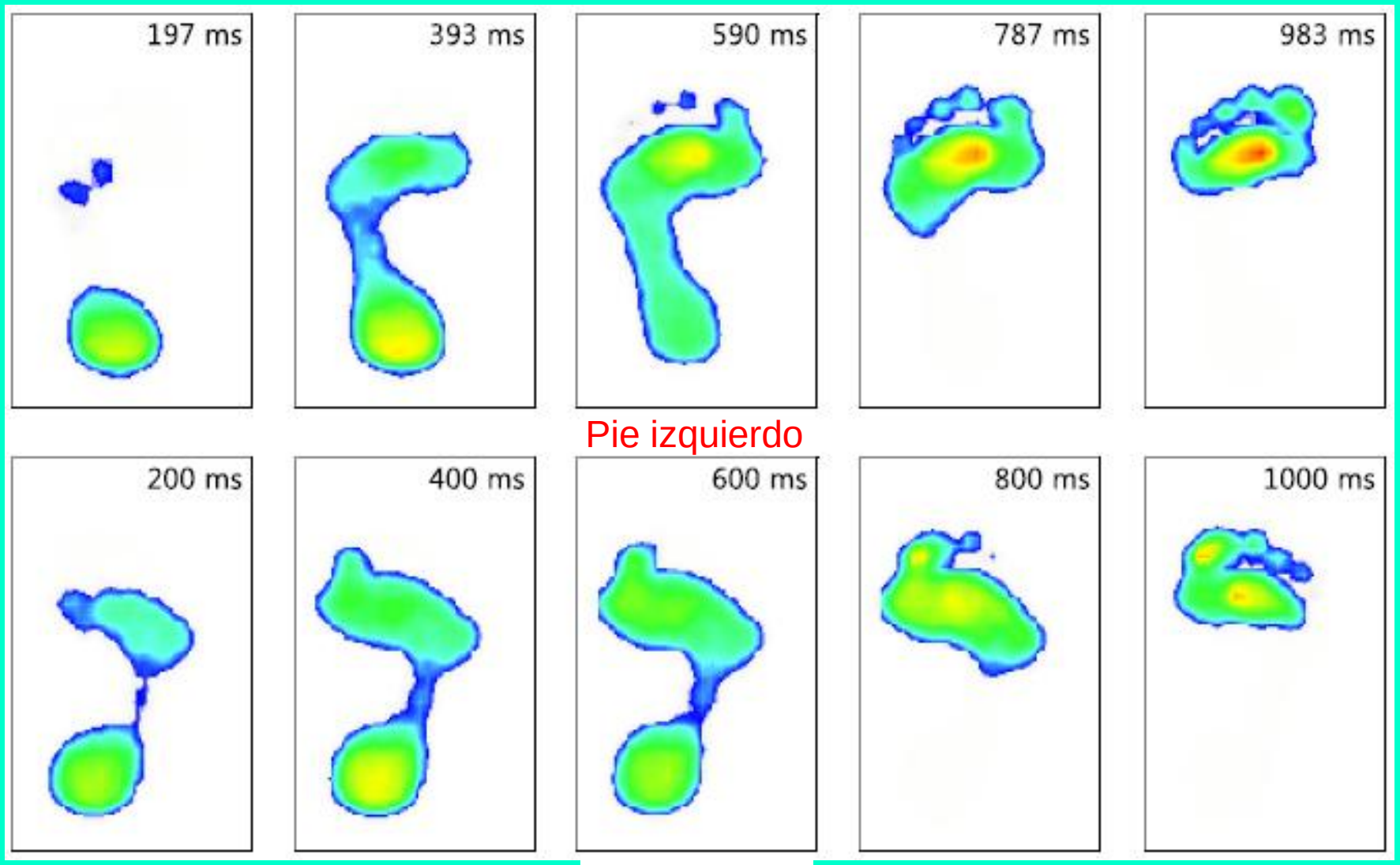

# IMPACTO DEL TALON

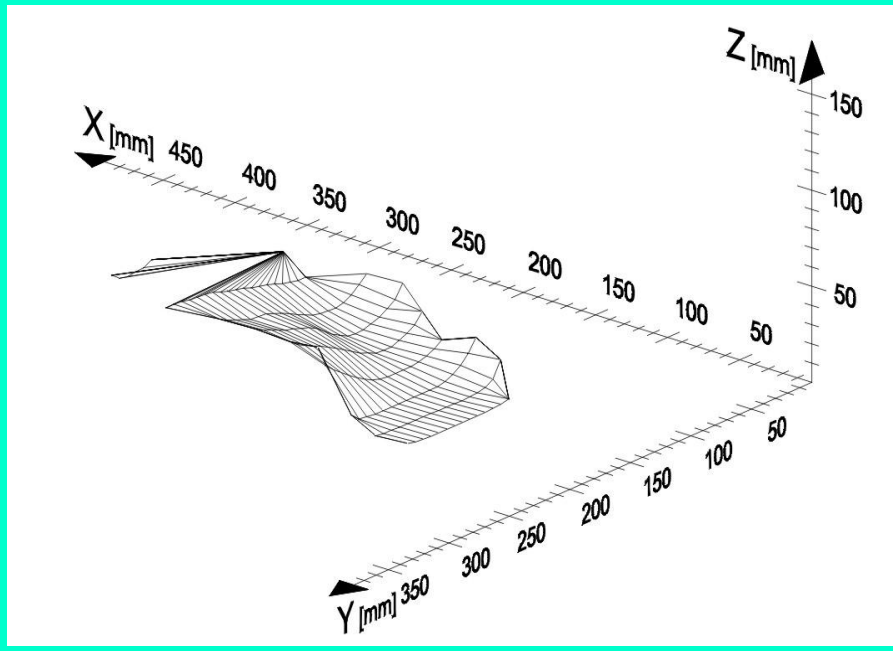


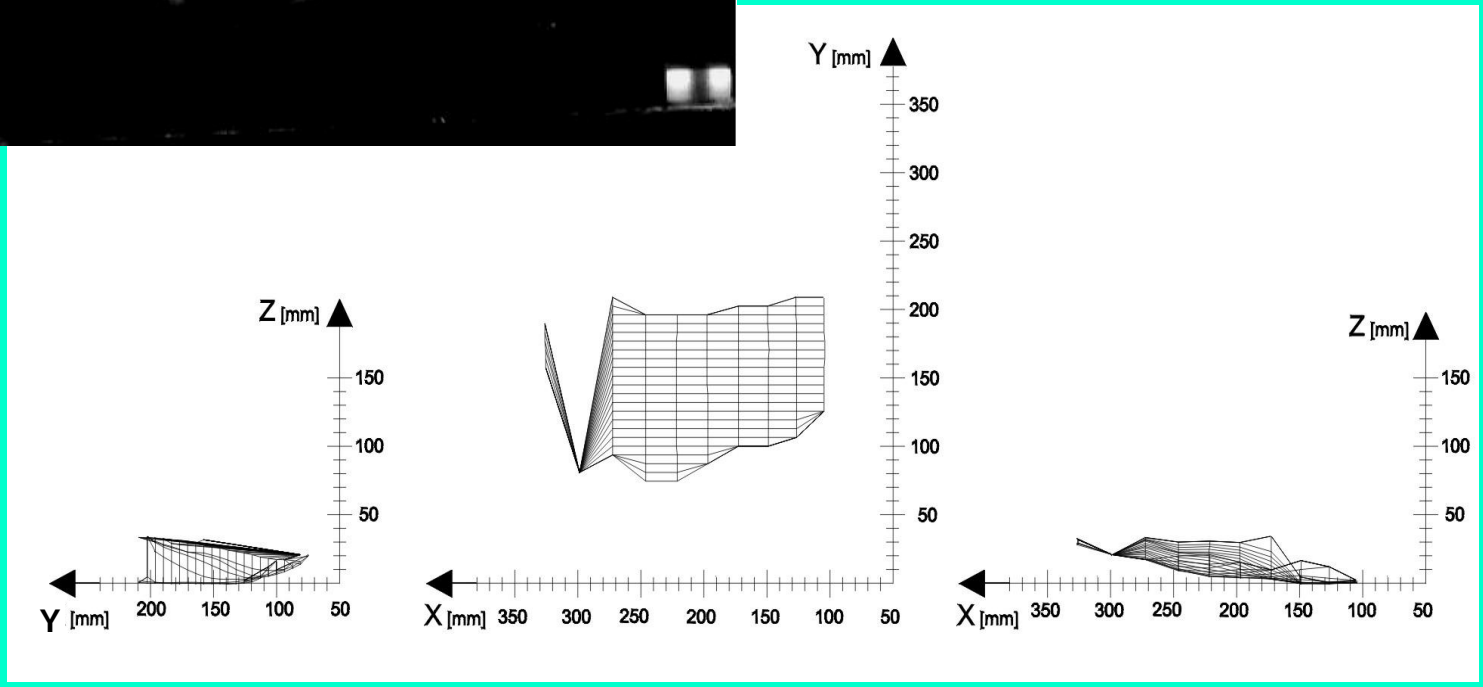

# SALIENDO EL PIE

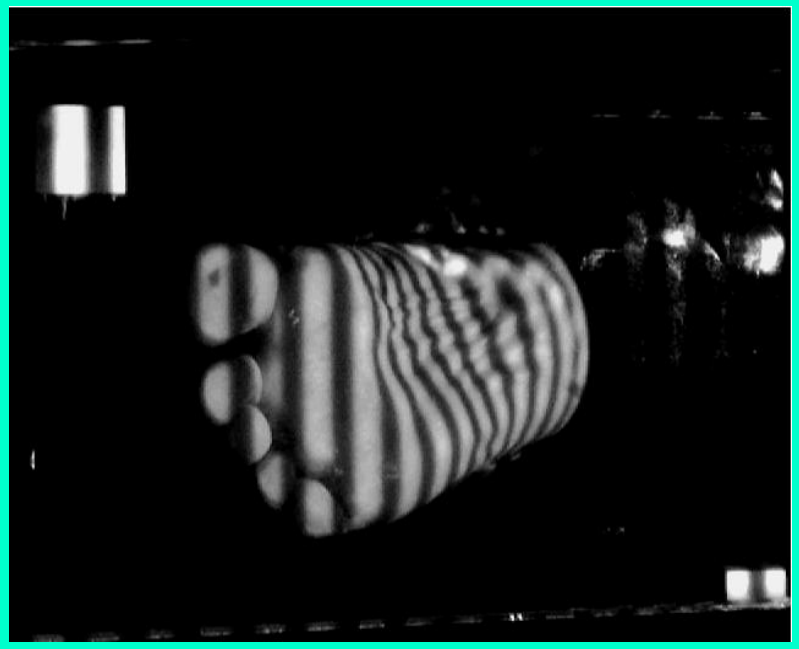

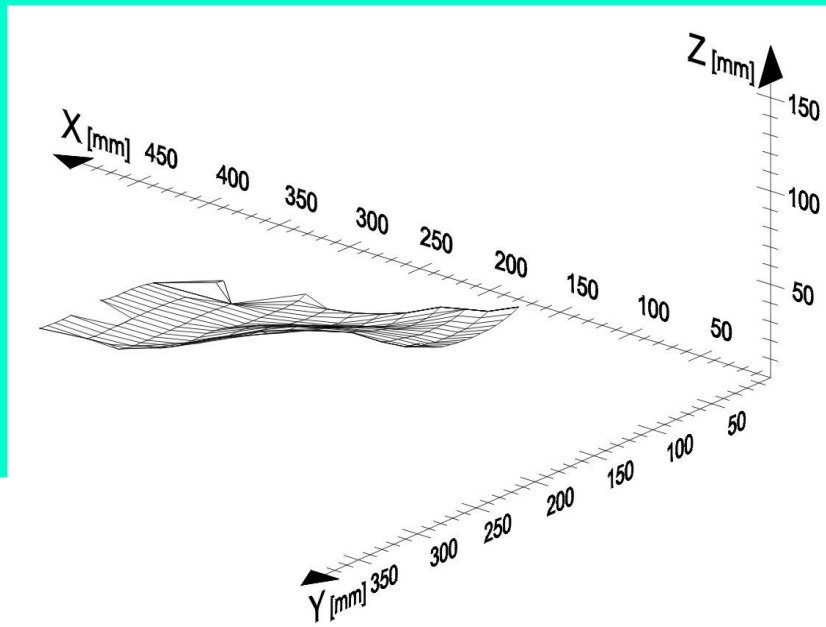


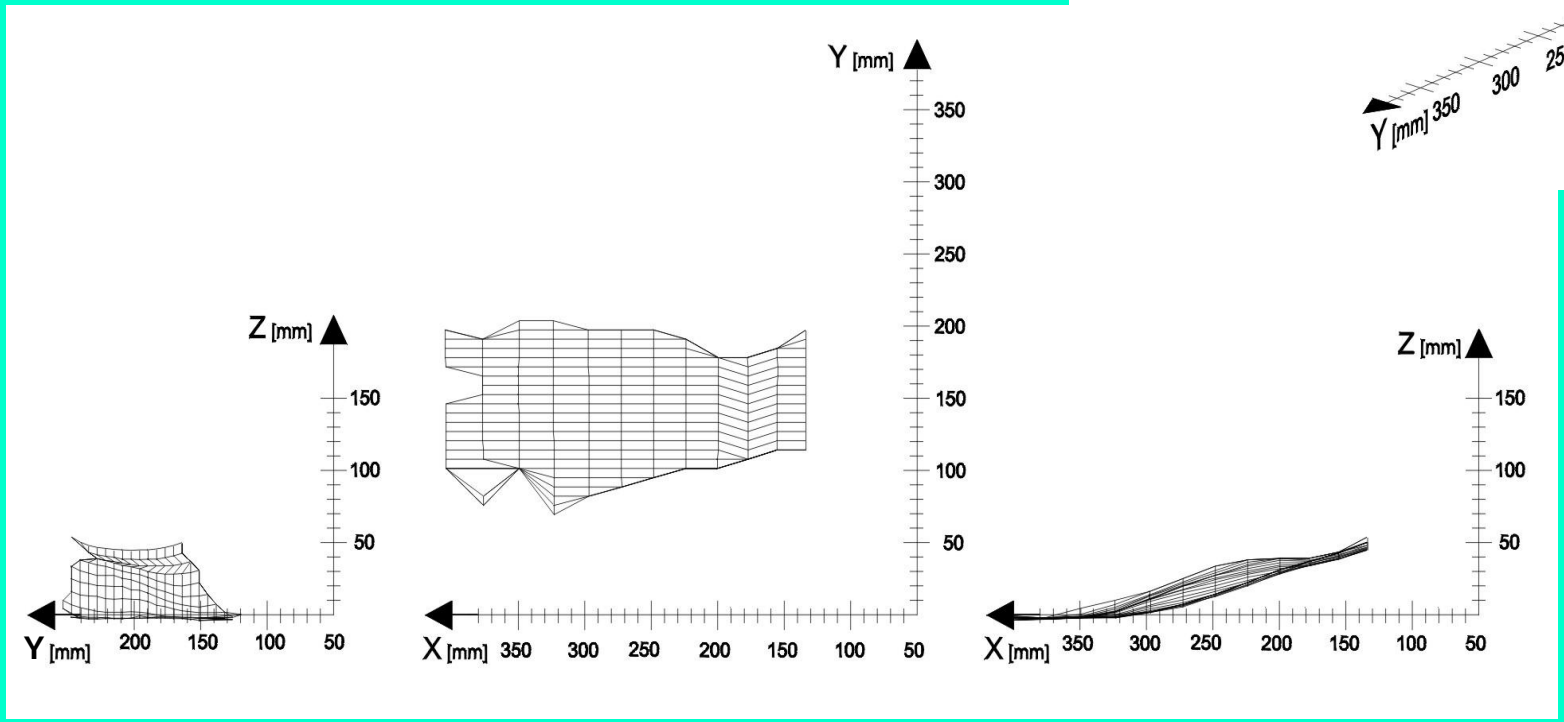

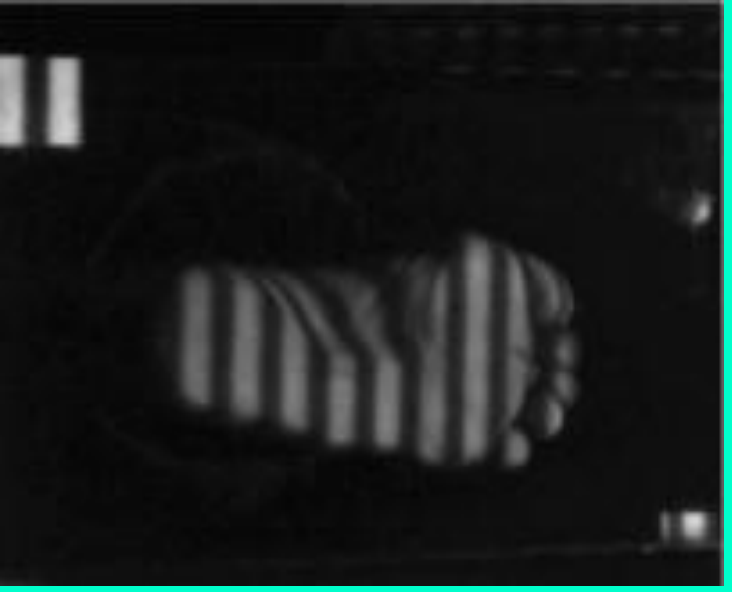

**Caminando**

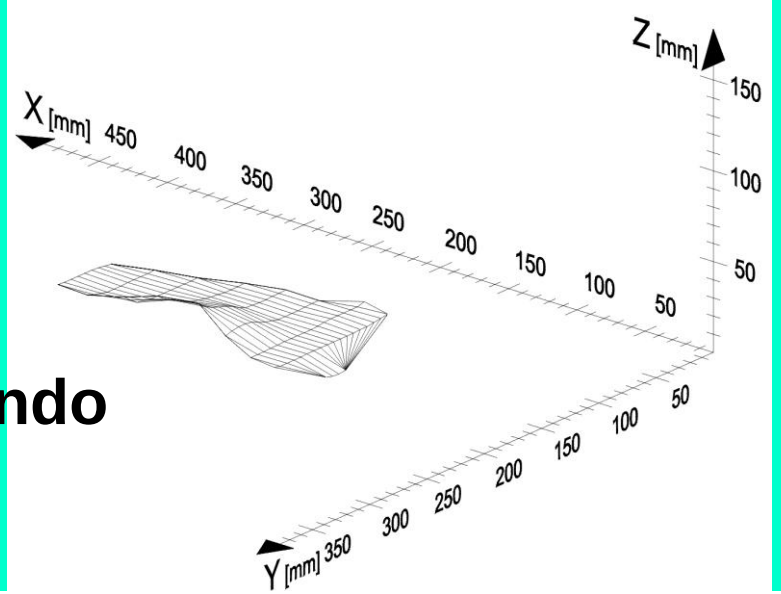


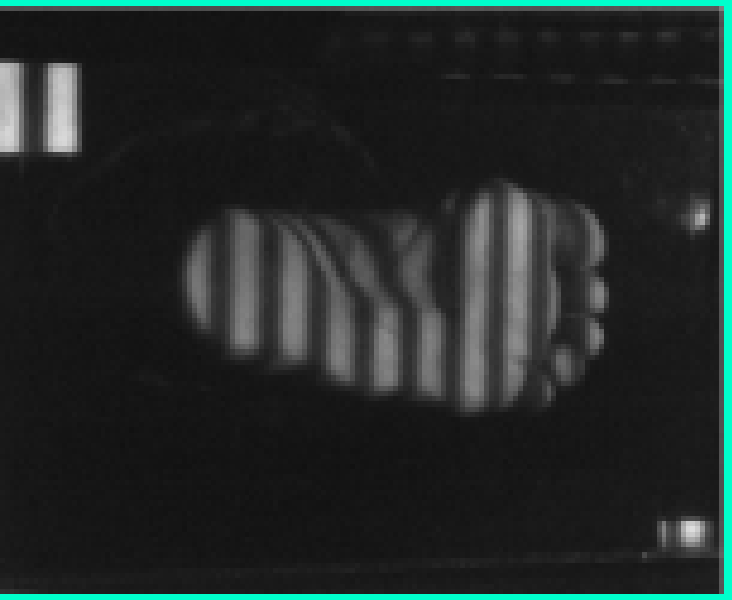

**Parada**

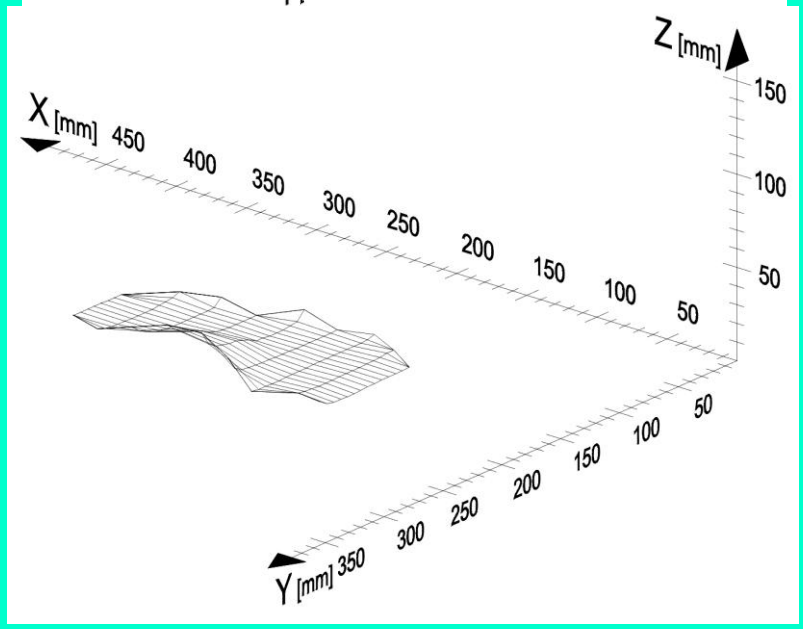


**Pisadas de mujer joven con una malformación en sus piernas, corregida quirúrgicamente.**

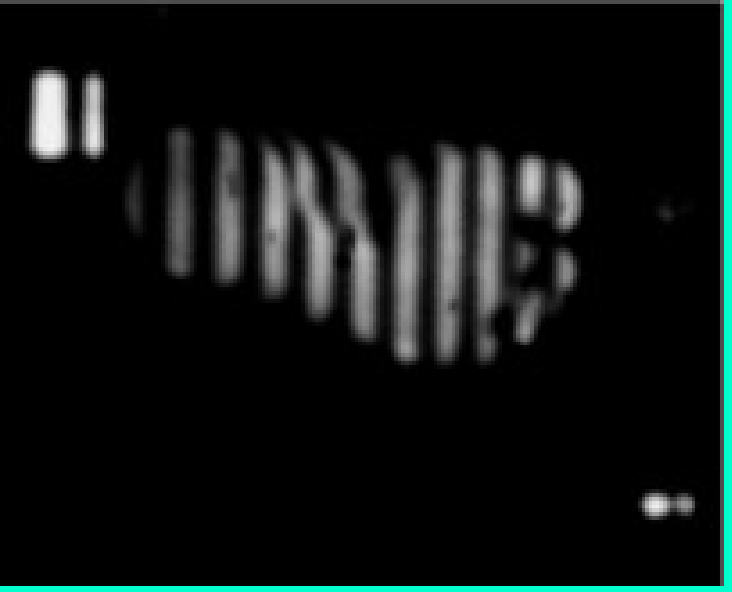

**Caminando**

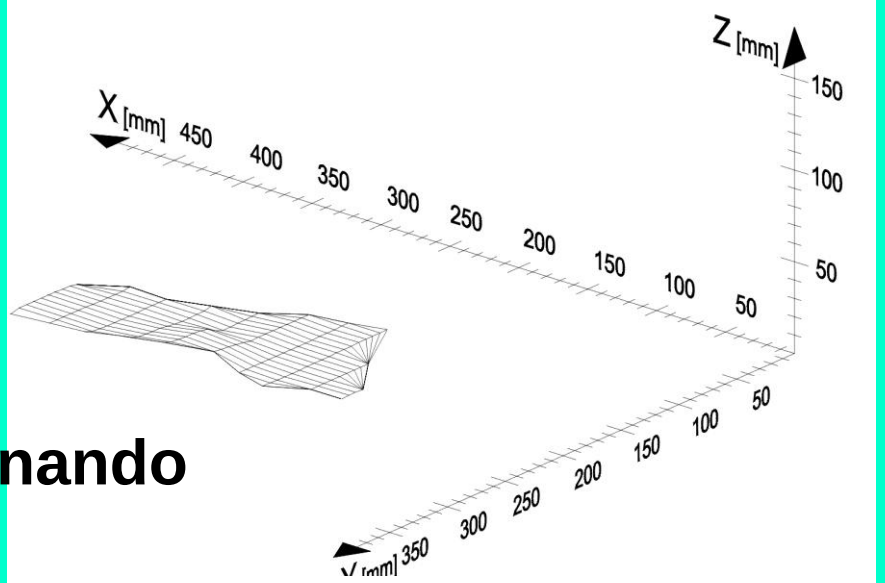


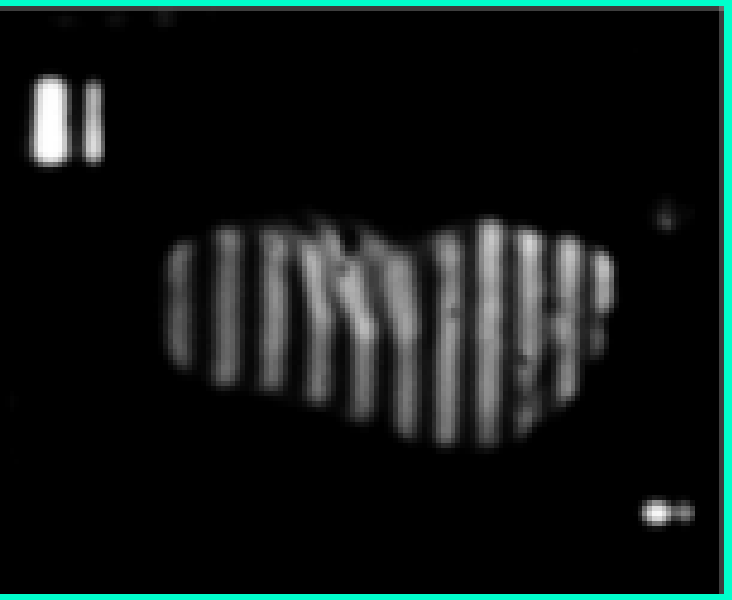

**Parado**

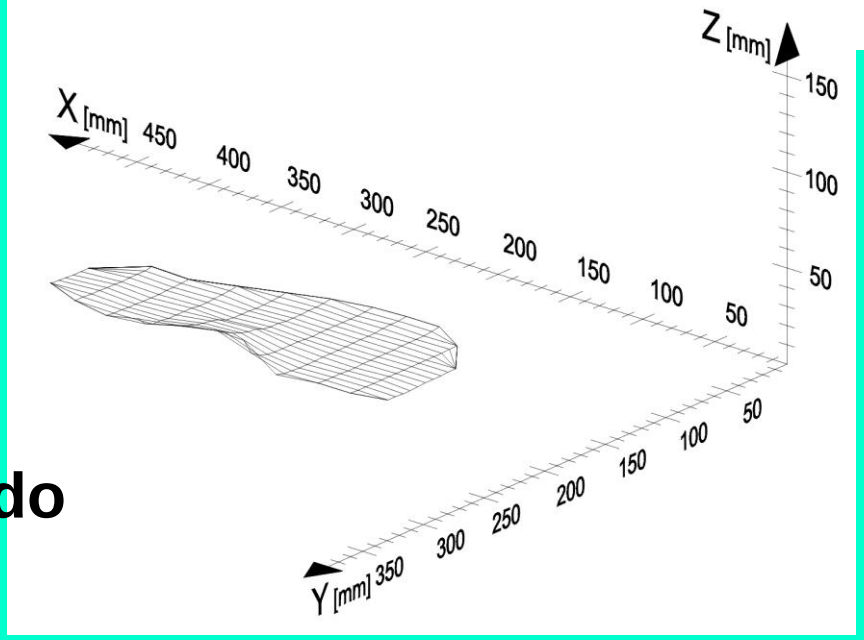


**Pisadas de hombre mayor con una pierna 1,5 cm más larga.**

**Caminando**

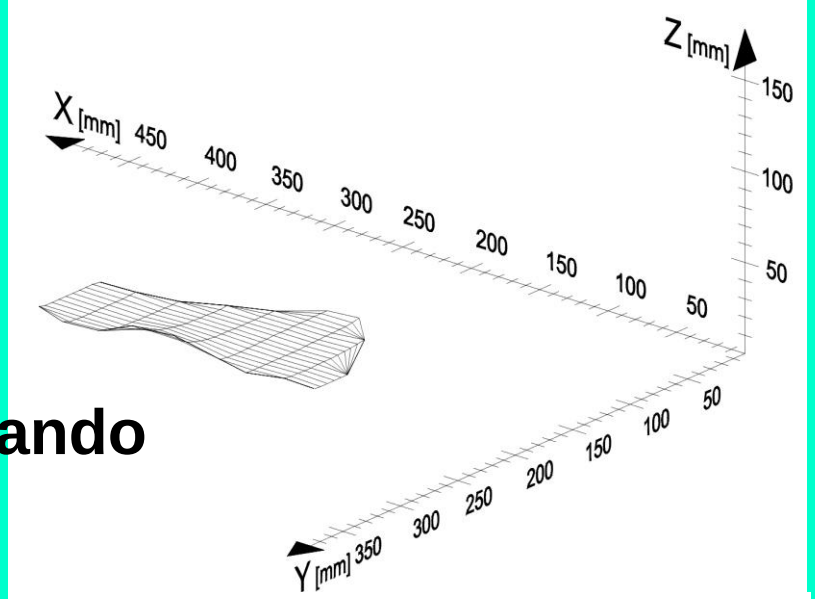


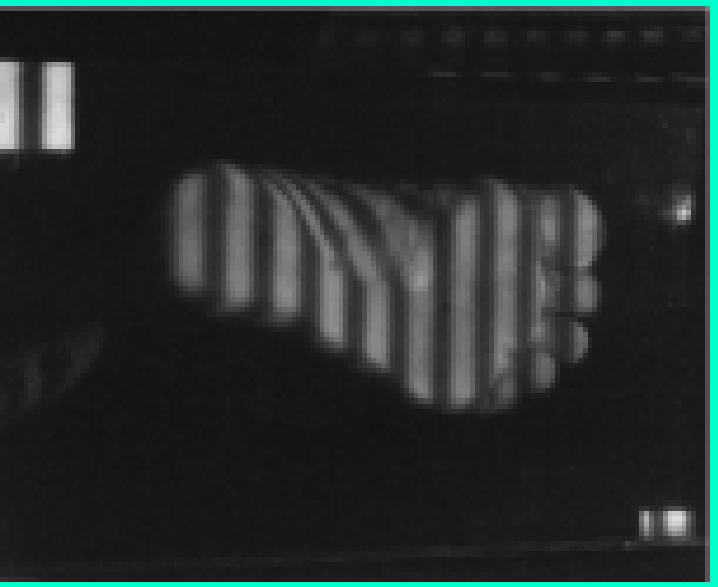

**Parada**

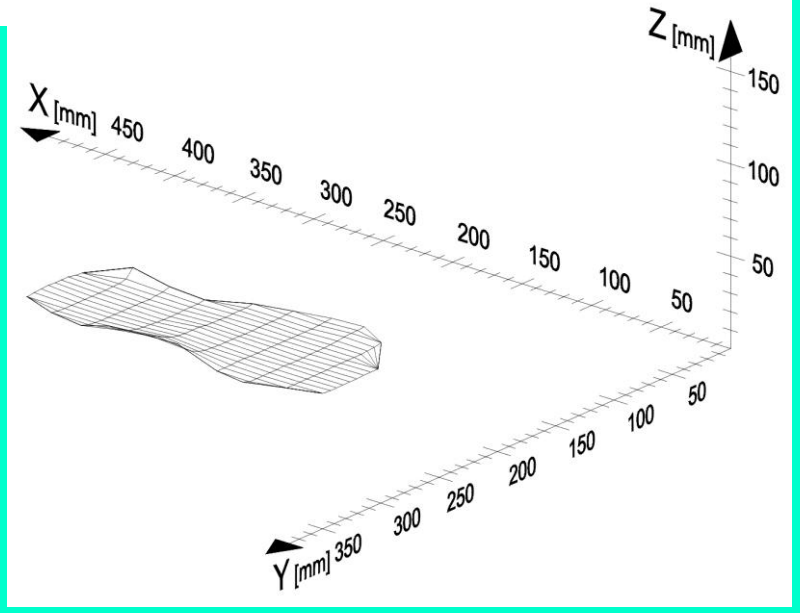


**Pisadas de bailarina clásica joven (2).**

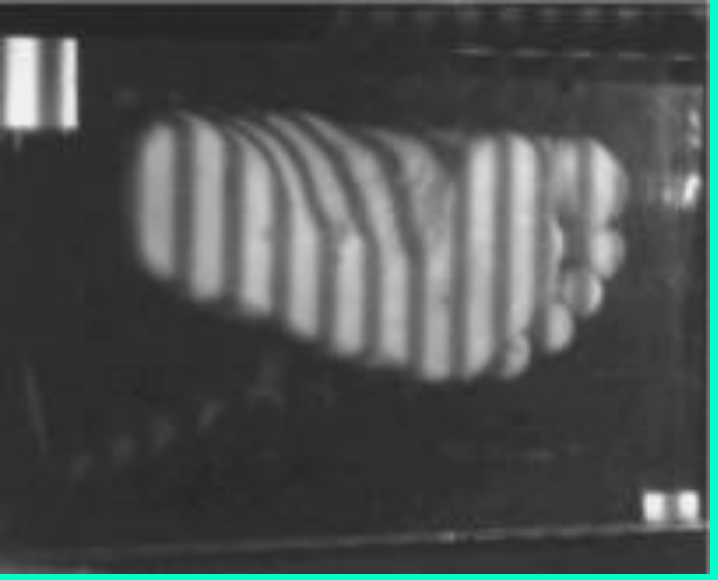

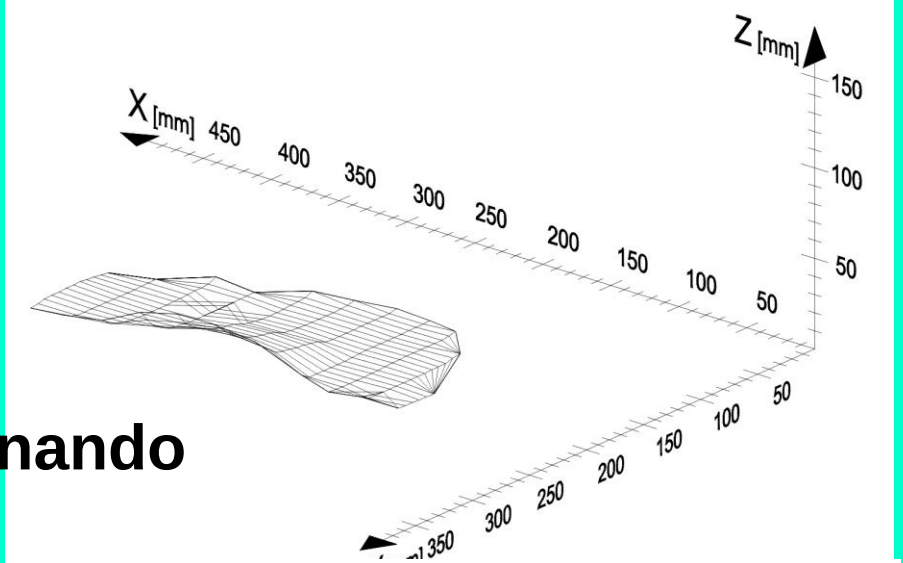


**Caminando**

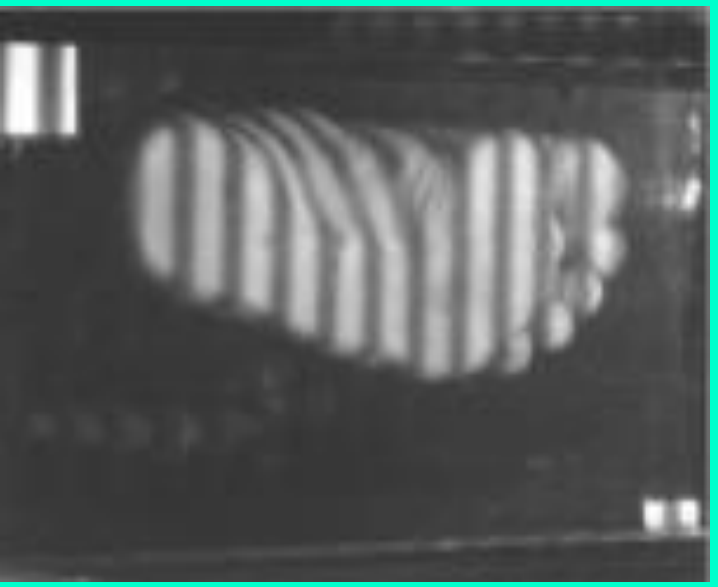

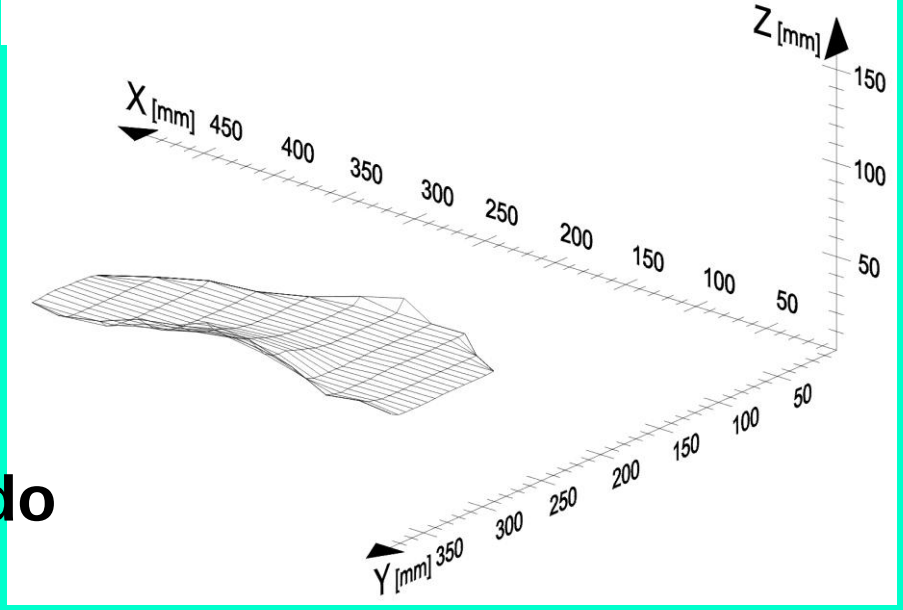


**Parado**

**Pisadas de un jugador de fútbol joven.**

**Caminando**

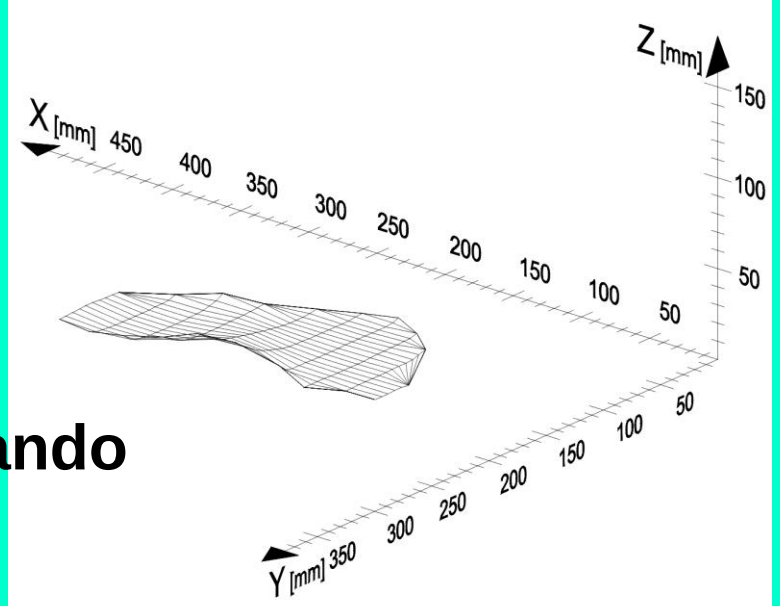


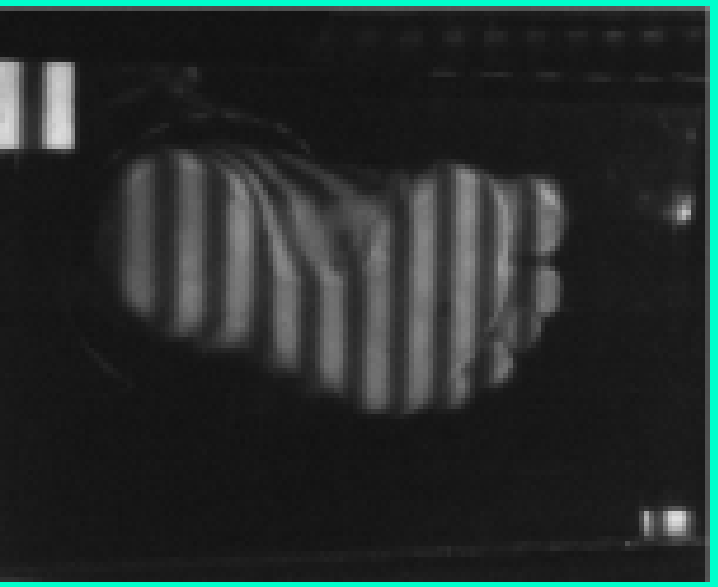

**Parado**

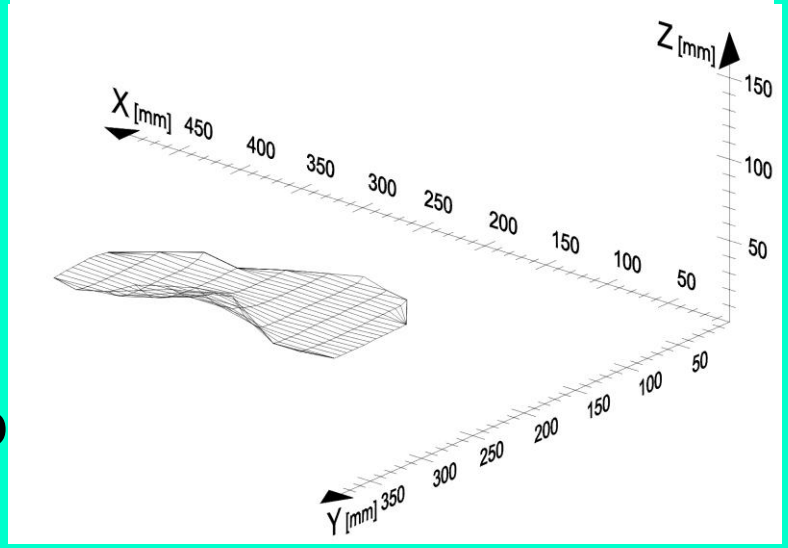


**Pisadas de un jugador de rugby joven.**

# ESTABILIDAD CAMINANDO I

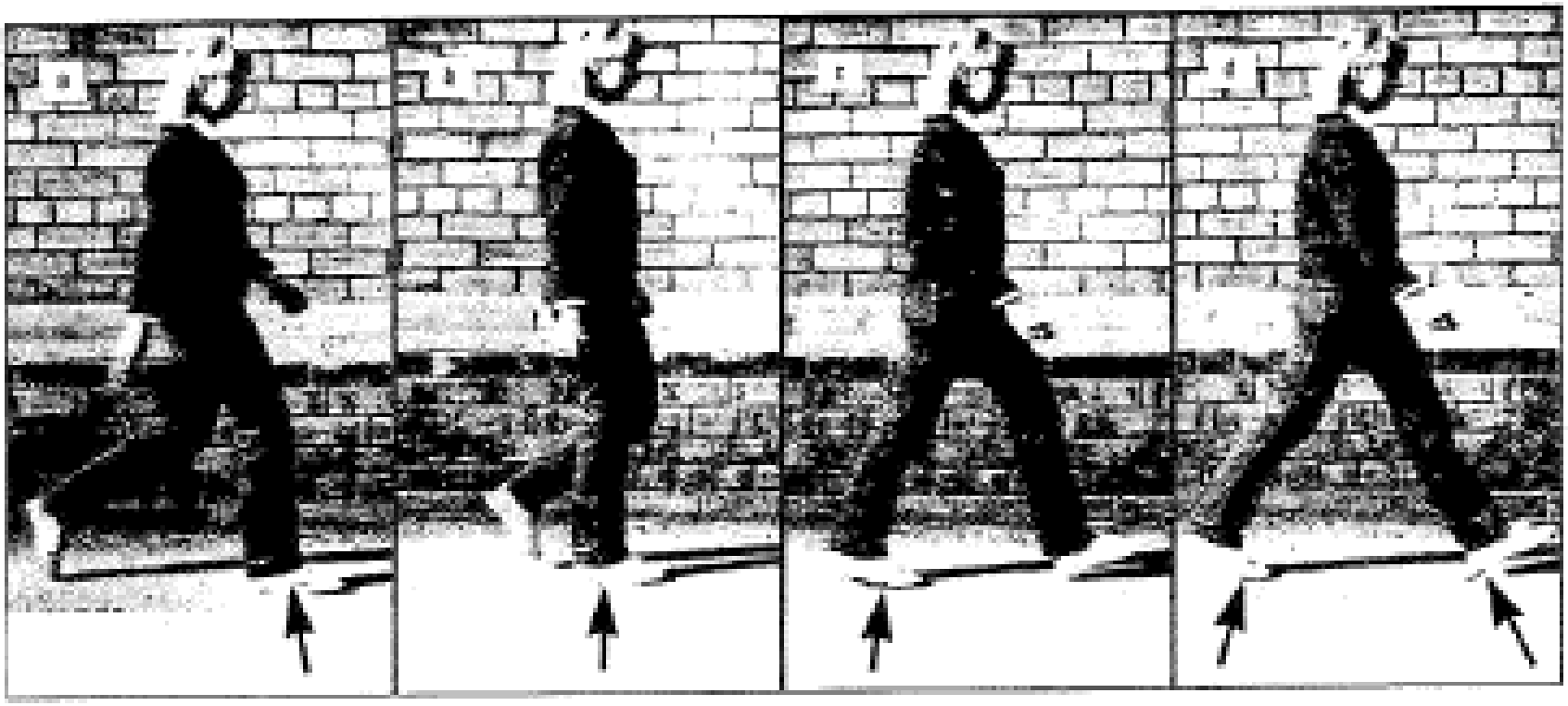

**Fig. 3.8.** Walking, with arrows showing the directions of the forces on the feet. (From [99]. Copyright 1992 Columbia University Press. Reprinted with the permission of the press)

# ESTABILIDAD CAMINANDO II

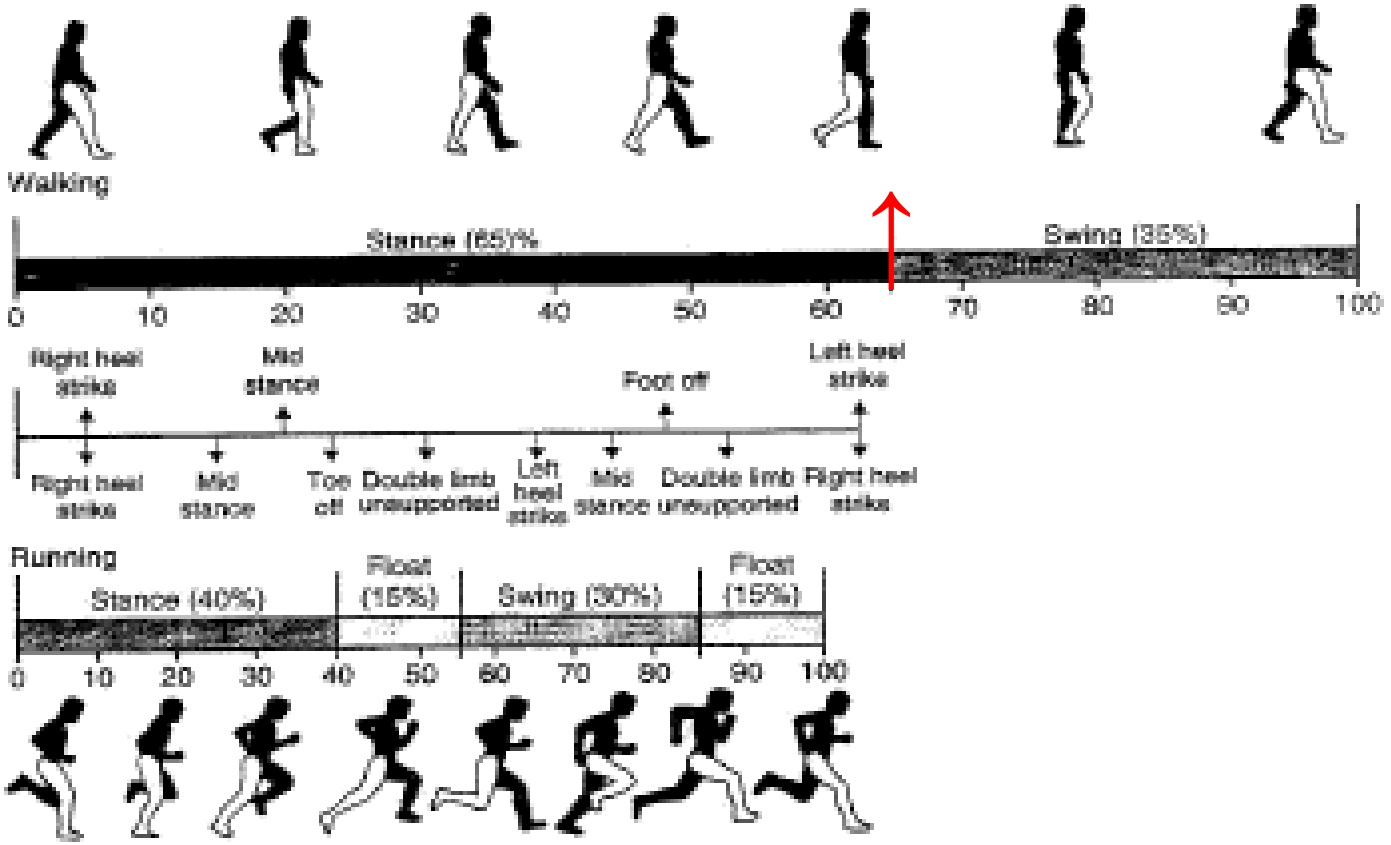


**Fig. 3.9.** Walking and running gait sequences. For walking, from foot strike (or heel strike) to toe off (or foot off) is the stance phase, with subdivisions sometimes called: foot flat or loading, midstance, terminal stance, and then preswing. From toe off to foot strike is the swing phase, with subdivisions called: initial swing, midswing, and then terminal swing. (From [166]. Used with permission)

# ESTABILIDAD CAMINANDO III

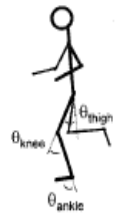


Fig. 3.1. One set of conventions for hip (thigh), knee (lower leg), and ankle (foot) angles. Other conventions are also used, such as with the thigh angle being relative to the vertical and the ankle angle defined as 90° less than here. (Based on 150])

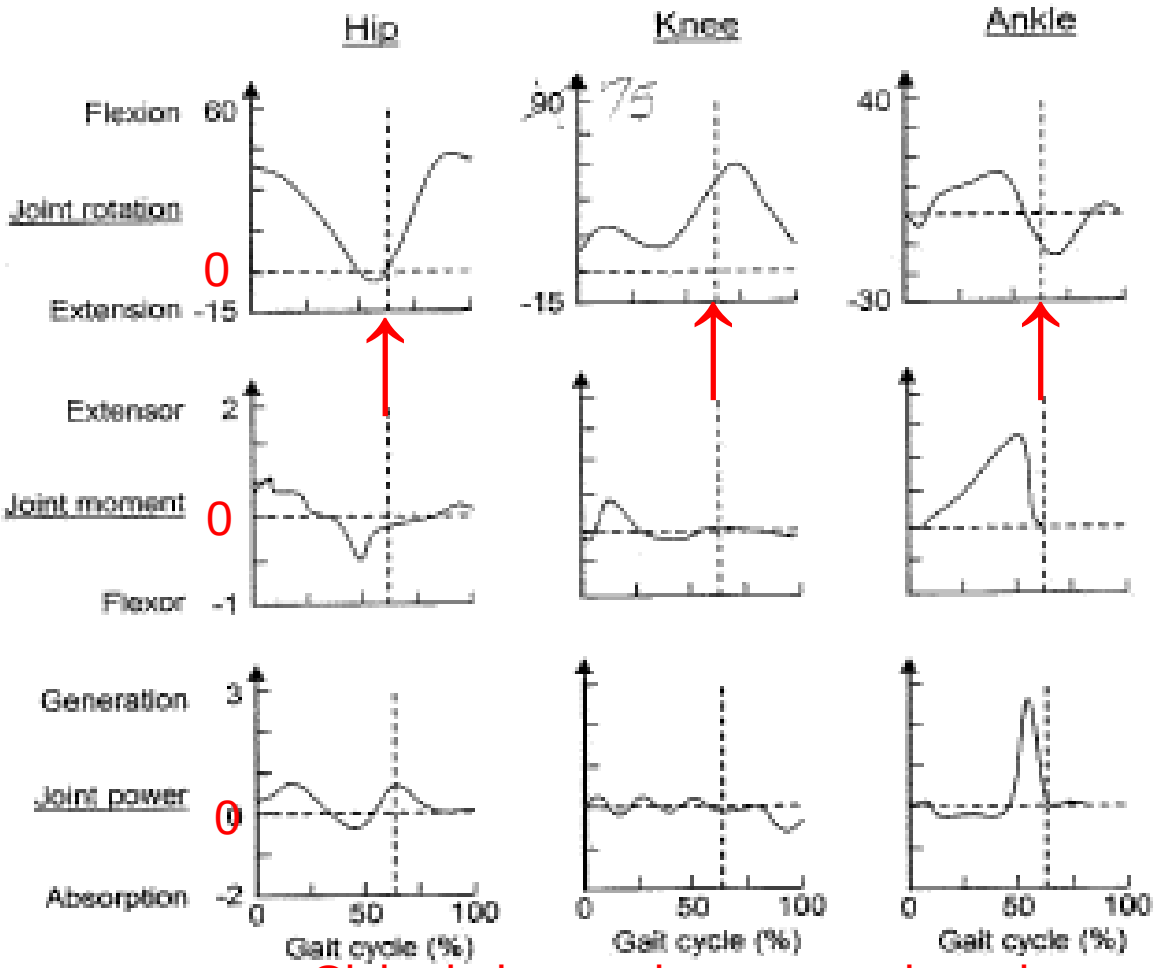


Ciclo de la marcha o paso al caminar

**Fig. 3.10.** Average values for sagittal plane joint rotation (in °), moment (torque) per mass (in N-m/kg body mass), and power per mass (in W/kg body mass) for the hip, knee, and ankle during a step in walking. (Based on [121]. Also see [104])

# ESTABILIDAD CAMINANDO IV

Contracción muscular concéntrica

Contracción muscular excéntrica

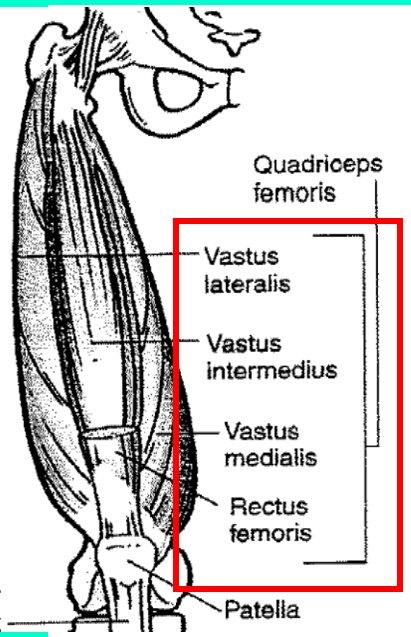


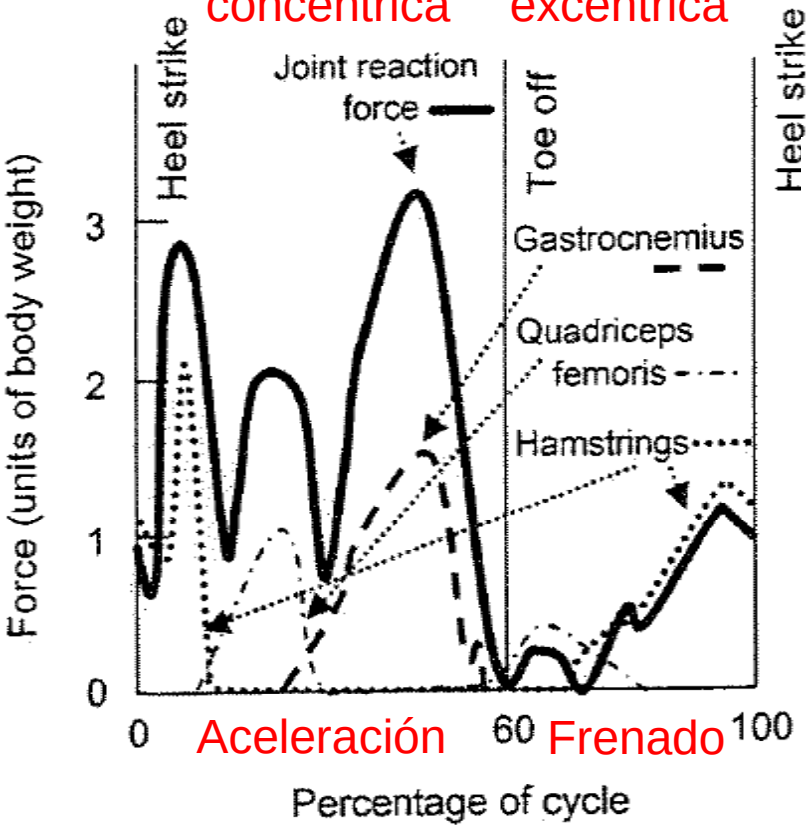


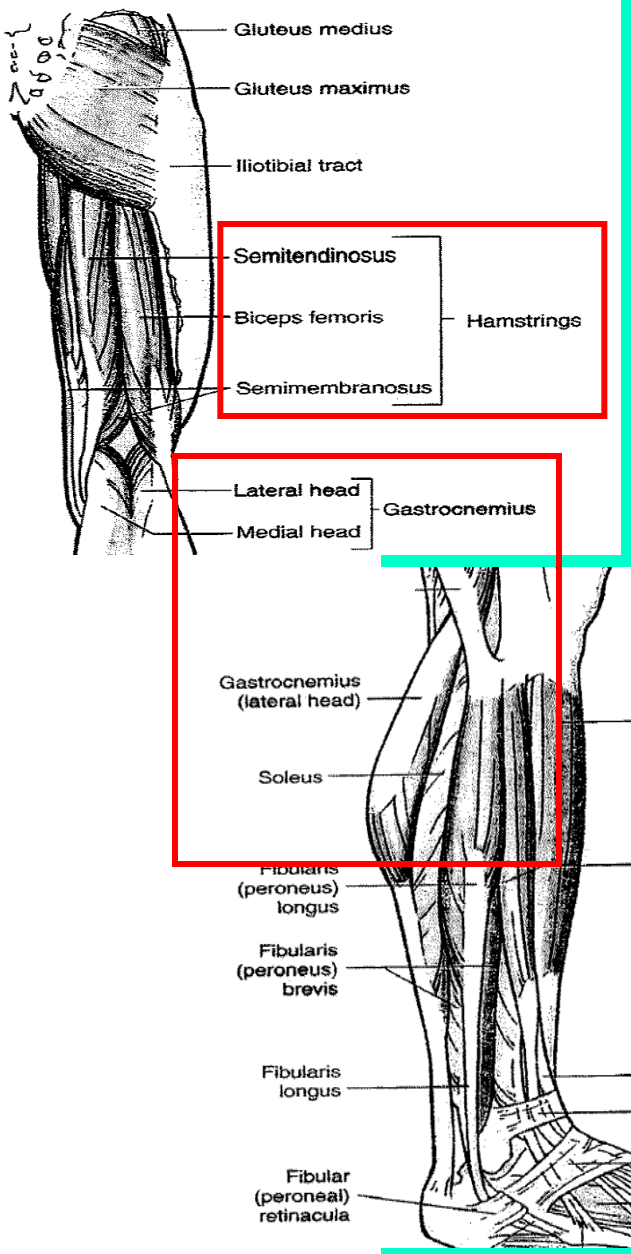


**Fig. 3.11.** Joint reaction forces transmitted through tibial plateau during one gait normal walking (*solid line*), along with the muscles forces – averaged for 12 subjects. (Based on [154] and [160]) (1970 y 2001)

# ESTABILIDAD CAMINANDO V

En contracción concéntrica los músculos realizan la fuerza necesaria para superar el esfuerzo.

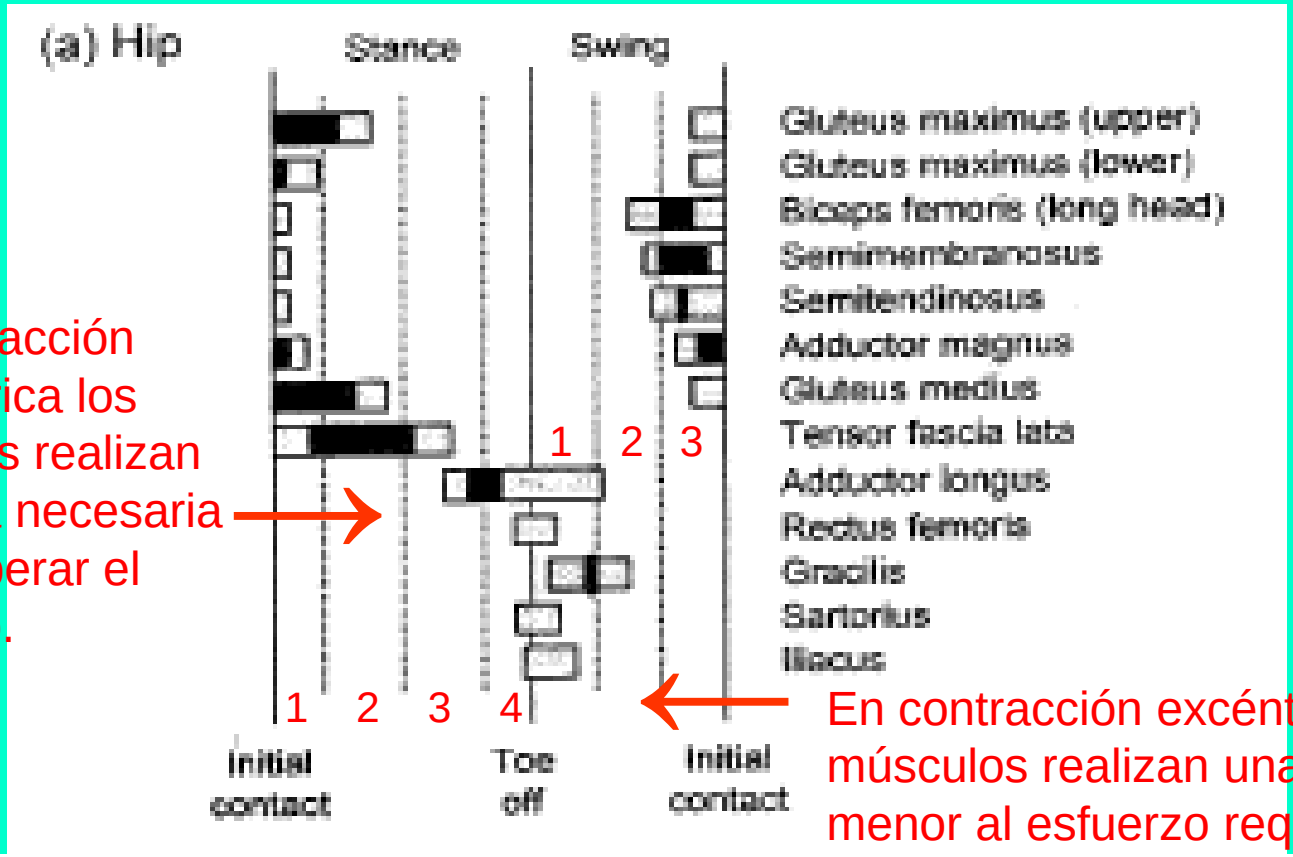


En contracción excéntrica los músculos realizan una fuerza menor al esfuerzo requerido.

**Fig. 3.12.** Electromyographic (EMG) activity of the muscles of the (a) hip, (b) knee, and (c) ankle and foot during walking in a healthy person. *Dotted* regions represent activation <20% of maximum voluntary contractions, while *black* regions represent >20% activation. *White* regions in (c) for the intrinsic muscles of the foot show at least some level of activation. The four phases of stance are, in time sequence, loading, midstance, terminal stance, and preswing; the three phases of swing are initial swing, midswing, and terminal swing. (Also see Fig. 3.9.) (Based on [104] and [162])

GLUTEO MAYOR

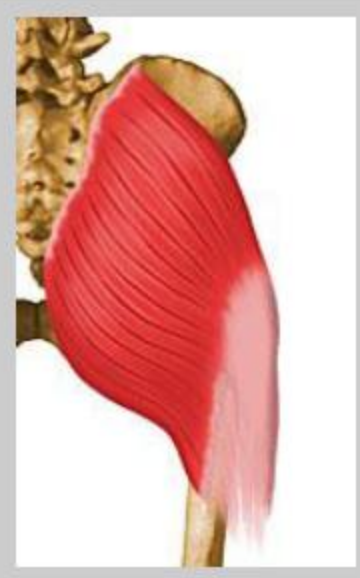

GLUTEO MEDIANO

GLUTEO MENOR

TENSOR DE LA FASCIA LATA

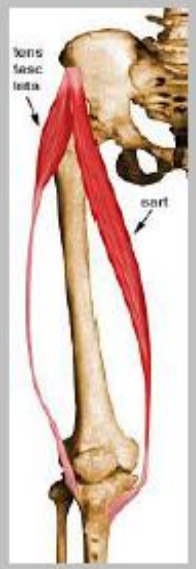


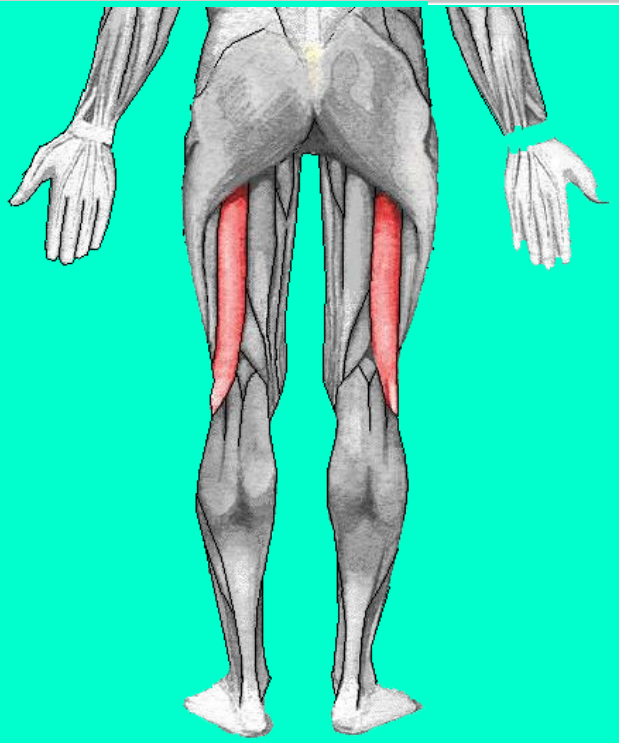

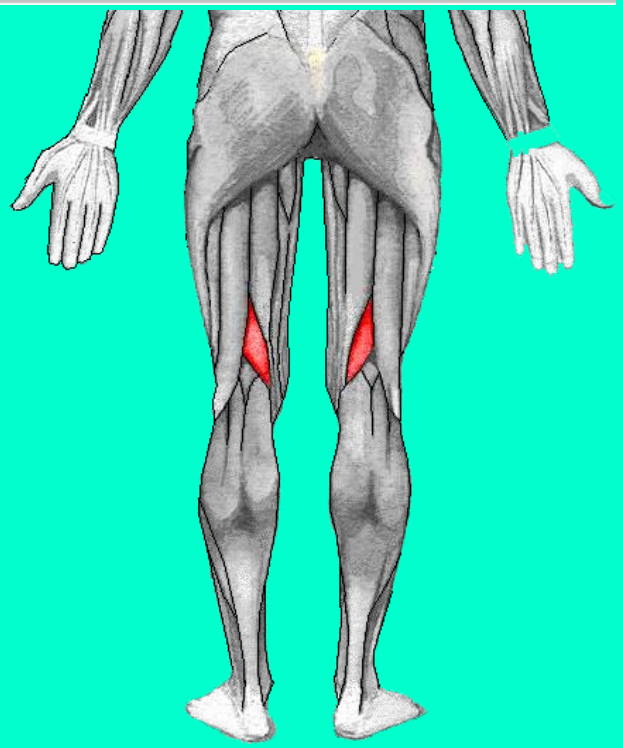

# ESTABILIDAD CAMINANDO VI

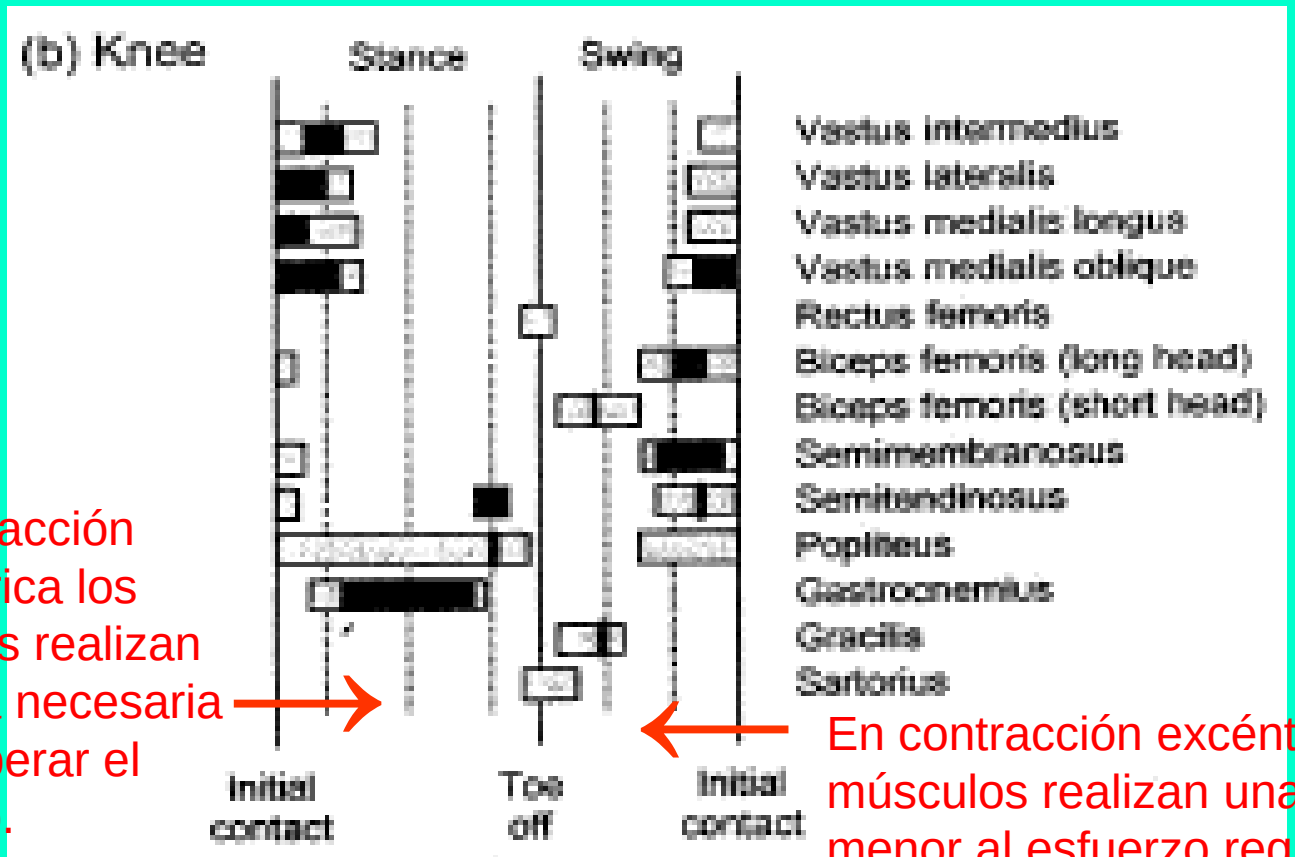


En contracción concéntrica los músculos realizan la fuerza necesaria para superar el esfuerzo.

En contracción excéntrica los músculos realizan una fuerza menor al esfuerzo requerido.

**Fig. 3.12.** Electromyographic (EMG) activity of the muscles of the (a) hip, (b) knee, and (c) ankle and foot during walking in a healthy person. *Dotted* regions represent activation <20% of maximum voluntary contractions, while *black* regions represent >20% activation. *White* regions in (c) for the intrinsic muscles of the foot show at least some level of activation. The four phases of stance are, in time sequence, loading, midstance, terminal stance, and preswing; the three phases of swing are initial swing, midswing, and terminal swing. (Also see Fig. 3.9.) (Based on [104] and [162])

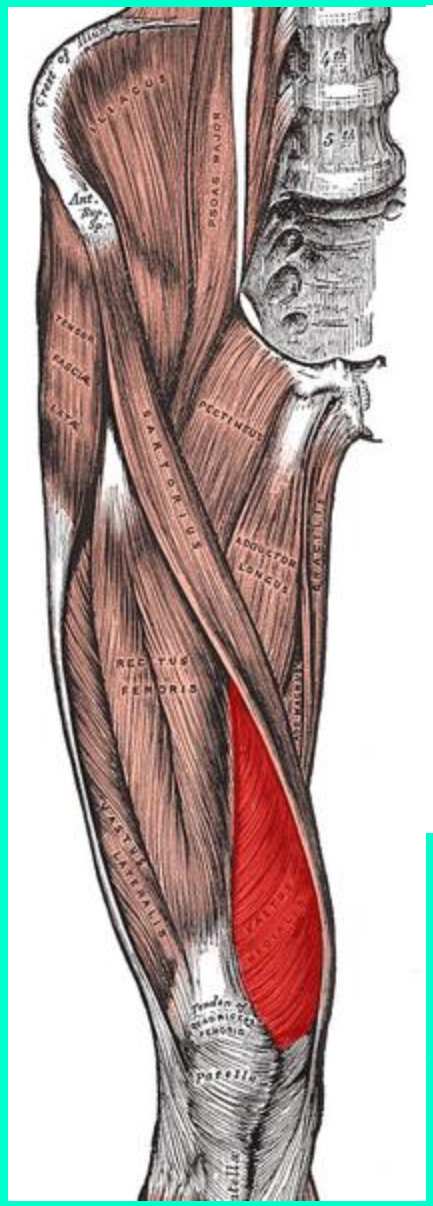

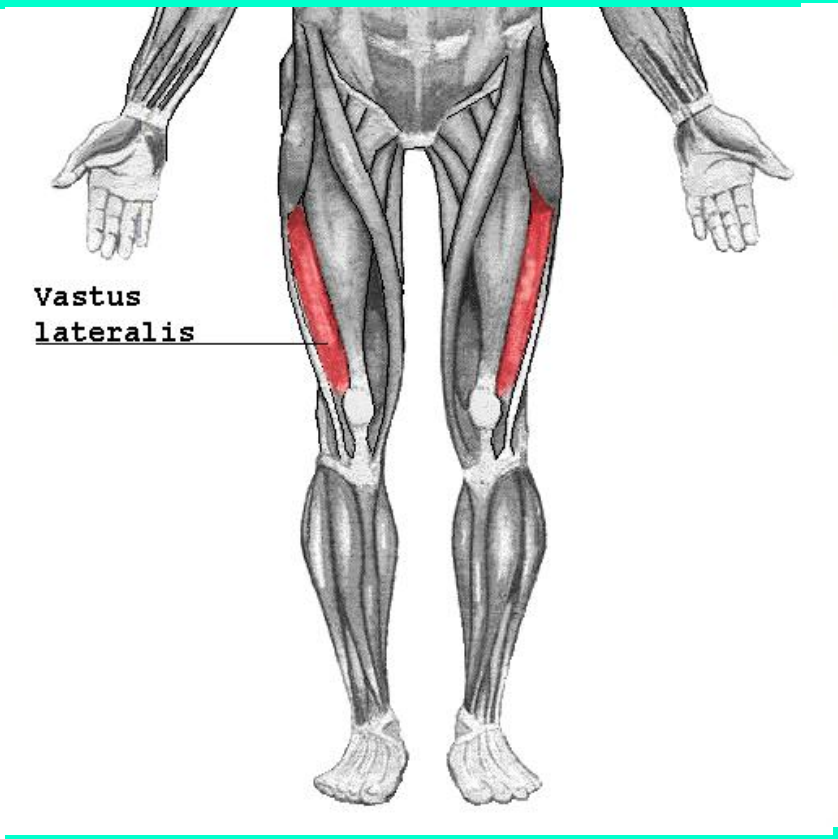
Vastus
lateralis

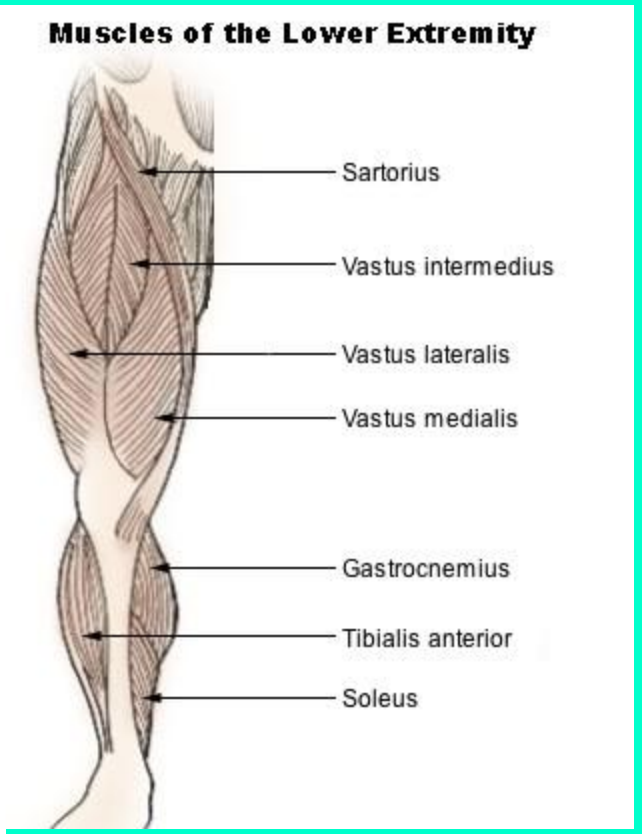
Muscles of the Lower Extremity
Sartorius
Vastus intermedius
Vastus lateralis
Vastus medialis
Gastrocnemius
Tibialis anterior
Soleus

# ESTABILIDAD CAMINANDO VII

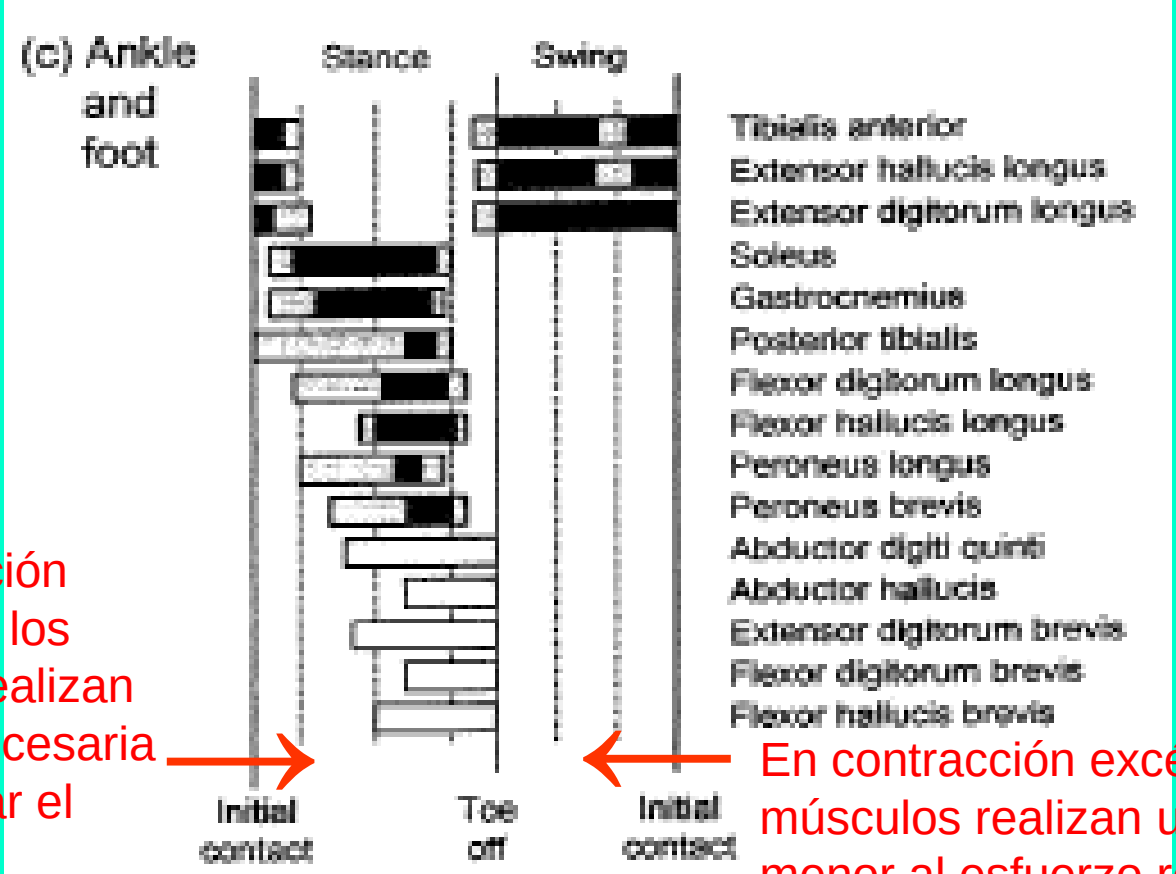


En contracción concéntrica los músculos realizan la fuerza necesaria para superar el esfuerzo.

En contracción excéntrica los músculos realizan una fuerza menor al esfuerzo requerido.

**Fig. 3.12.** Electromyographic (EMG) activity of the muscles of the (a) hip, (b) knee, and (c) ankle and foot during walking in a healthy person. *Dotted* regions represent activation <20% of maximum voluntary contractions, while *black* regions represent >20% activation. *White* regions in (c) for the intrinsic muscles of the foot show at least some level of activation. The four phases of stance are, in time sequence, loading, midstance, terminal stance, and preswing; the three phases of swing are initial swing, midswing, and terminal swing. (Also see Fig. 3.9.) (Based on [104] and [162])

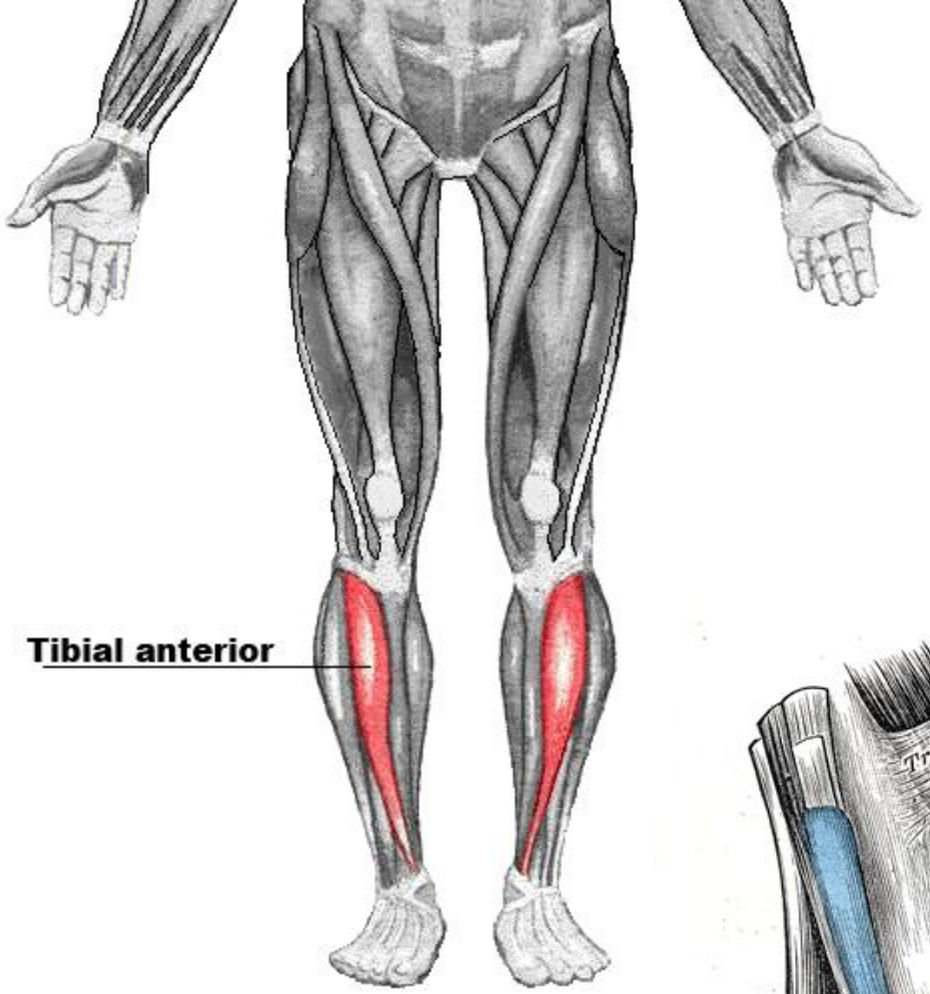
Tibial anterior

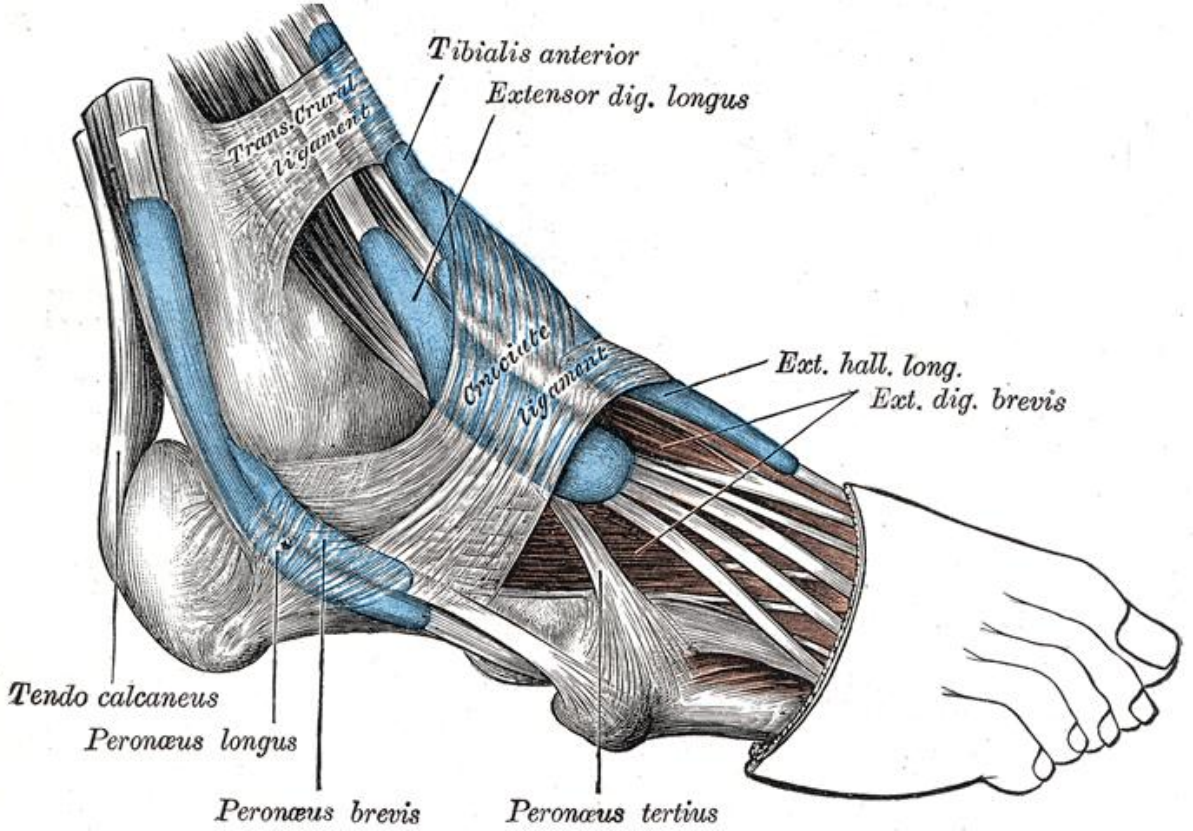
Tibialis anterior
Extensor dig. longus
Trans. Crural ligament
Cruciate ligament
Ext. hall. long.
Ext. dig. brevis
Tendo calcaneus
Peronæus longus
Peronæus brevis
Peronæus tertius

# ESTABILIDAD CAMINANDO VIII

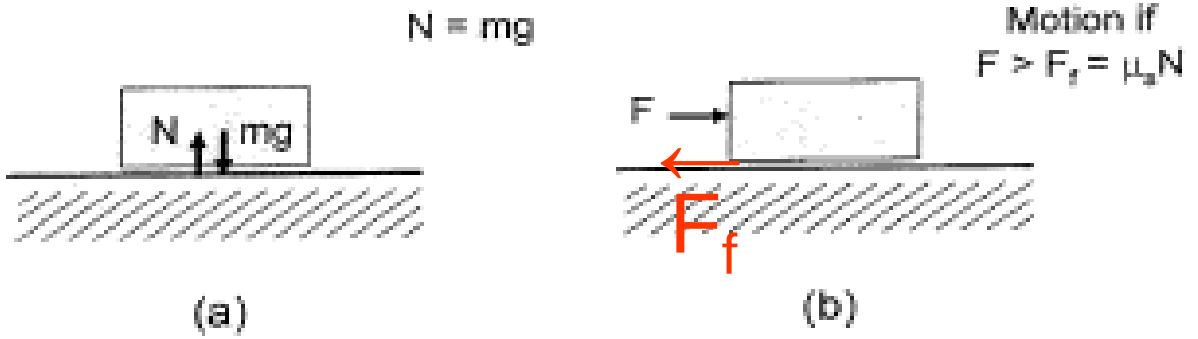


**Fig. 3.13.** (a) Static equilibrium of an object on a table and (b) lateral force required to overcome static friction to enable motion

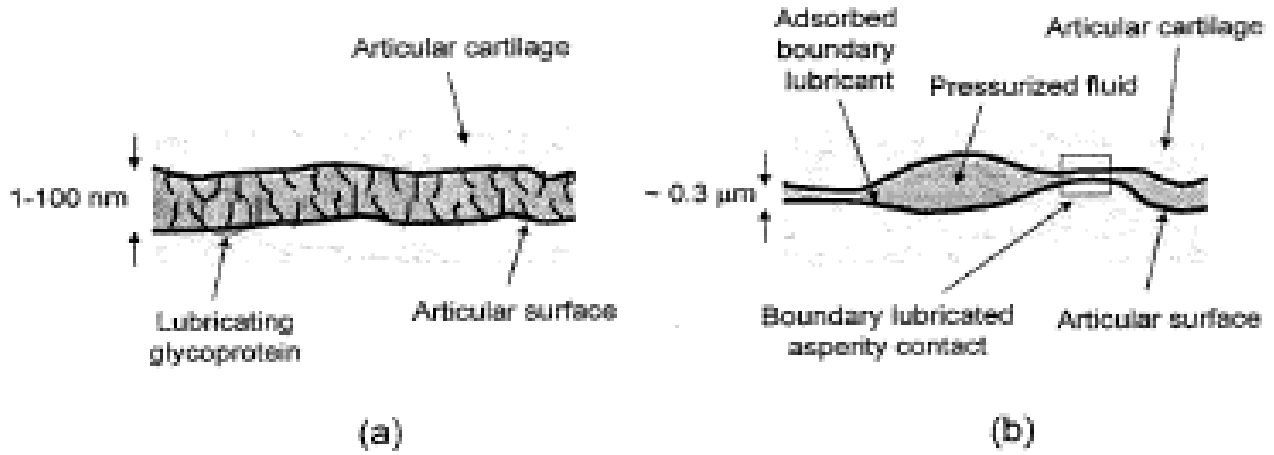


**Fig. 3.14.** In synovial joints (a) boundary layer lubrication of the articular cartilage surfaces for relatively flat and nearby surfaces and (b) mixed lubrication at articular cartilage, showing boundary lubrication when the separation is on the order of the surface roughness and fluid-film lubrication in areas of more widely separated surfaces. (Based on [155])

# ESTABILIDAD CAMINANDO X

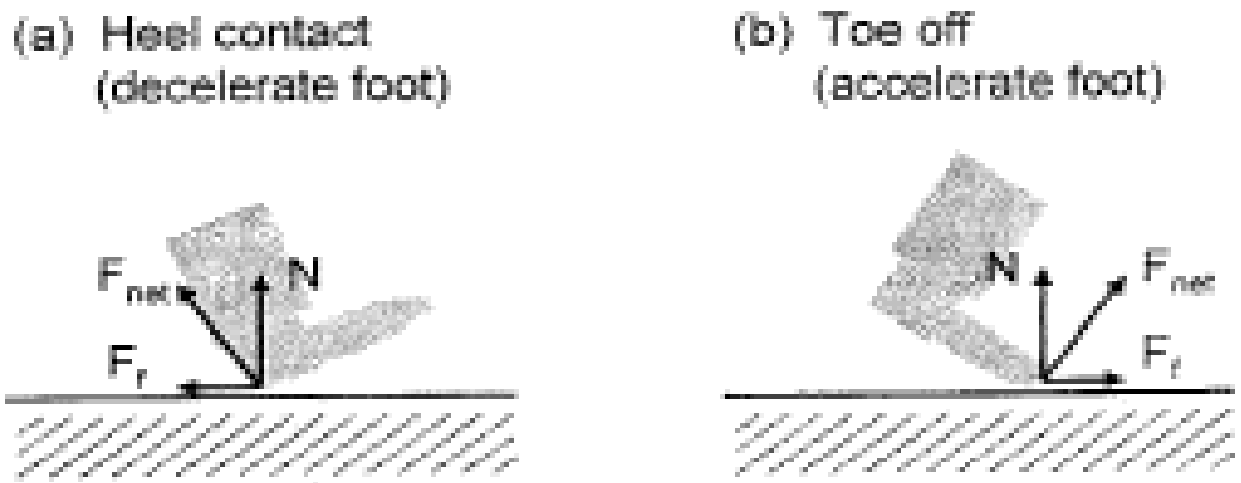


**Fig. 3.15.** (a) Heel contact stage and decelerating the foot and (b) toe-off stage and accelerating the foot

# ESTABILIDAD CAMINANDO XI

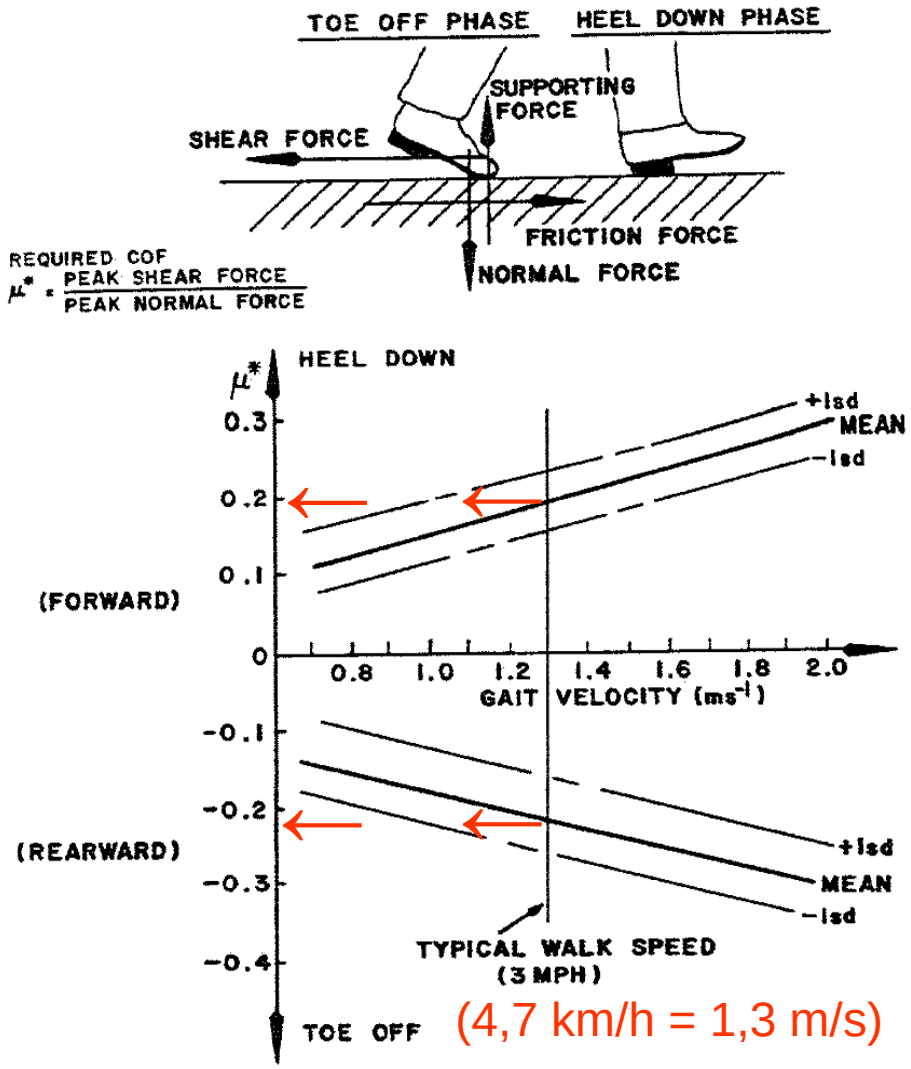


**Fig. 3.16.** Coefficient of friction required during walking at different speeds. (From [114]. Reprinted with permission of Wiley)

# ESTABILIDAD CAMINANDO XII

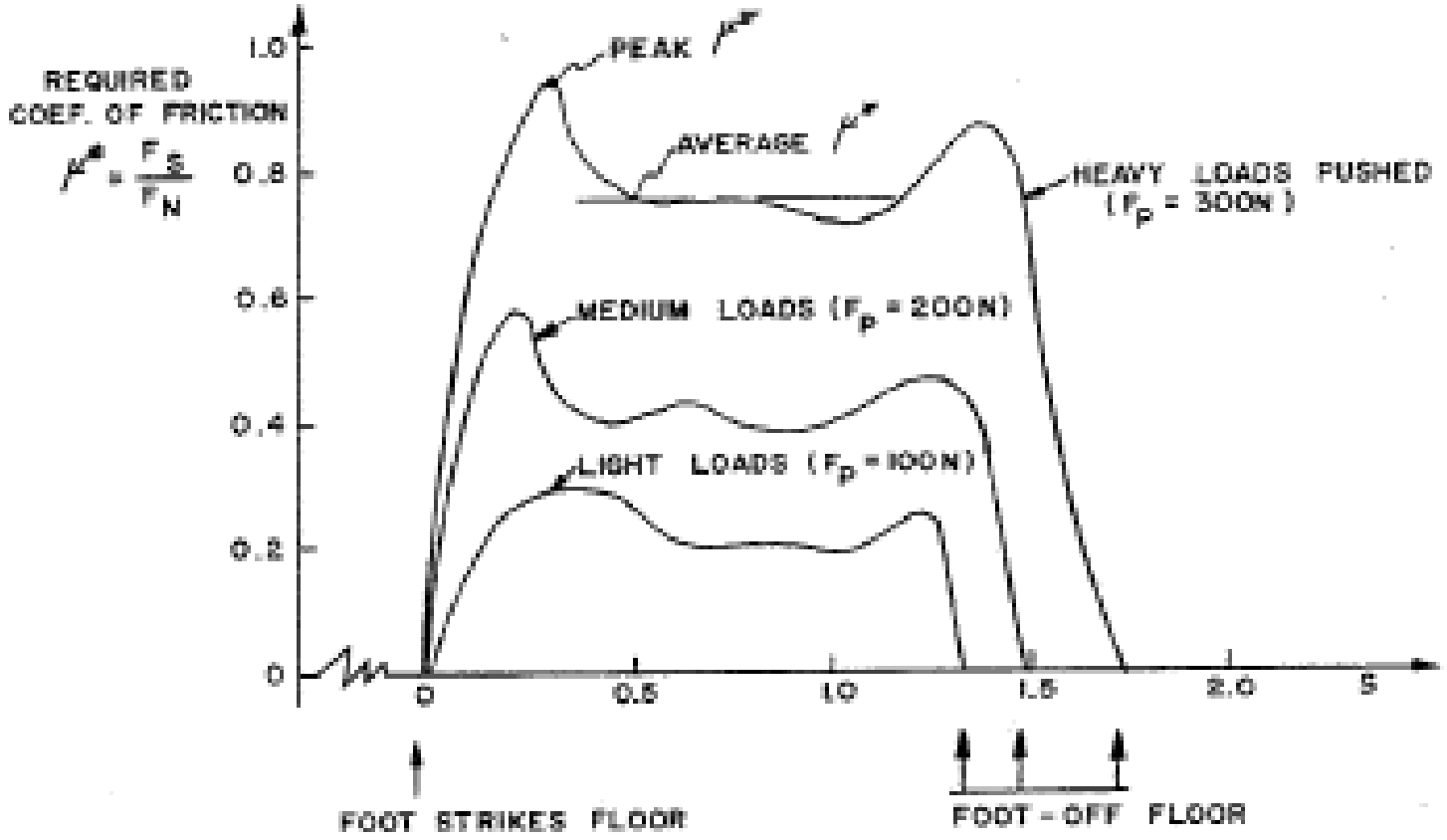


**Fig. 3.17.** Dynamic coefficient of friction required to push a weighted cart with different loads. (From [113]. Reprinted with permission of Wiley)

# ESTABILIDAD CAMINANDO XIII

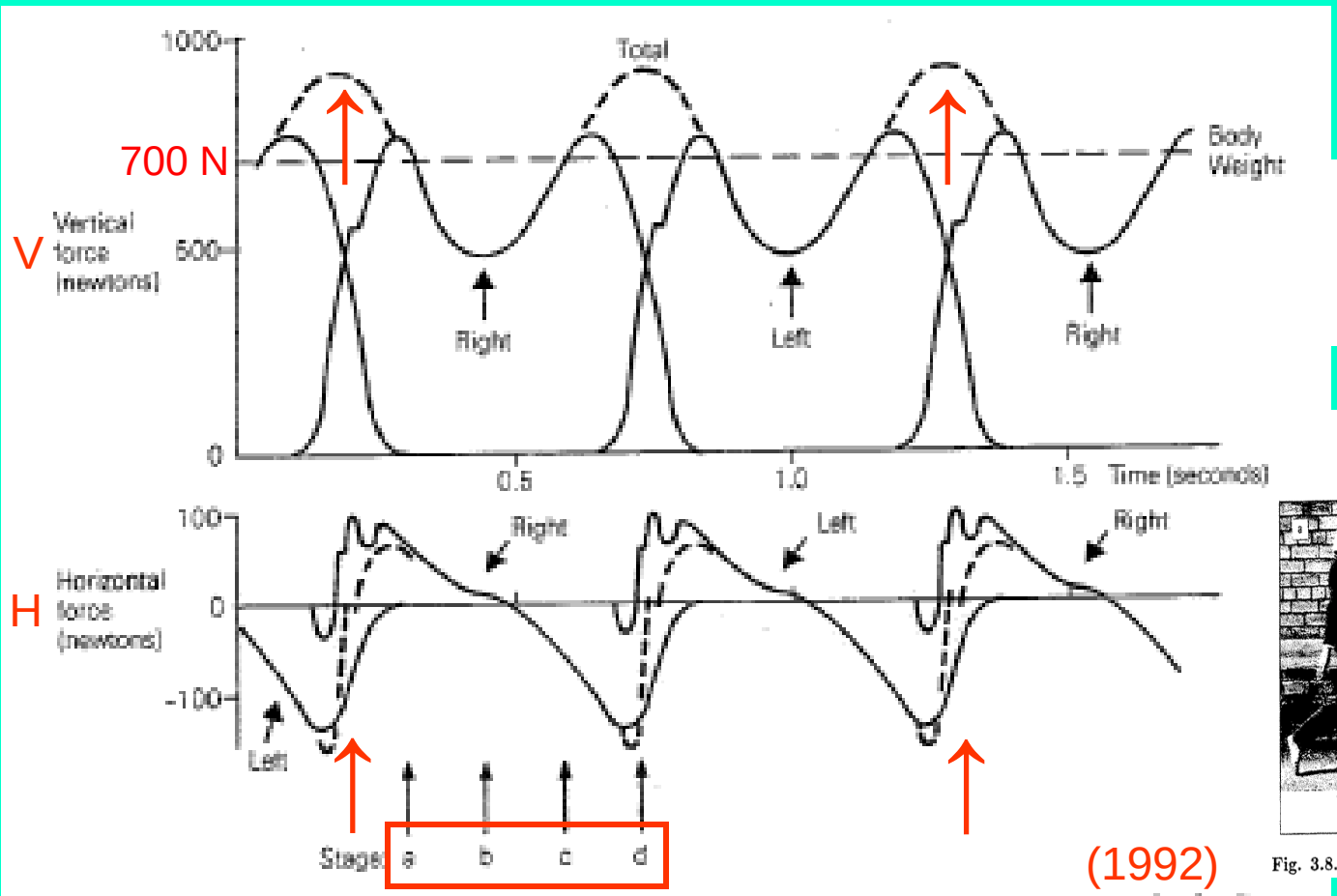


(1992)

**Fig. 3.18.** Vertical and horizontal forces on feet during walking. (From [99]. Copyright 1992 Columbia University Press. Reprinted with the permission of the press)

Las componentes V y H están fuera de fase

a b c d

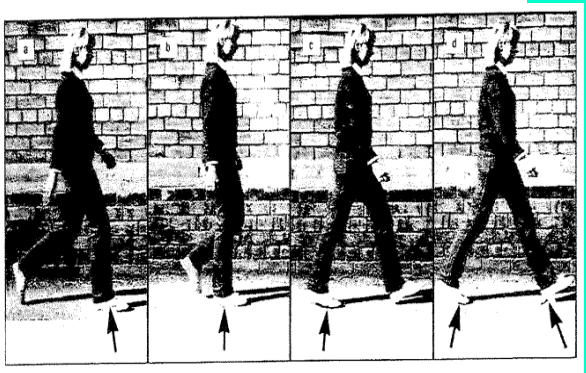

Fig. 3.8. Walking, with arrows showing the directions of the forces on the feet.

# ESTABILIDAD CAMINANDO XIV

Las componentes H y V están fuera de fase

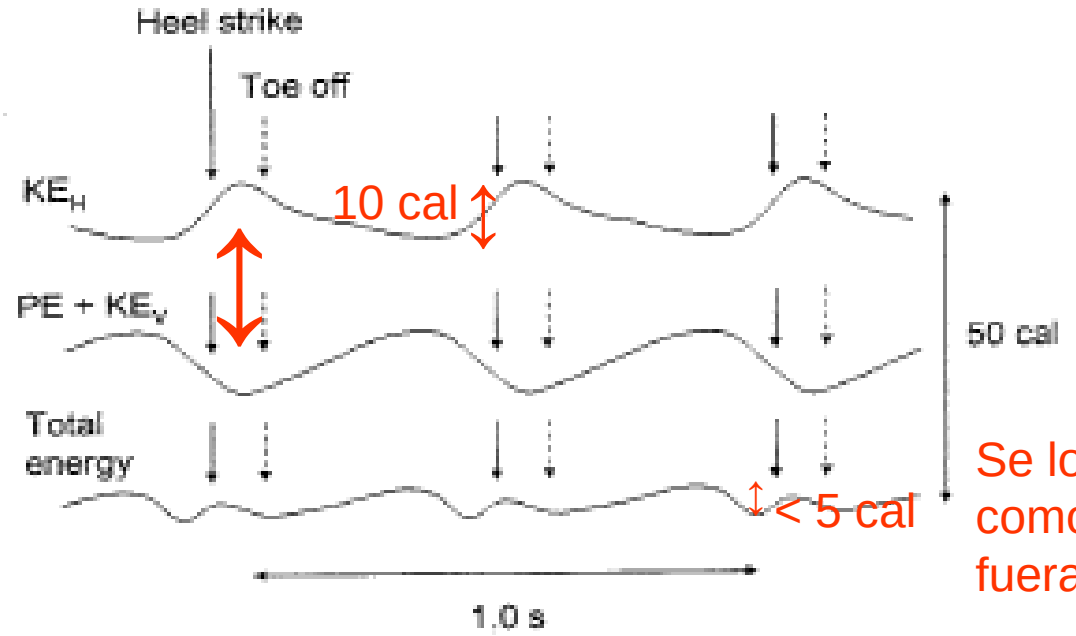


Se lo intenta modelar como si la Energía Total fuera constante

**Fig. 3.19.** Changes in mechanical energy during walking from force plates, with heel strike and toe off shown, for (from top to bottom curve) forward kinetic energy, gravitational potential energy plus vertical kinetic energy, and total energy. (Based on [112] and [146])

$$KE = KE_H + KE_V,$$

$$KE_H = \frac{1}{2} m_b v_x^2 = \frac{1}{2} m_b \left(\frac{dx}{dt}\right)^2,$$

$$KE_V = \frac{1}{2} m_b v_z^2 = \frac{1}{2} m_b \left(\frac{dz}{dt}\right)^2.$$

$$PE = m_b g z_{CM},$$

$$E = KE + PE.$$

# ESTABILIDAD CAMINANDO XV

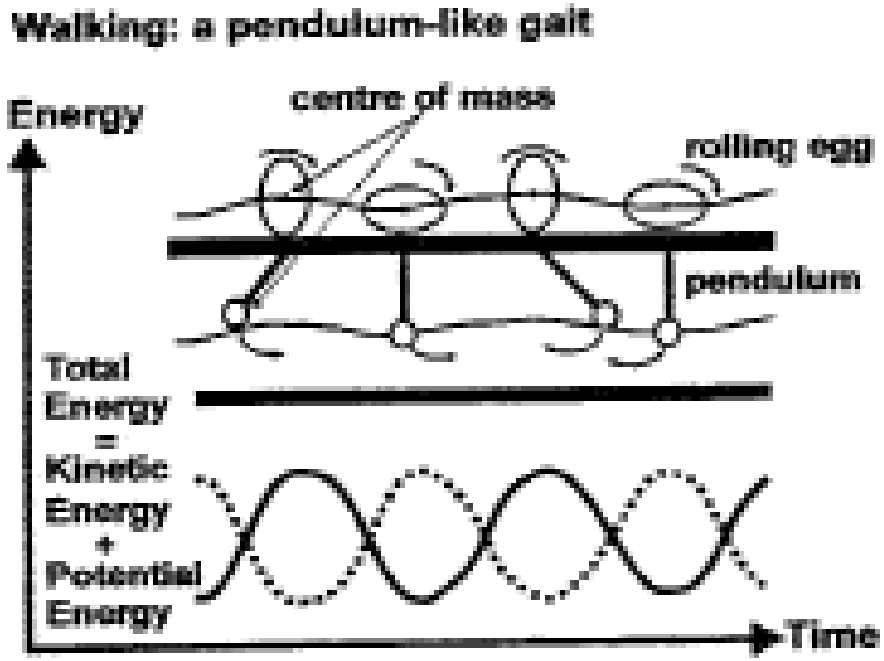


Fig. 3.20. The cyclic exchange of kinetic and potential energy in a pendulum and a rolling egg, with constant total energy, is similar to that in walking. (From [151]. Used with permission)

(2000)

# ESTABILIDAD CAMINANDO XVI Fuerzas y Energías

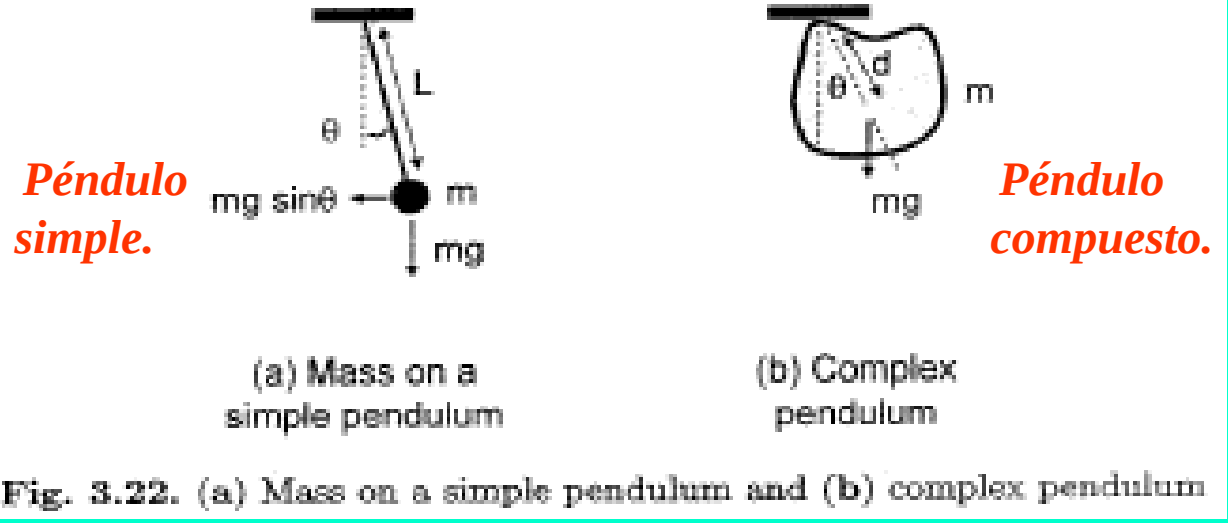


***Péndulo simple.***

***Péndulo compuesto.***

Fig. 3.22. (a) Mass on a simple pendulum and (b) complex pendulum

$$\mathrm{KE} = \frac{1}{2}mv^2 = \frac{1}{2}m\left(L\frac{\mathrm{d}\theta}{\mathrm{d}t}\right)^2 = \frac{1}{2}mB^2L^2\omega^2\sin^2(\omega t+\beta),$$

$$\mathrm{PE} = mgL(1-\cos\theta) \approx \frac{1}{2}mgL\theta^2,$$

$$mL\frac{\mathrm{d}^2\theta}{\mathrm{d}t^2} = -mg\sin\theta.$$

$$\sin\theta \approx \theta$$

$$\theta(t) = B\cos(\omega t+\beta),$$

$$\omega = (g/L)^{1/2}$$

$$\mathrm{PE} \approx \frac{1}{2}mgLB^2\cos^2(\omega t+\beta) = \frac{1}{2}mB^2L^2\omega^2\cos^2(\omega t+\beta)$$

$$\begin{aligned} E &= \mathrm{KE}+\mathrm{PE} \\ &= \frac{1}{2}mB^2L^2\omega^2\sin^2(\omega t+\beta) + \frac{1}{2}mB^2L^2\omega^2\cos^2(\omega t+\beta) \\ &= \frac{1}{2}mB^2L^2\omega^2 \end{aligned}$$

$B$ es la amplitud, $\omega$ es la frecuencia, y $\beta$ es la fase.

***Péndulo simple.***

# ESTABILIDAD CAMINANDO XVII
# Torques y Momentos de Inercia

$$mL\frac{d^2\theta}{dt^2} = -mg\sin\theta.$$

$$mL^2\frac{d^2\theta}{dt^2} = -mgL\sin\theta.$$

***Péndulo simple.***

***Momento de Inercia.***

$$I = \sum_i m_i R_i^2$$

$$I = \int \rho(\mathbf{r}) R^2 dV.$$

¡No confundir!

$$\tau = mgL\sin(360^\circ - \theta) = -mgL\sin\theta = mL^2\frac{d^2\theta}{dt^2}.$$

Torque

¡No confundir!

***Péndulo compuesto.***

$$\tau = -mgd\sin\theta = I\frac{d^2\theta}{dt^2}$$

***Momento de la Cantidad de Movimiento o Momento Cinético.***

$$L = I\Omega$$

$$\Omega = d\theta/dt$$

$$\tau = dL/dt.$$

$$\frac{d^2\theta}{dt^2} = -\frac{mgd}{I}\sin\theta \approx -\frac{mgd}{I}\theta.$$

$$\omega = (mgd/I)^{1/2}$$

¡No confundir!

$$I = m\rho^2.$$

***Siendo*** $\rho$ ***el radio de giro.***

# ESTABILIDAD CAMINANDO XIX
# Caso a) Modelo 1

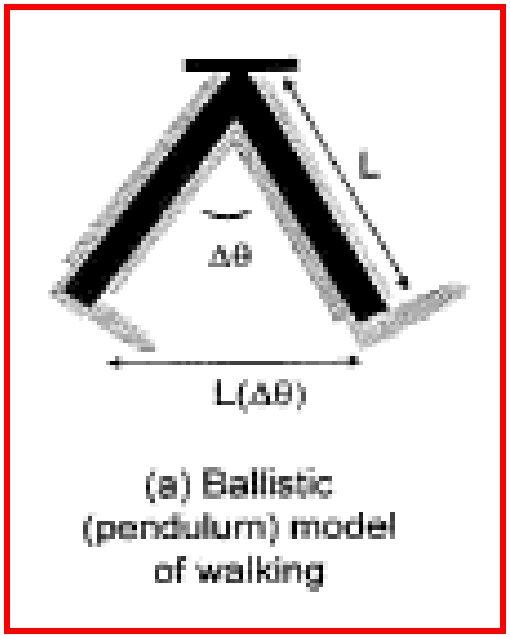


(a) Ballistic (pendulum) model of walking

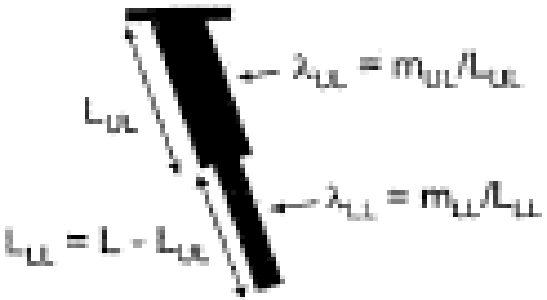


(b) Complex leg

**Fig. 3.24.** (a) Ballistic (pendulum) model of walking, with simple leg of uniform linear mass density, and with (b) complex leg with upper and lower legs with different linear mass densities

$$\omega = (g/L)^{1/2},$$

$$T_{\text{half period}} = \pi(L_{\text{leg}}/g)^{1/2}.$$

$$\omega = (g/L_{\text{leg}})^{1/2},$$

$$v = \frac{\omega}{\pi} L_{\text{leg}}(\Delta\theta).$$

# ESTABILIDAD CAMINANDO XX
# Caso a) Modelo 1

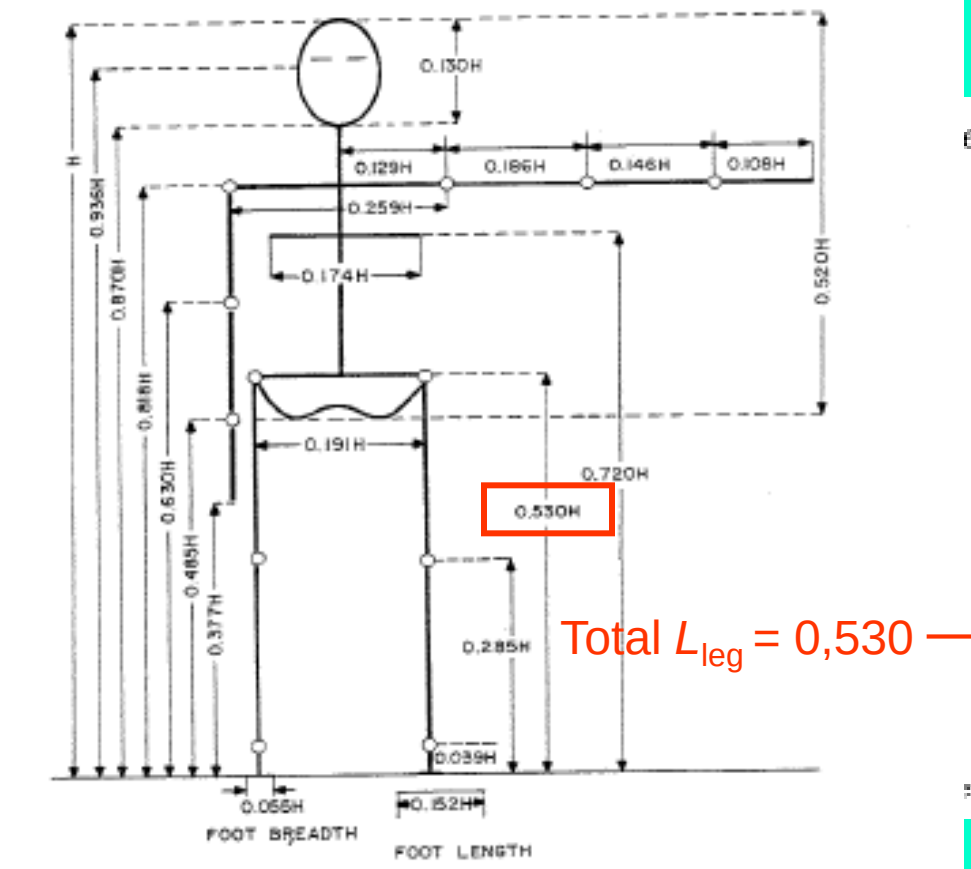


**Fig. 1.15.** Body segments length, relative to body height $H$. (From [38], as from [53]. Reprinted with permission of Wiley)

6. Body segment lengths. Also see Fig. 1.15. (Using data from [63])

| segment | segment length*/ body height $H$ |
|---|---|
| head height | 0.130 |
| neck height | 0.052 |
| shoulder width | 0.259 |
| upper arm | 0.186 |
| lower arm | 0.146 |
| hand | 0.108 |
| shoulder width | 0.259 |
| chest width | 0.174 |
| hip width/leg separation | 0.191 |
| upper leg (thigh) | 0.245 |
| lower leg (calf) | 0.246 |
| ankle to bottom of foot | 0.039 |
| foot breadth | 0.055 |
| foot length | 0.152 |

erwise specified.

Total $L_{leg}$ = 0,530 →

# ESTABILIDAD CAMINANDO XXI
## Caso a) Modelo 1

Sea una persona de $H = 1,8m$, luego su $L_{leg} = 0,53H = 0,95m$

$$T/2 = \pi \left( L_{leg} / g \right)^{1/2} \cong 3,14 \left( 0,95/9,8 \right)^{1/2} \cong 0,98s \approx 1,0s$$

**Pero en realidad**, si la persona camina lentamente a: $v = 0,5m/s$ con un paso de longitud: $l_p = 0,3m$, lo dará en:

$$T/2 = \left( v/l_p \right) = \left( 0,5/0,3 \right) = 0,6s$$

Y si acelera a: $v = 2,0m/s$, con un paso de longitud: $l_p = 0,7m$, lo dará en:

$$T/2 = \left( v/l_p \right) = \left( 2,0/0,7 \right) = 0,35s$$

Con lo que el Modelo 1 no es adecuado para la caminata.

# ESTABILIDAD CAMINANDO XXII
# Caso b) Modelo 2

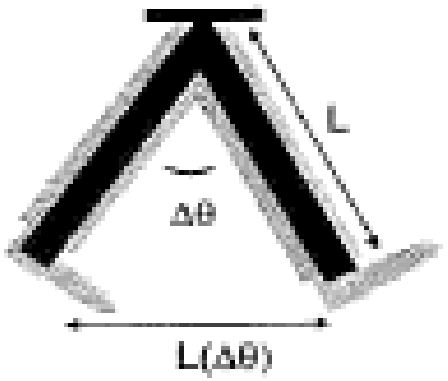


(a) Ballistic (pendulum) model of walking

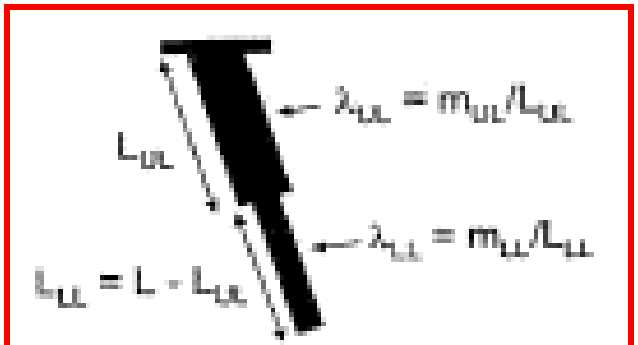


(b) Complex leg

**Fig. 3.24.** (a) Ballistic (pendulum) model of walking, with simple leg of uniform linear mass density, and with (b) con pierna como en (a) de densidad lineal λ constante.

$$I = \int \rho(\mathbf{r}) R^2 \mathrm{d}V = \int_0^{L_{\mathrm{leg}}} \lambda R^2 \mathrm{d}R = \frac{m_{\mathrm{leg}}}{L_{\mathrm{leg}}} \frac{L_{\mathrm{leg}}^3}{3} = \frac{1}{3} m_{\mathrm{leg}} L_{\mathrm{leg}}^2.$$

# ESTABILIDAD CAMINANDO XXIII
# Caso a) Modelo 2

Luego la velocidad angular será:

$$\omega = \left(mgd/I\right)^{1/2} = \left[\left(m_{leg} g L_{leg}/2\right)/\left(m_{leg} L^2_{leg}/3\right)\right]^{1/2} = \left(\frac{3}{2} g / L_{leg}\right)^{1/2}$$

Y el paso lo dará en:

$$T/2 = \pi\left(2L_{leg}/3g\right)^{1/2} = \left(2\times 0,95/3\times 9,80\right)^{1/2} \approx 0,81s$$

Luego, el Modelo 2 ajusta mejor que el Modelo 1, aunque se puede realizar otro refinamiento planteando el Modelo 3.

# ESTABILIDAD CAMINANDO XXIV
# Caso b) Modelo 3

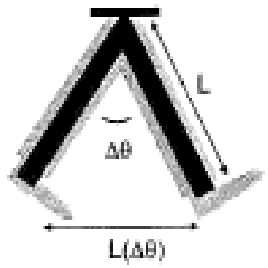


(a) Ballistic (pendulum) model of walking

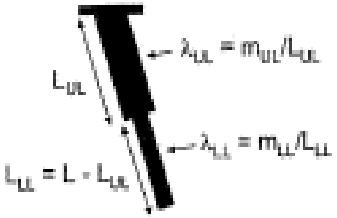


(b) Complex leg

**Fig. 3.24.** (a) Ballistic (pendulum) model of walking, with simple leg of uniform linear mass density, and with (b) complex leg with upper and lower legs with different linear mass densities

$$r_{CM} = \frac{m_1 r_1 + m_2 r_2}{m_1 + m_2},$$

**Table 1.7.** Masses and mass densities of body segments. (Using data from [63])

| segment | segment mass/ total body mass $m_b$ | mass density ($g/cm^3$) |
|---|---|---|
| hand | 0.006 | 1.16 |
| forearm | 0.016 | 1.13 |
| upper arm | 0.028 | 1.07 |
| forearm and hand | 0.022 | 1.14 |
| total arm | 0.050 | 1.11 |
| foot | 0.0145 | 1.10 |
| lower leg (calf) | 0.0465 | 1.09 |
| upper leg (thigh) | 0.100 | 1.05 |
| foot and lower leg | 0.061 | 1.09 |
| total leg | 0.161 | 1.06 |
| head and neck | 0.081 | 1.11 |
| trunk | 0.497 | 1.03 |

$$d = \frac{m_{u,leg}(L_{u,leg}/2) + m_{l,leg}(L_{u,leg} + L_{l,leg}/2)}{m_{u,leg} + m_{l,leg}}$$
$$= \frac{(0.621 m_{leg})(0.231 L_{leg}) + (0.379 m_{leg})(0.731 L_{leg})}{m_{leg}} = 0.421 L_{leg}.$$

# ESTABILIDAD CAMINANDO XXV
# Caso b) Modelo 3

$$I = \int_0^{L_{u,leg}} \lambda_{u,leg} R^2 dR + \int_{L_{u,leg}}^{L_{leg}} \lambda_{L,leg} R^2 dR = \frac{1}{3}\lambda_{u,leg} L_{u,leg}^3 + \frac{1}{3}\lambda_{L,leg}(L_{leg}^3 - L_{u,leg}^3),$$

Table 1.7. Masses and mass densities of body segments. (Using data from [63])

| segment | segment mass/ total body mass $m_b$ | mass density ($g/cm^3$) |
|---|---|---|
| hand | 0.006 | 1.16 |
| forearm | 0.016 | 1.13 |
| upper arm | 0.028 | 1.07 |
| forearm and hand | 0.022 | 1.14 |
| total arm | 0.050 | 1.11 |
| foot | 0.0145 | 1.10 |
| lower leg (calf) | 0.0465 | 1.09 |
| upper leg (thigh) | 0.100 | 1.05 |
| foot and lower leg | 0.061 | 1.09 |
| total leg | 0.161 | 1.06 |
| head and neck | 0.081 | 1.11 |
| trunk | 0.497 | 1.03 |

(2005)

(¿Cómo se hace un promedio?)

# ESTABILIDAD CAMINANDO XXVI
# Caso b) Modelo 3

## Algunos detalles de cálculo I

En el cálculo de la posición del centro de masas, *d*:

$$d = \frac{m_{u,leg}(L_{u,leg}/2) + m_{l,leg}(L_{u,leg} + L_{l,leg}/2)}{m_{u,leg} + m_{l,leg}}$$
$$= \frac{(0.621 m_{leg})(0.231 L_{leg}) + (0.379 m_{leg})(0.731 L_{leg})}{m_{leg}} = 0.421 L_{leg}.$$

Se hace, por ejemplo:

$$m_{uleg} = 0,100 m_b = 0,100\left(m_{leg}/0,161\right) = 0,621 m_{leg}$$

$$L_{uleg} = 0,245H = 0,245 L_{leg}/2 \times 0,530 = 0,231 L_{leg}$$

$$m_{lleg} = 0,061 m_b = 0,061\left(m_{leg}/0,161\right) = 0,379 m_{leg}$$

$$L_{lleg} = 0,285H = 0,538 L_{leg}$$

$$L_{uleg} + \left(L_{lleg}/2\right) = 0,462 L_{leg} + 0,269 L_{leg} = 0,731 L_{leg}$$

# ESTABILIDAD CAMINANDO XXVII
## Caso b) Modelo 3
### Algunos detalles de cálculo II

En el cálculo del momento de inercia, $I$:

$$I = \int_0^{L_{u,leg}} \lambda_{u,leg} R^2 dR + \int_{L_{u,leg}}^{L_{leg}} \lambda_{L,leg} R^2 dR = \frac{1}{3}\lambda_{u,leg} L_{u,leg}^3 + \frac{1}{3}\lambda_{L,leg}(L_{leg}^3 - L_{u,leg}^3),$$

Se hace:

$$I = \frac{1}{3}\lambda_{uleg} L^3_{uleg} + \frac{1}{3}\lambda_{leg}\left(L^3_{leg} - L^3_{uleg}\right) = 0,256 m_{leg} L^3_{leg}$$

Con lo que:

$$T/2 = 0,76s$$

# ESTABILIDAD CAMINANDO XXVIII
# Péndulo invertido. Modelo 4

v ≡ Velocidad lineal
≡ Velocidad tangencial

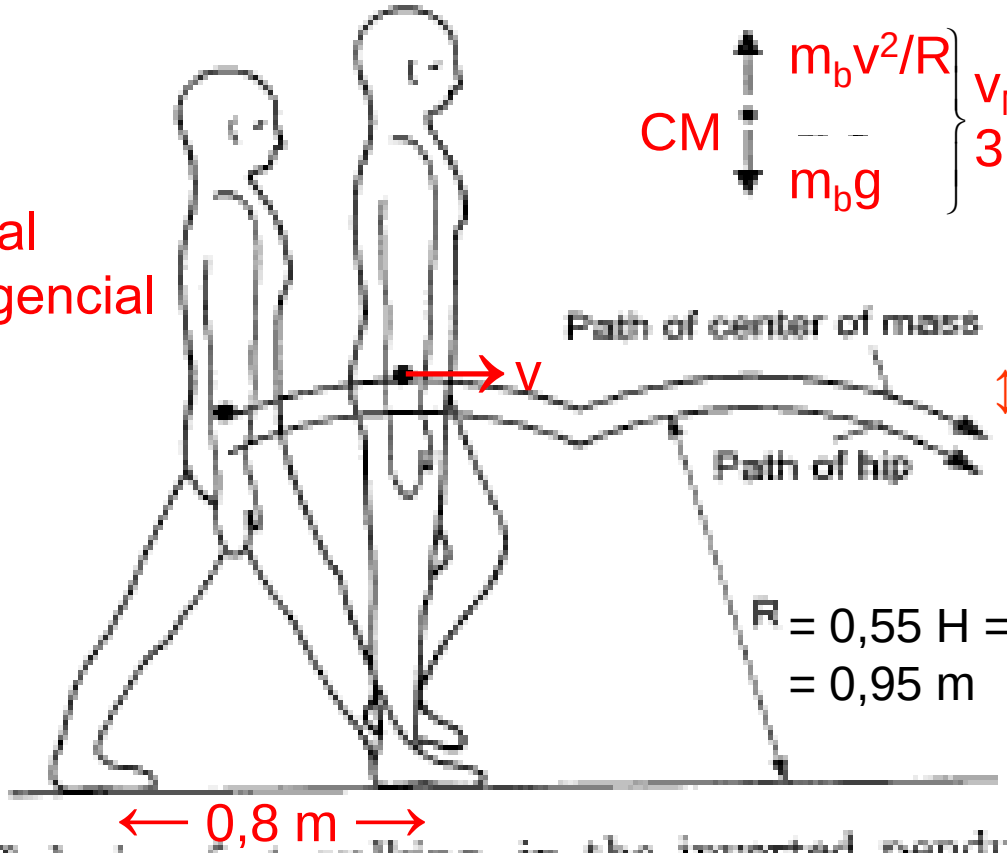


**Fig. 3.26.** Takeoff during fast walking, in the inverted pendulum model. (From [99]. Copyright 1992 Columbia University Press. Reprinted with the permission of the press)

El Modelo 4 responde muy bien a pesar de su tremenda simplicidad

# ESTABILIDAD CAMINANDO XXIV

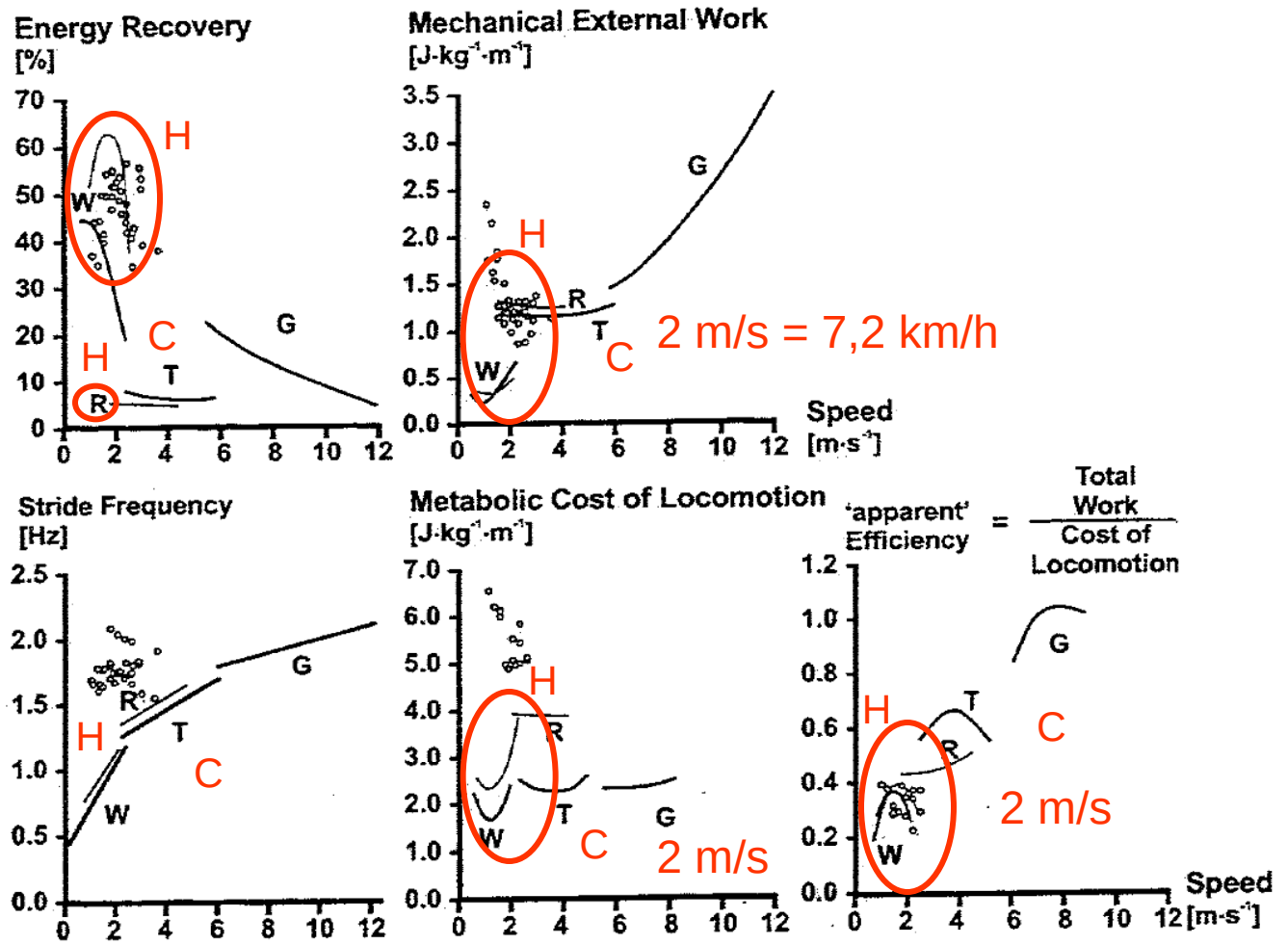


**Fig. 3.25.** Gait parameters as a function of speed for humans (*thin curves*) and horses (*thick curves*), for different gaits: walking (W), running (R), trotting (T), galloping (G), and human skipping (*open circles*). (From [151]. Used with permission. Also see [123])

# ESTABILIDAD CAMINANDO XXV

**Table 3.6.** Comparison of motion in bipeds and quadrupeds

| biped type | foot sequence[a] | features |
|---|---|---|
| walk | R, L, R, L, etc. | no flight phase |
| run | R, flight, L, flight, etc. | |
| skip | | |
| right unilateral skipping | L, R, flight; L, R, flight; etc. | left unilateral is R, L, flight, etc. |
| bilateral skipping | L, R, flight; R, L, flight; etc. | |
| **quadruped type (biped analog)** | **foot sequence[b]** | **features** |
| walk (walk) | FL, HR, FR, HL | stride: up to 3 hooves on ground |
| trot (run) | two running bipeds w/50% phase lag | rack is trot with 0% phase lag |
| gallop (none) | | |
| slow gallop or canter | HL, HR, FL simul.; FR flight | right cantor; left switches R and L |
| transverse gallop (fast run) | HL, HR flight; FL, FR flight | right transverse |
| rotary gallop (fast run) | HL, HR flight; FR, FL flight | clockwise or counterclockwise |

[a] R right foot, L left foot.
[b] FL: fore left, HR: hind right, FR: fore right, HL: hind left. (From [151].)

Delantero Trasero

# ESTABILIDAD CORRIENDO I

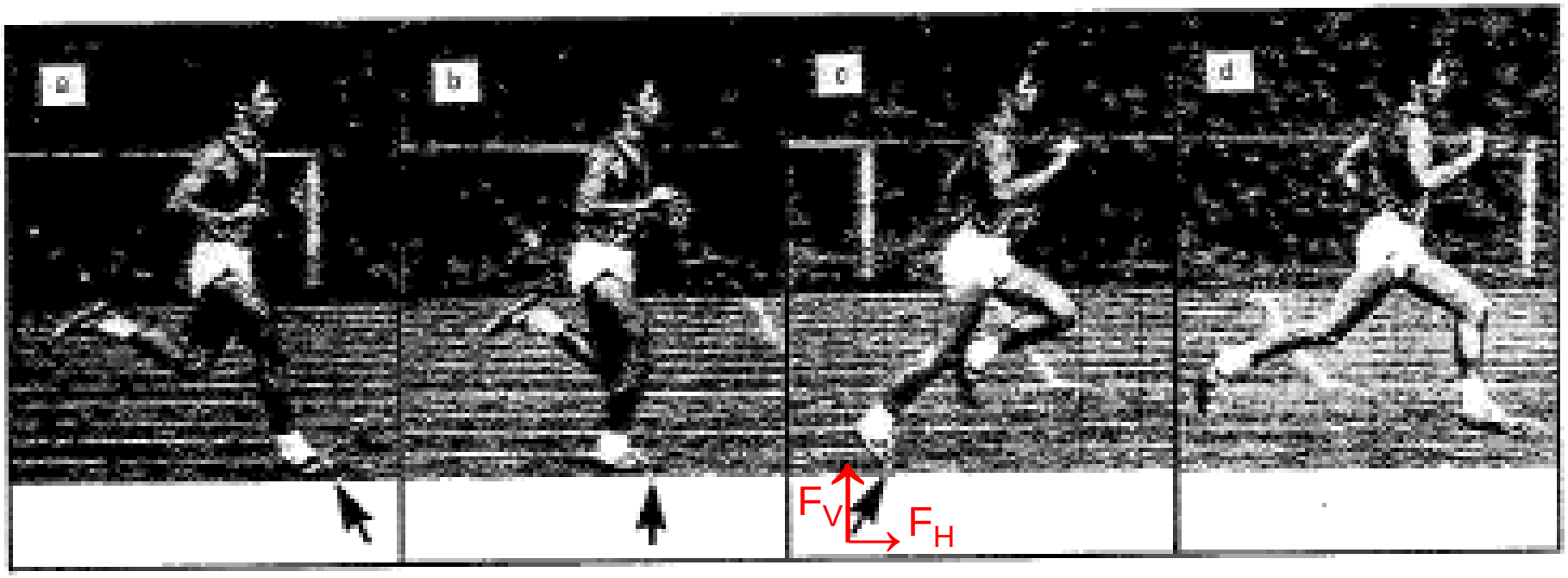


**Fig. 3.27.** Stages of a running stride, with the arrows indicating the directions of the forces on the feet. (From [99]. Copyright 1992 Columbia University Press. Reprinted with the permission of the press)

# ESTABILIDAD CORRIENDO II

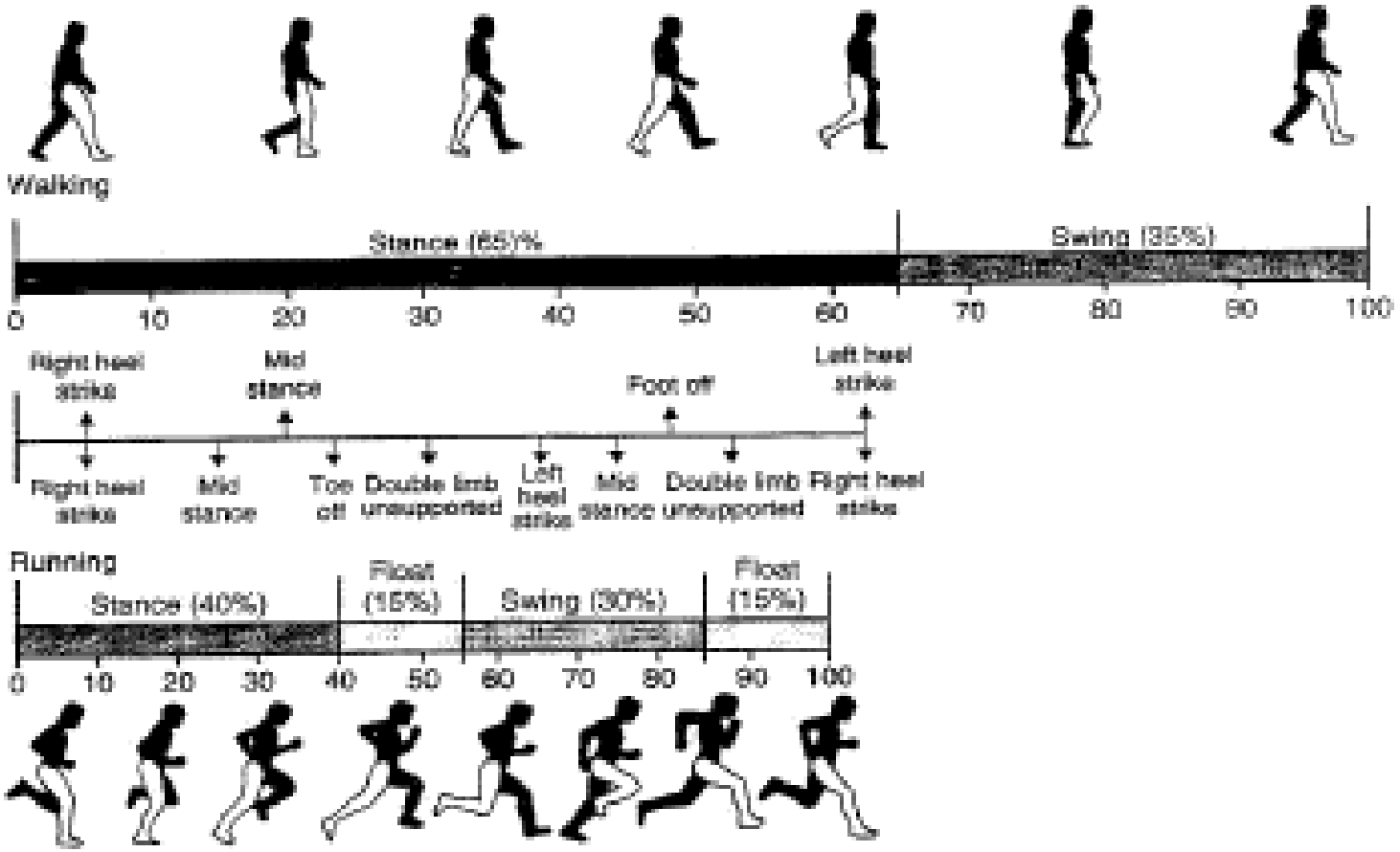


**Fig. 3.9.** Walking and running gait sequences. For walking, from foot strike (or heel strike) to toe off (or foot off) is the stance phase, with subdivisions sometimes called: foot flat or loading, midstance, terminal stance, and then preswing. From toe off to foot strike is the swing phase, with subdivisions called: initial swing, midswing, and then terminal swing. (From [166]. Used with permission)

# ESTABILIDAD CORRIENDO IV

**Table 3.5.** Maximum thigh, knee, and ankles angles (in degrees) for running at different speeds and grades on a treadmill. (Using data from [150])

| | level | | | ramp | | |
|---|---|---|---|---|---|---|
| speed (m/s) | 3.4 | 4.2 | 5.0 | 3.4 | 3.4 | 3.4 |
| grade | 0% | 0% | 0% | −20% | 0% | 20% |
| *thigh* | | | | | | |
| flexion | 39.0 | 41.0 | 46.6 | 25.8 | 39.0 | 54.5 |
| extension | −20.6 | −23.1 | −28.0 | −18.4 | −20.6 | −18.7 |
| *knee* | | | | | | |
| extension before footstrike | 13.4 | 16.7 | 15.5 | 4.0 | 13.4 | 37.7 |
| cushioning flexion | 40.6 | 39.4 | 42.9 | 41.2 | 40.6 | 46.3 |
| propulsion phase extension | 15.1 | 16.8 | 14.2 | 32.1 | 15.1 | 13.0 |
| swing phase flexion | 103.9 | 108.1 | 117.3 | 99.6 | 103.9 | 113.2 |
| *ankle* | | | | | | |
| dorsiflexion before footstrike | 91.3 | 91.8 | 92.5 | – | 91.3 | 97.6 |
| stance phase dorsiflexion | 112.4 | 108.7 | 110.8 | 103.5 | 112.4 | 116.4 |
| plantar flexion | 64.2 | 58.7 | 57.1 | 76.4 | 64.2 | 59.4 |

# ESTABILIDAD CORRIENDO V

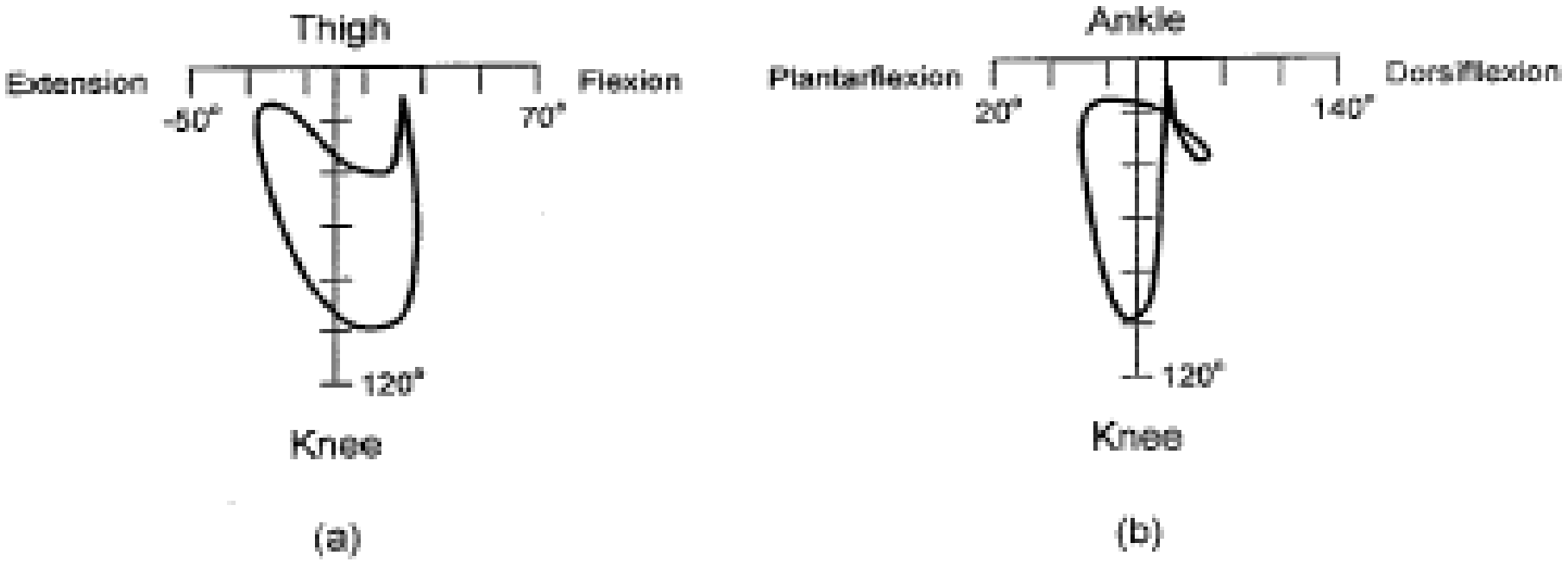


**Fig. 3.28.** Mean locus of (a) thigh angle vs. knee angle and (b) ankle angle vs. knee angle during running at 3.57 m/s, using joint angles as defined in Fig. 3.1 (Based on [150] and [175])

# ESTABILIDAD CORRIENDO VI

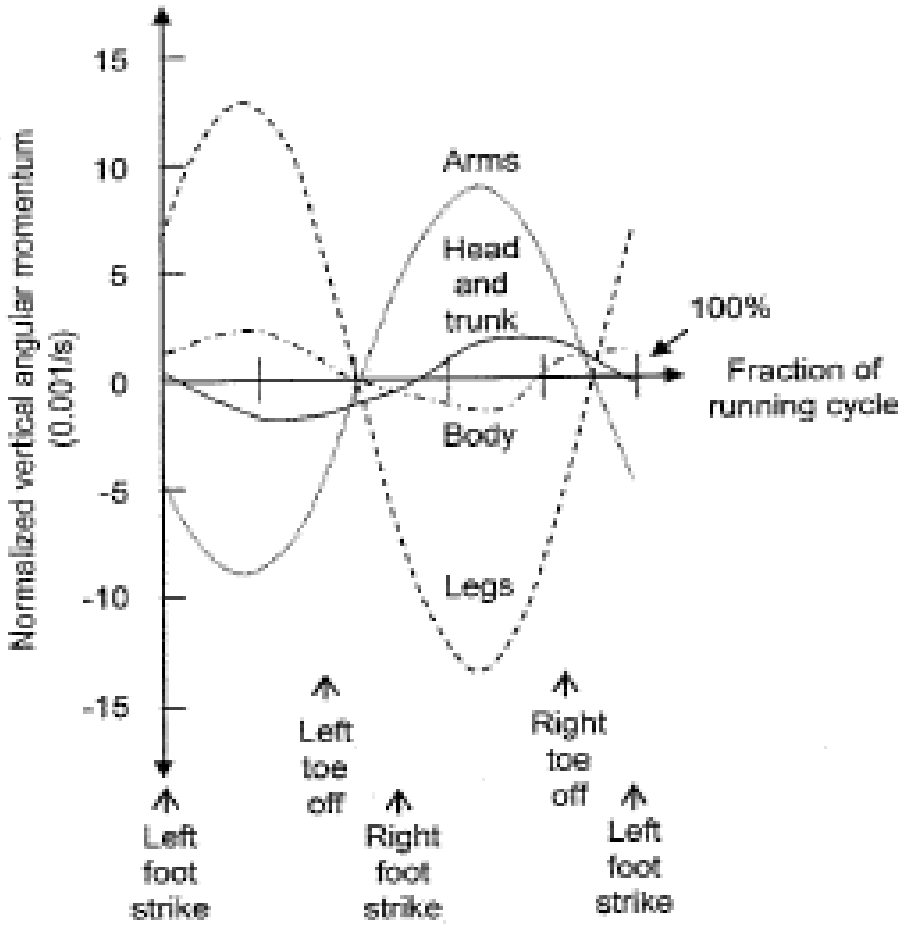


**Fig. 3.29.** Normalized mean vertical angular momenta of the arms, head-plus-trunk, legs, and whole body during a running cycle, at 4.5 m/s. The normalized vertical angular momentum is obtained by dividing the vertical angular momentum (in kg-$m^2$/s) by body mass (in kg) and the square of the runner's standing height (height in m). (Based on [128] and [129])

# ESTABILIDAD CORRIENDO VII

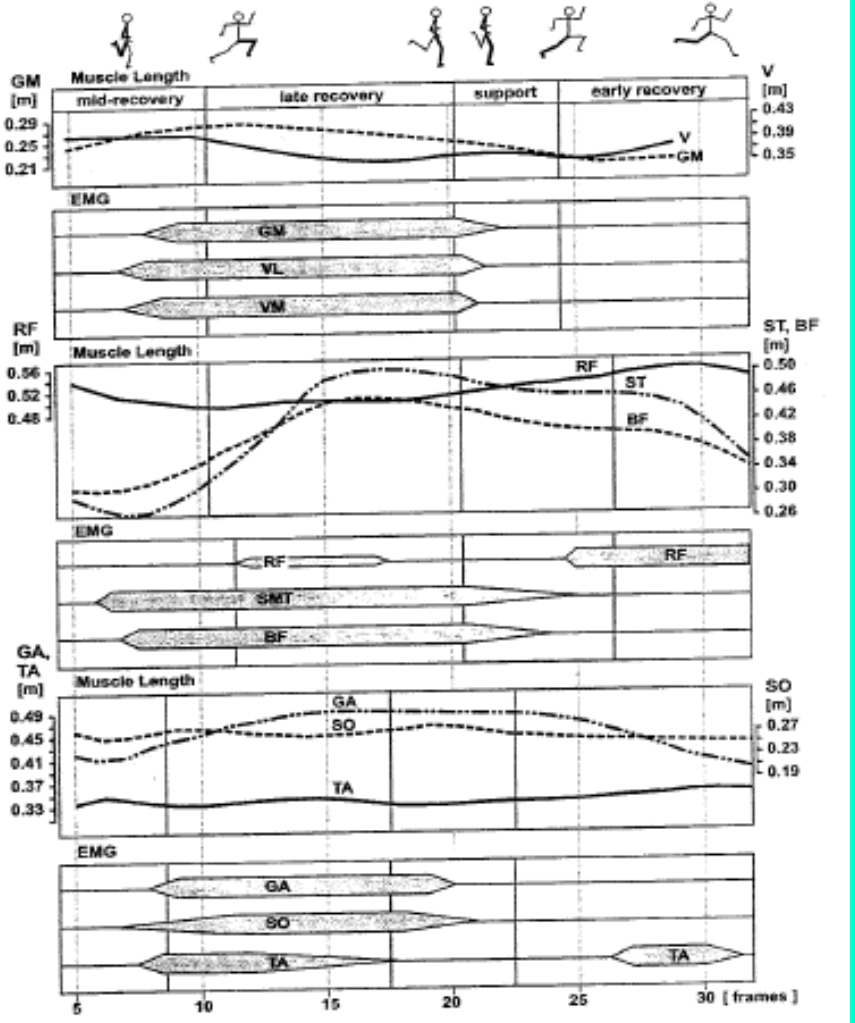


**Fig. 3.30.** Muscle length and electromyographic (EMG) activity vs. time during one running cycle of the right leg, for the gluteus maximus (GM), vastus lateralis (VL), biceps femoris (BF), vastus medialis (VM), combined VL and VM (V), rectus femoris (RF), semitendinosus (ST), combined semimembranosus (SM) and ST (SMT), gastrocnemius (GA), soleus (SO), and tibialis anterior (TA). (From [126]. Used with permission). Also see [145] (1990) (2000)

# ESTABILIDAD CORRIENDO VIII

$$\mathrm{KE_H}(t = \text{stage b}) < \mathrm{KE_H}(t = \text{stage d}),$$

$$\mathrm{PE}(t = \text{stage b}) < \mathrm{PE}(t = \text{stage d})$$

$$\mathrm{KE_H}(t = \text{stage b}) + \mathrm{PE}(t = \text{stage b}) \ll \mathrm{KE_H}(t = \text{stage d}) + \mathrm{PE}(t = \text{stage d}).$$

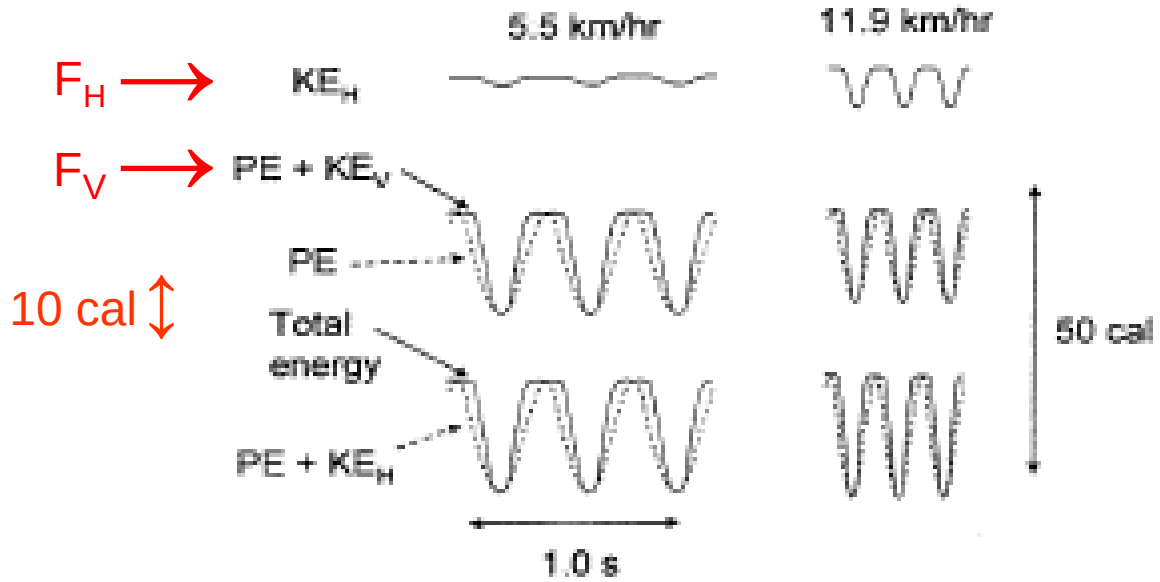


**Fig. 3.31.** Changes in mechanical energy during running at two different speeds from force plates, for (from top to bottom curve) horizontal kinetic energy; gravitational potential energy plus vertical kinetic energy and gravitational potential energy; and total energy and gravitational potential energy plus horizontal kinetic energy. (Based on [112] and [146])

# ESTABILIDAD CORRIENDO IX

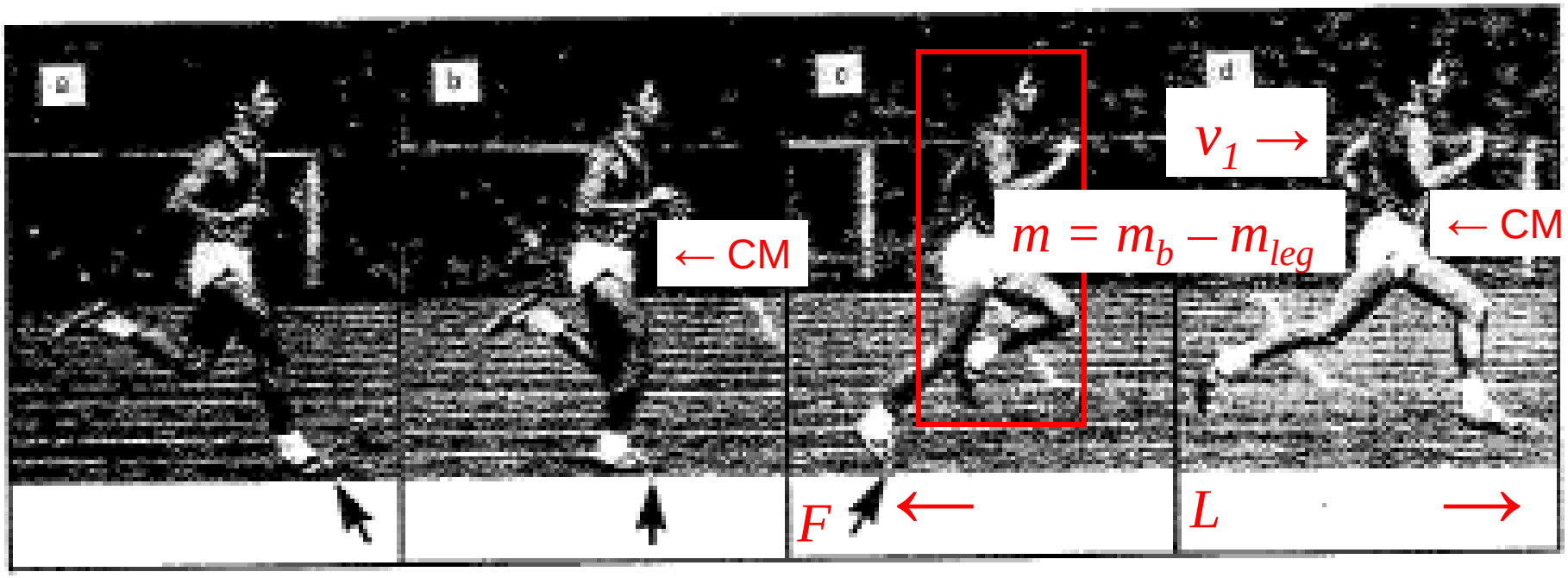


**Fig. 3.27.** Stages of a running stride, with the arrows indicating the directions of the forces on the feet. (From [99]. Copyright 1992 Columbia University Press. Reprinted with the permission of the press)

$$F \times L = \frac{1}{2}\left(m_b - m_{leg}\right)v_1^2$$

Trabajo

$$v_1^2 = \frac{2 \times F \times L}{m_b - m_{leg}}$$

Energía cinética

# ESTABILIDAD CORRIENDO X

El primer paso puede ser el de la salida de la lanzadera, el siguiente paso se realiza con el mismo trabajo que el primero y la parte alta del cuerpo acelera de $v_1$ a $v_2$, mientras que la pierna que estaba en reposo ($v = 0$) acelera hasta $v_2$, quedando:

$$F \times L = \frac{1}{2}\left(m_b - 2m_{leg}\right)\left(v_2^2 - v_1^2\right) + \frac{1}{2} m_{leg} v_2^2 =$$

$$= \frac{1}{2}\left(m_b - m_{leg}\right)v_2^2 - \frac{1}{2}\left(m_b - 2m_{leg}\right)v_1^2$$

con lo que:

$$v_2^2 = \frac{1}{m_b - m_{leg}}\left[2 \times F \times L + \left(m_b - 2m_{leg}\right)v_1^2\right]$$

y reemplazando $v_1$ del cálculo inicial, queda:

$$v_2^2 = \frac{2 \times F \times L}{m_b - m_{leg}}\left(1 + \frac{m_b - 2m_{leg}}{m_b - m_{leg}}\right)$$

# ESTABILIDAD CORRIENDO XI

Y después de $n$ pasos, resulta:

$$v_n^2 = \frac{2 \times F \times L}{m_b - m_{leg}} \left[ 1 + \frac{m_b - 2m_{leg}}{m_b - m_{leg}} + \left( \frac{m_b - 2m_{leg}}{m_b - m_{leg}} \right)^2 + \ldots + \left( \frac{m_b - 2m_{leg}}{m_b - m_{leg}} \right)^n \right]$$

cuyo corchete es una serie geométrica; reemplazando por su suma, queda:

$$v_n^2 = \frac{2 \times F \times L}{m_b - m_{leg}} \frac{\left[ 1 - \left( \frac{m_b - 2m_{leg}}{m_b - m_{leg}} \right)^n \right]}{\left[ 1 - \left( \frac{m_b - 2m_{leg}}{m_b - m_{leg}} \right) \right]} = \frac{2 \times F \times L}{m_{leg}} \left[ 1 - \left( \frac{m_b - 2m_{leg}}{m_b - m_{leg}} \right)^n \right]$$

Considerando un corredor de:

$$m_b = 70kg \quad \text{y} \quad m_{leg} = 0,161 \times m_b = 0,161 \times 70kg = 11,27kg$$

el corchete resulta:

$$\left( \frac{m_b - 2m_{leg}}{m_b - m_{leg}} \right)^n \approx 0,81^n$$

# ESTABILIDAD CORRIENDO XII

Y en el límite:

$\lim_{n\to\infty} 0,81^n \to 0$ , queda: $v_{final\infty} = \sqrt{\frac{2\times F\times L}{m_{leg}}}$

Luego, para el mismo corredor con:

$$L = 1m \quad \text{y} \quad F = 560N$$

resulta:

$$v_{final(\infty)} \cong 10,0\,\frac{m}{s}$$

Y para 32 pasos, $n$ = 32, resulta:

$$v_{final(32)} = 9,96\,\frac{m}{s}$$

# ESTABILIDAD CORRIENDO XIII

Jessie Owen (1936)

10,2 s ⟶ v = 9,80 m/s

Usain Bolt (2009)

9,69 s ⟶ v = 10,32m/s

**Table 6.34.** World record running speeds. (As of 2006)

| distance (m) | average running speed (m/s) |
|---|---|
| 100 | 10.22 |
| 200 | 10.35 |
| 400 | 9.26 |
| 1,500 | 7.28 |
| 10,000 | 6.32 |
| 42,200[a] | 6.12 |
| 100,000 | 4.46 |

[a] Marathon, 26 miles, 385 yd

# ESTABILIDAD CORRIENDO XIV

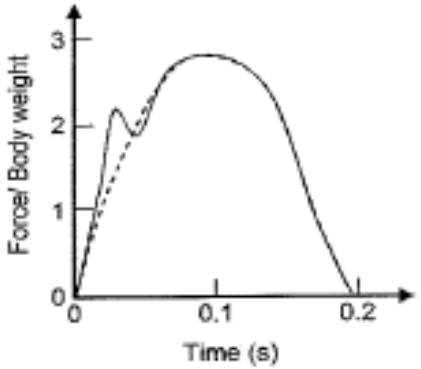


**Fig. 3.32.** Vertical force exerted on the ground during a running stride (*solid line*, with *dashed line* approximation). This was calculated from force plates and was averaged for five-runners running at 4.5 m/s. (Based on [99])

15,2 km/h

Usain Bolt

37,15 km/h

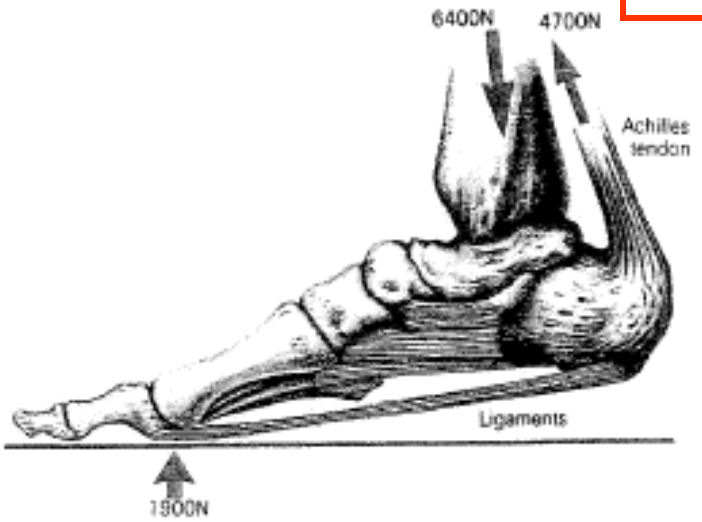


**Fig. 3.33.** Peak forces on foot during running stride. (From [99]. Copyright 1992 Columbia University Press. Reprinted with the permission of the press)

2520 N

Carrera con paso largo

# ESTABILIDAD CORRIENDO XVII

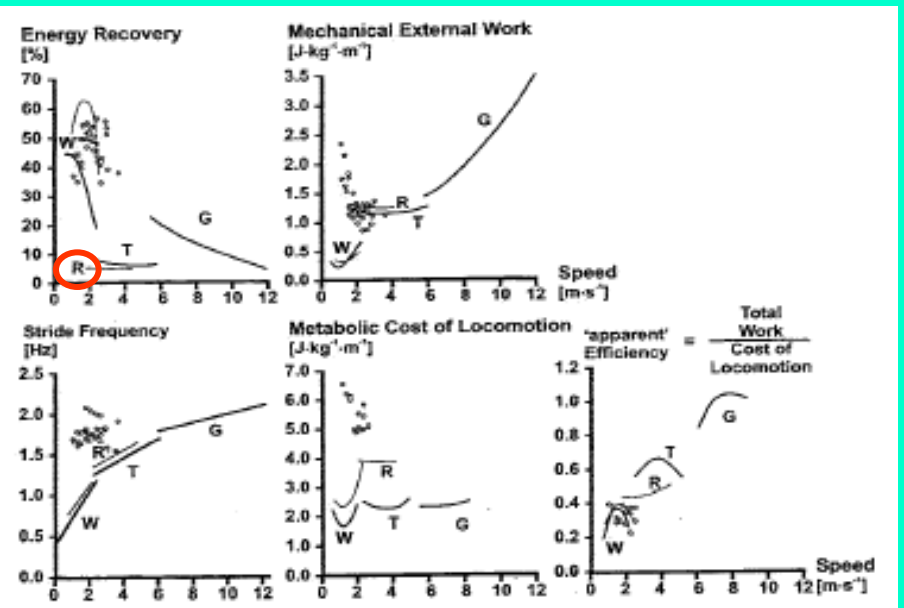


Fig. 3.25. Gait parameters as a function of speed for humans (*thin curves*) and horses (*thick curves*), for different gaits: walking (W), running (R), trotting (T), galloping (G), and human skipping (*open circles*). (From [151]. Used with permission. Also see [123])

Table 3.8. Energy return from elastic sports equipment. (Using data from [171])

| equipment | $k$ (1,000 N/m) | $\Delta x_{max}$ (cm) | $KE_{max}$ (J) | $H_{max}$ (cm) |
|---|---|---|---|---|
| trampoline | 5 | 80 | 1,600 | 230 |
| tumbling floor | 50 | 10 | 250 | 36 |
| gymnastic floor | 120 | 5 | 150 | 22 |
| running track | 240 | 1 | 12 | 2 |
| gymnasium floor | 400 | 0.5 | 5 | 1 |

$\Delta x_{max}$ and $KE_{max}$ are the maximum deformation and stored energy ($KE_{max} = k\Delta x_{max}^2/2$) and $H_{max}$ is the maximum height of a $m_b = 70$ kg person with this energy, $H_{max} = KE_{max}/m_b g$.

# ESTABILIDAD CORRIENDO XVIII

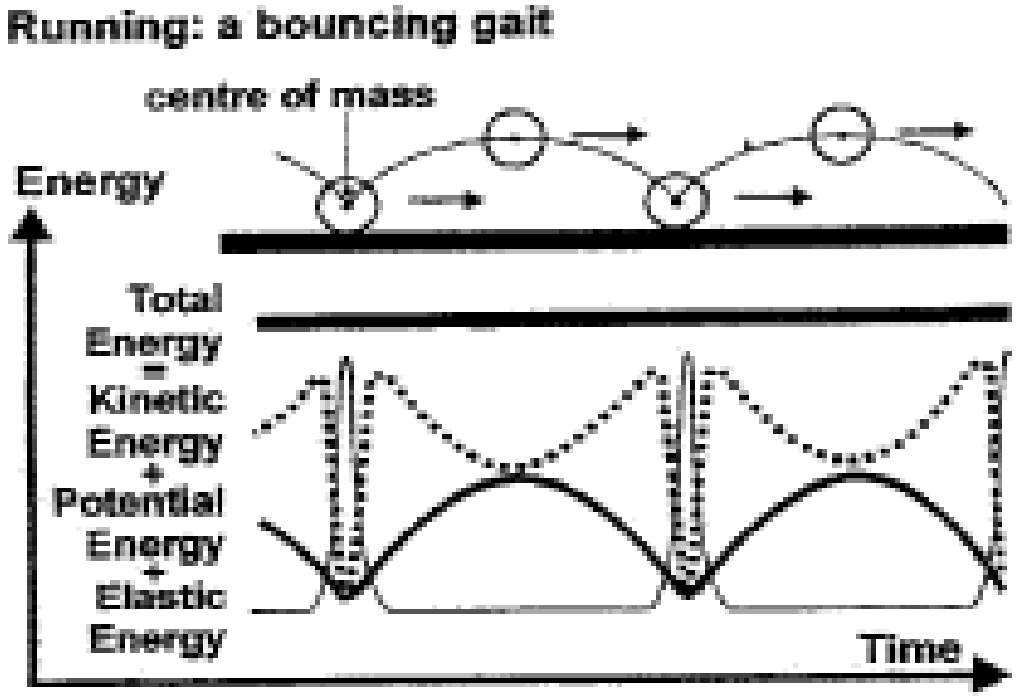


Fig. 3.34. Bouncing ball model of running, showing that the sum of the ball kinetic energy (*dotted line*), gravitational potential energy (*thick line*), and elastic potential energy (*thin line*) is constant (*very thick line*) during bounces. (From [151]. Used with permission)

# Fluctuaciones en la caminata

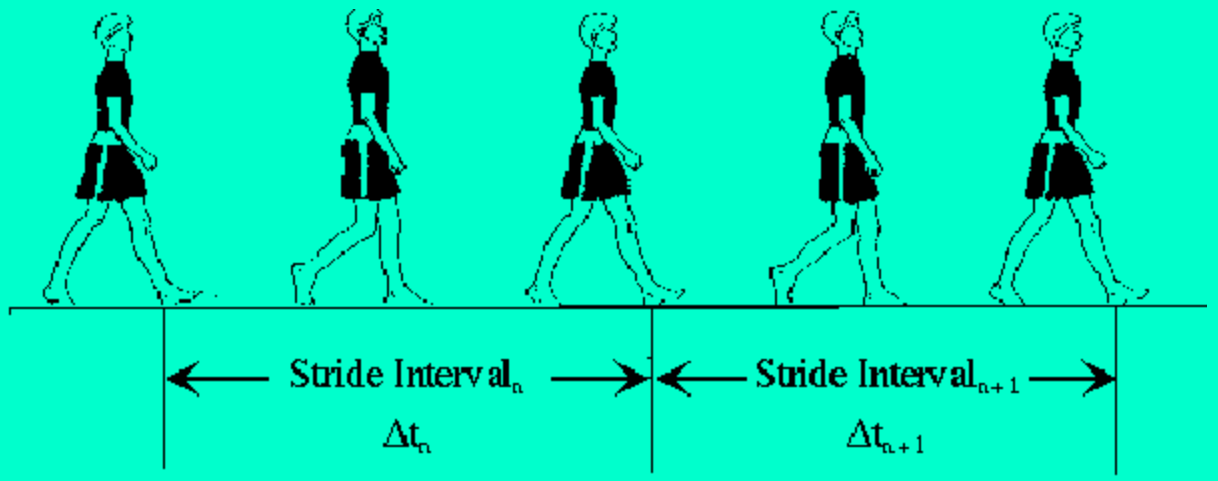


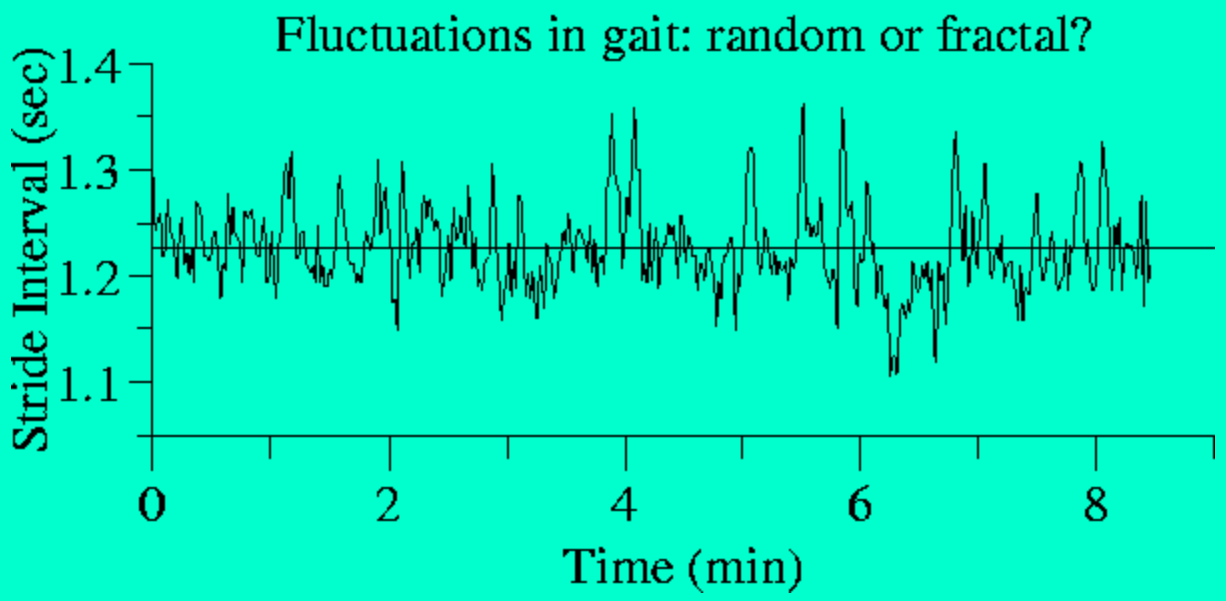

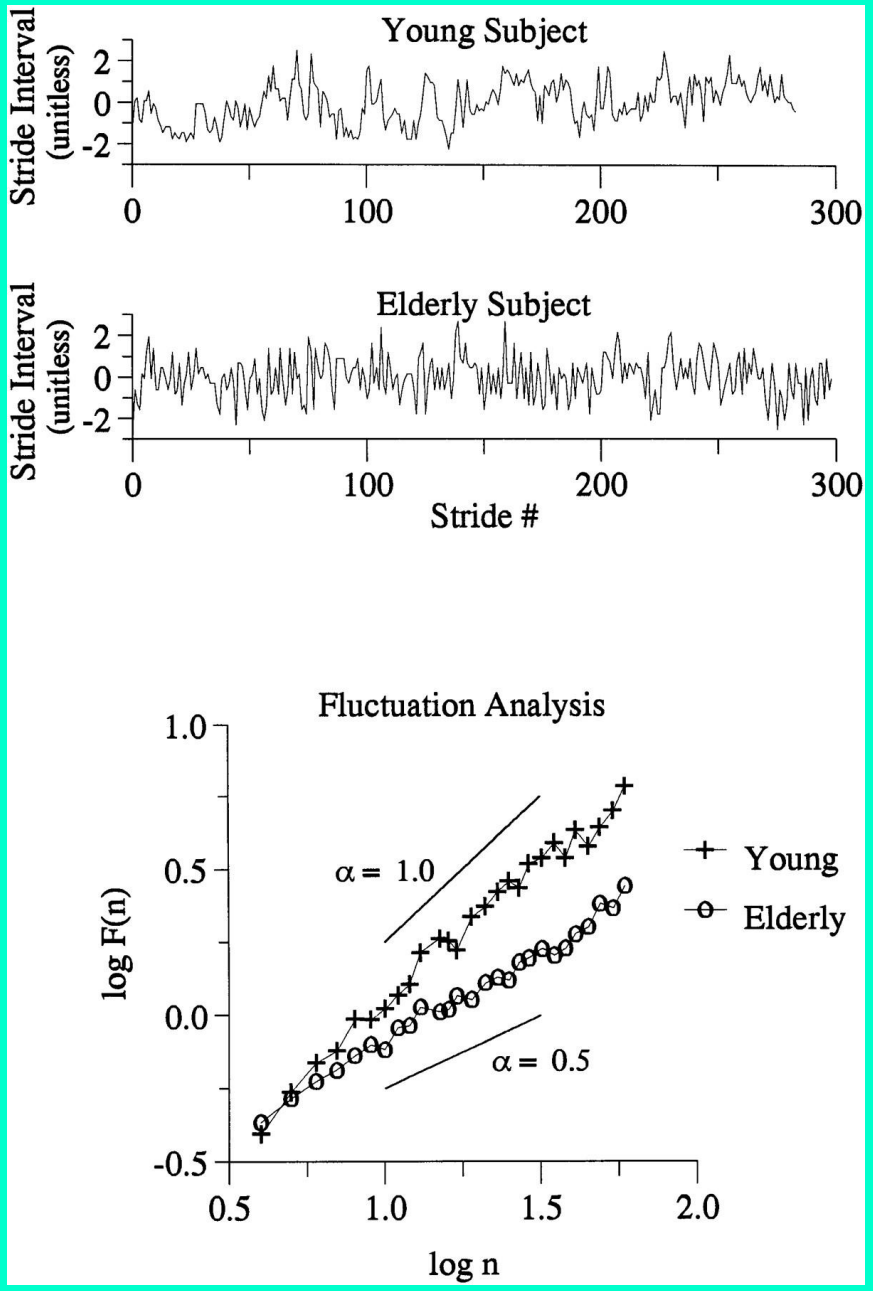
Young Subject
Stride Interval (unitless)
2
0
-2
0
100
200
300
Elderly Subject
Stride Interval (unitless)
2
0
-2
0
100
200
300
Stride #
Fluctuation Analysis
1.0
0.5
0.0
-0.5
log F(n)
α = 1.0
α = 0.5
Young
Elderly
0.5
1.0
1.5
2.0
log n

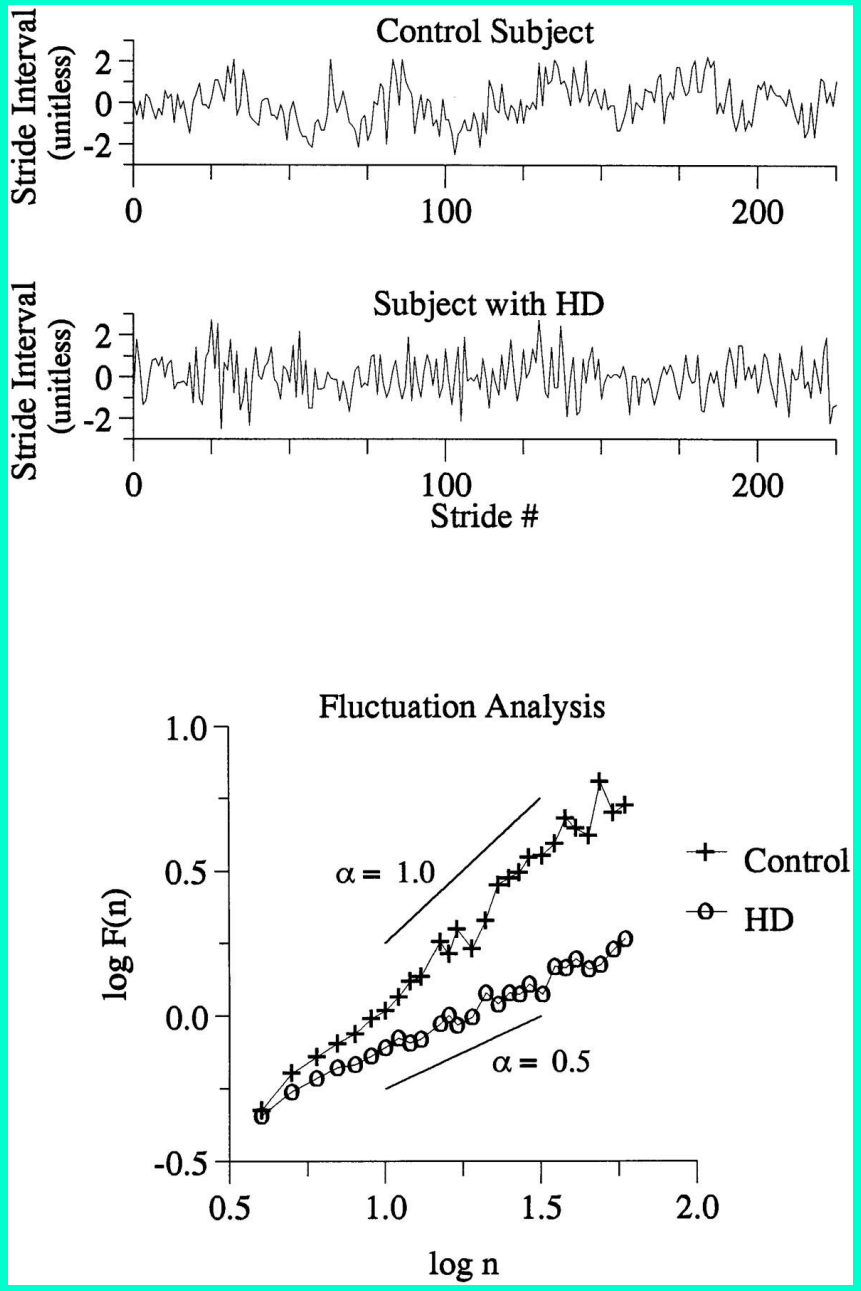
Control Subject
Stride Interval (unitless)
2
0
-2
0
100
200
Subject with HD
Stride Interval (unitless)
2
0
-2
0
100
200
Stride #
Fluctuation Analysis
1.0
0.5
0.0
-0.5
log F(n)
α = 1.0
α = 0.5
Control
HD
0.5
1.0
1.5
2.0
log n

# ESTABILIDAD SALTANDO I

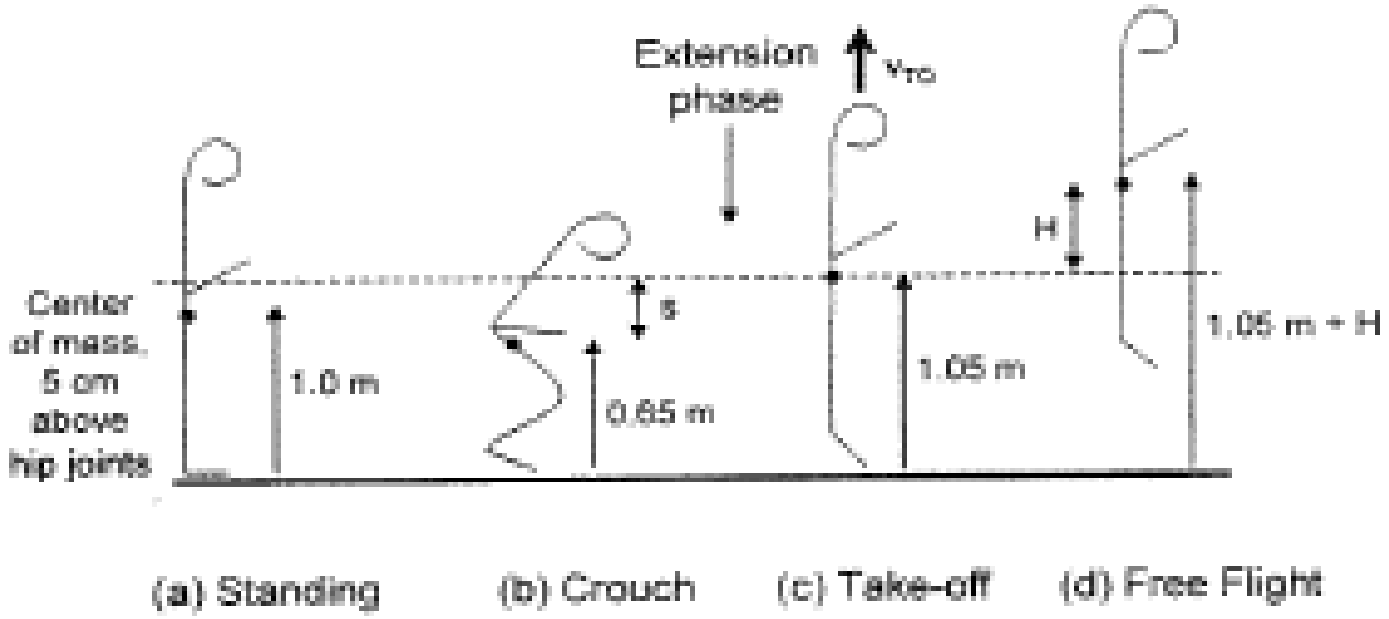


**Fig. 3.36.** Stick diagram of a vertical jump, including initial standing in (a), crouching in (b) and then extension to take-off in (c) and free flight in (d). (Based on [161])

# ESTABILIDAD SALTANDO II

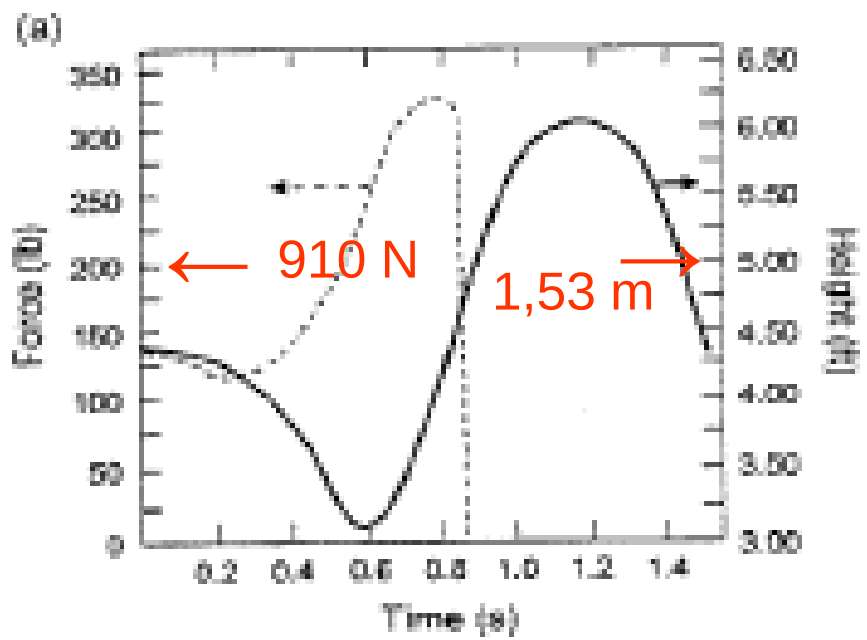


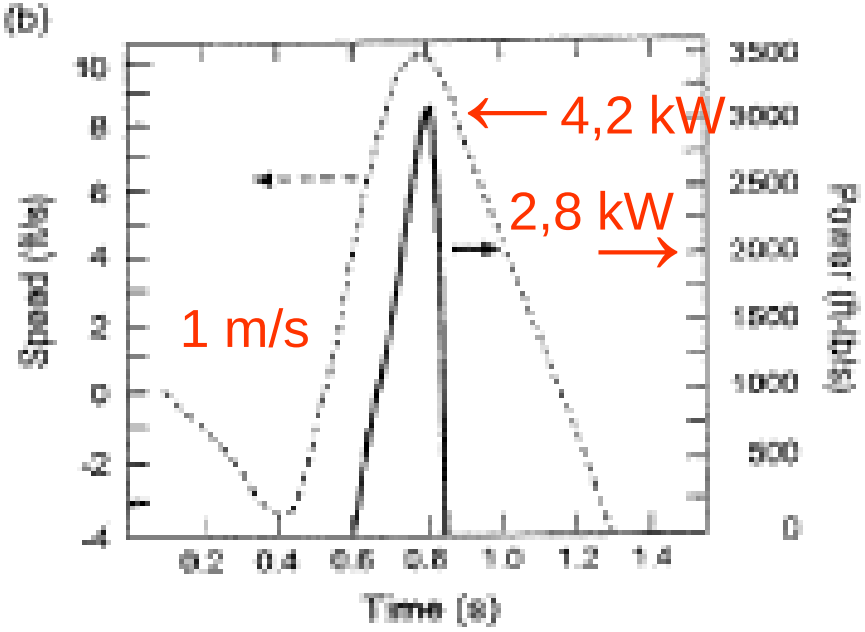


**Fig. 3.37.** Kinematic and dynamic data during a vertical jump, including (a) reaction force from the ground (left scale) and height of the center of mass (right scale), and (b) vertical speed of the center of mass (left scale) and applied power (right scale, this power is the product of the force in (a) and speed in (b)). (Based on [161])

$$\frac{1}{2}m_b v_{TO}^2 + m_b g(1.05\,\mathrm{m}) = 0 + m_b g(1.05\,\mathrm{m} + H)$$

$$\frac{1}{2}m_b v_{TO}^2 = m_b g H, \qquad \int_0^s F_V(t)\,dz = \frac{1}{2}m_b v_{TO}^2 = m_b g H$$

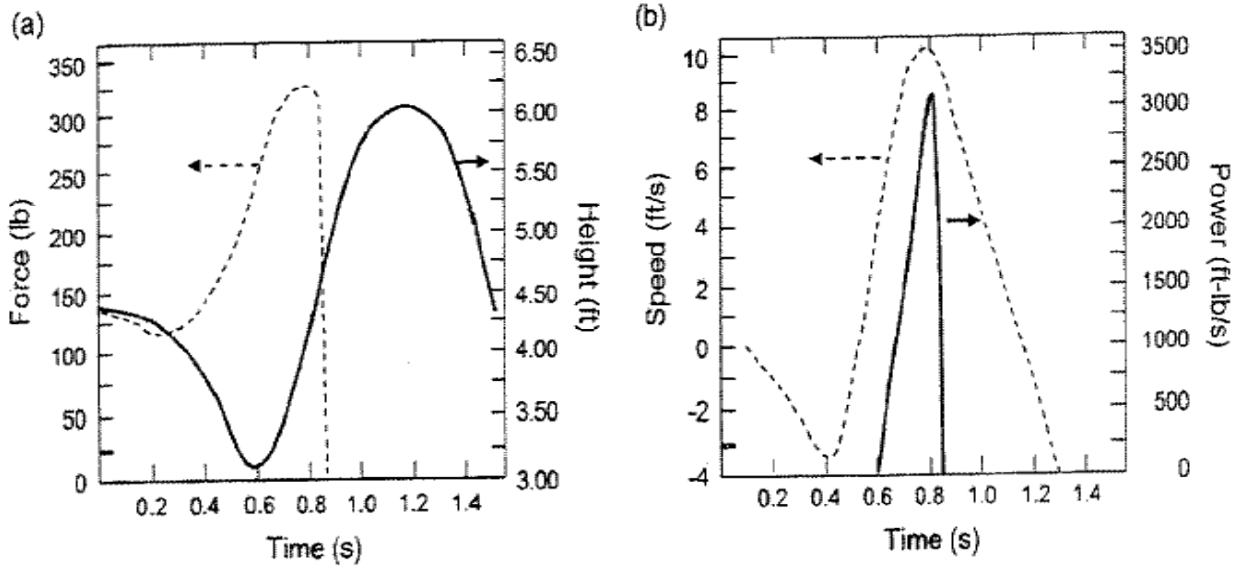


**Fig. 3.37.** Kinematic and dynamic data during a vertical jump, including (a) reaction force from the ground (left scale) and height of the center of mass (right scale), and (b) vertical speed of the center of mass (left scale) and applied power (right scale, this power is the product of the force in (a) and speed in (b)). (Based on [161])

$$H = \frac{\int_0^s F_V(t)\,dx}{m_b g} = \frac{(N(t) - m_b g)s}{m_b g}$$

$$= \frac{(300\,\text{lb} - 140\,\text{lb})1.4\,\text{ft}}{140\,\text{lb}} = 1.6\,\text{ft}\,(0.49\,\text{m}).$$

$$v_{TO} = \frac{2s}{\tau},$$

$$H = \frac{v_{TO}^2}{2g} = \frac{(2s/\tau)^2}{2g} = \frac{2s^2}{g\tau^2}.$$

$$a = \frac{N(t) - m_b g}{m_b}.$$

$$v_{TO} = a\tau$$

$$s = \frac{1}{2}a\tau^2$$

$$\tau^2 = 2\left(\frac{m_b g}{N(t) - m_b g}\right)\left(\frac{s}{g}\right) = 2\left(\frac{140\,\text{lb}}{160\,\text{lb}}\right)\left(\frac{1.4\,\text{ft}}{32.2\,\text{ft/s}^2}\right)$$

$$v_{TO} = \frac{2s}{\tau},$$

$$H = \frac{v_{TO}^2}{2g} = \frac{(2s/\tau)^2}{2g} = \frac{2s^2}{g\tau^2}.$$

# ESTABILIDAD SALTANDO III

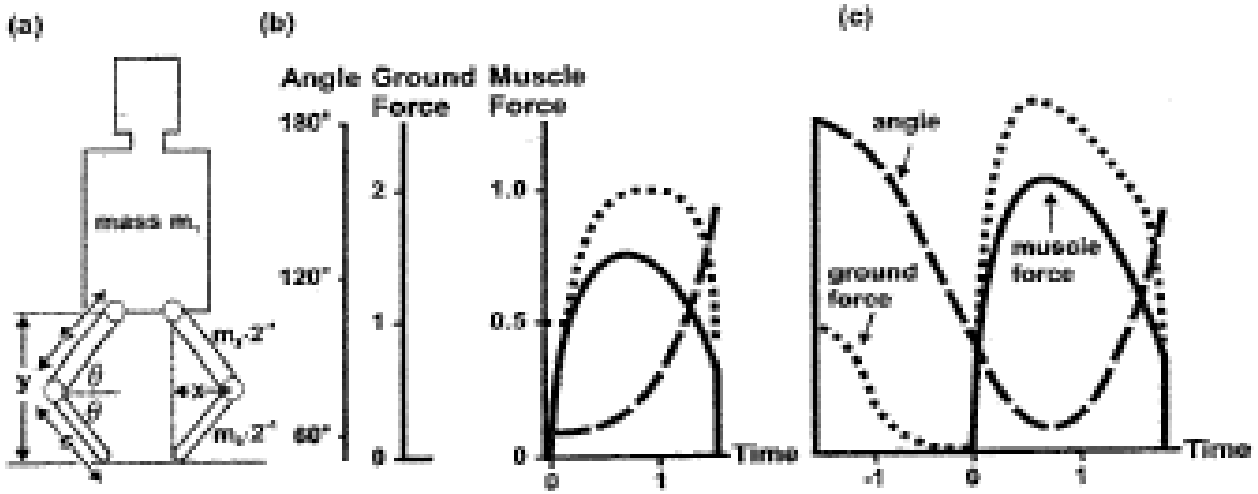


**Fig. 3.38.** (a) A mechanical model of vertical jumping, with (b) a simulated jump and (c) a simulated countermovement jump, with muscle force, ground reaction force, and angle plotted vs. time in (b) and (c). (From [101], as from [100]. Used with permission)

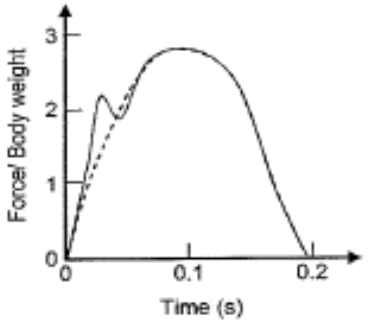


**Fig. 3.32.** Vertical force exerted on the ground during a running stride (*solid line*, with *dashed line* approximation). This was calculated from force plates and was averaged for five-runners running at 4.5 m/s. (Based on [99])

# ESTABILIDAD SALTANDO CON GARROCHA

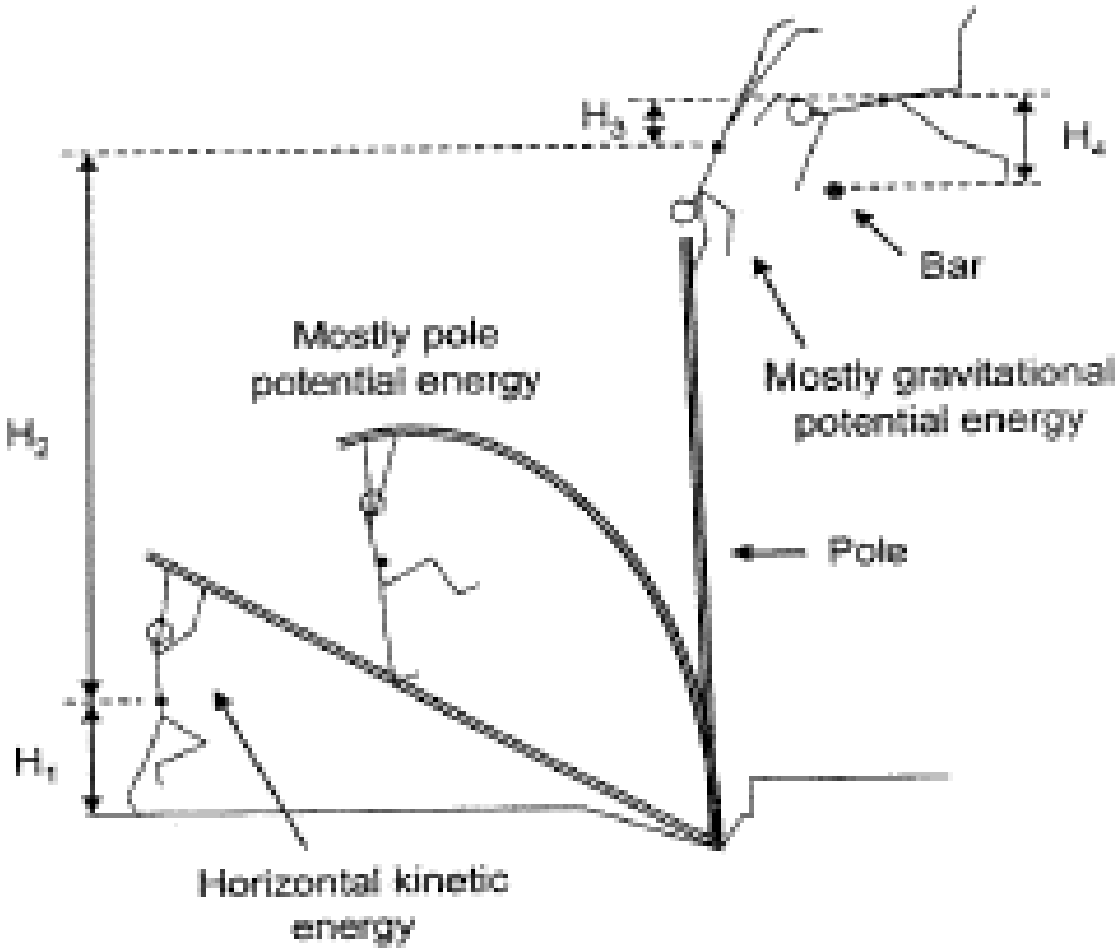


**Fig. 3.39.** Schematic of the heights involved in the pole vault. (Based on [127])

# ESTABILIDAD EN BICICLETA

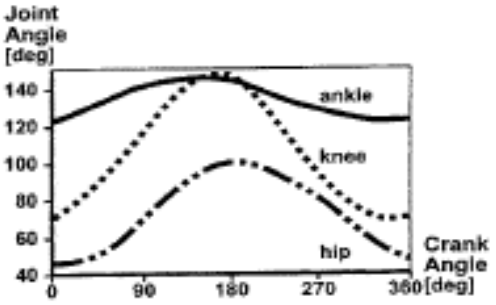


Angulo del pedaleo

**Fig. 3.51.** Joint angles in the right leg during a crank cycle in bicycling. The hip angle is that between the pelvis and the upper leg (thigh) (180° with full extension), the knee angle is that between the lower leg (shank, calf) and upper leg (thigh) (180° with full extension), and the ankle angle is that between the lower leg and a line from the ankle joint axis to the pedal spindle axis. (From [126], as from [131]. Used with permission)

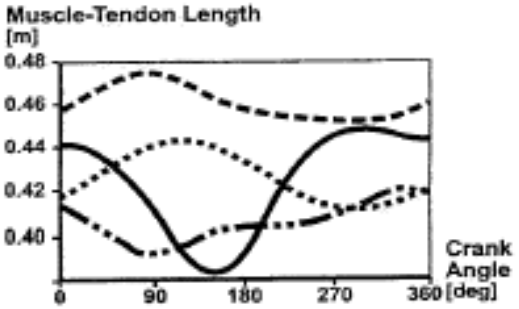


**Fig. 3.52.** Changes in the muscle/tendon lengths in biarticulate muscles (that span two joints) during a crank cycle in bicycling, for the rectus femoris (*dashes*), biceps femoris (*dots*), semimembranosus (*solid line*), and gastrocnemius (*dashes and dots*). (From [126], as from [131]. Used with permission)

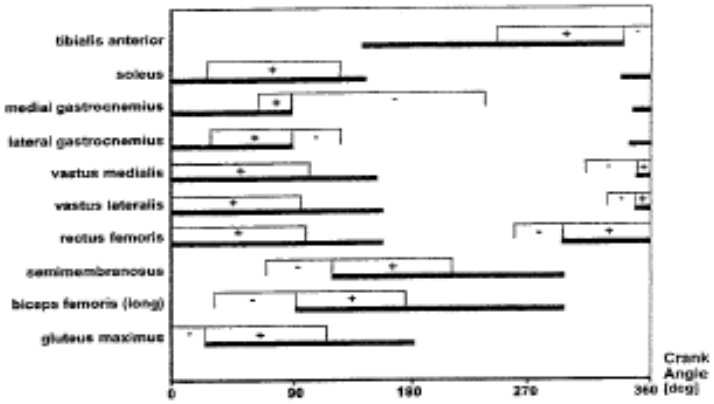


**Fig. 3.53.** Crank angles corresponding to positive work (contracting muscles) and negative work (extending muscles) for ten muscles during one crank cycle in bicycling. (From [126], as from [131]. Used with permission)

# ESTABILIDAD EN SALTOS DESDE TRAMPOLIN Y EN BARRA ALTA

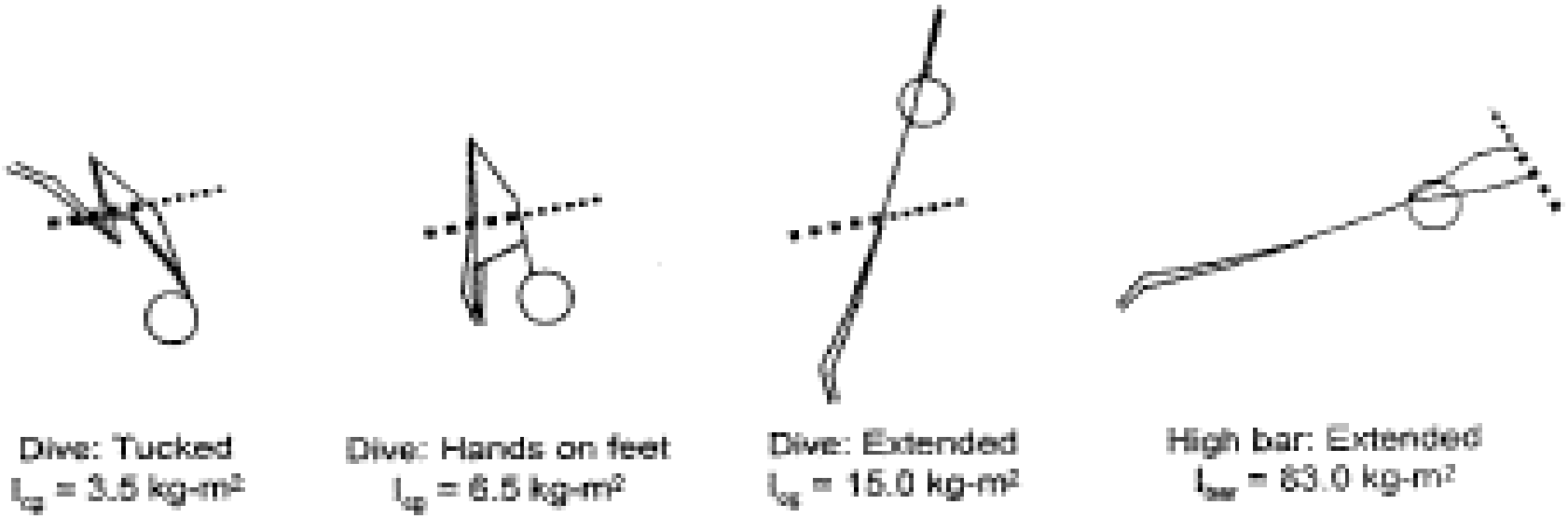


**Fig. 3.54.** Moments of inertia during diving positions (about the axis through center of mass) and in the high bar gymnastic event (about the bar). (Based on [127])

# ESTABILIDAD EN SALTOS DESDE TRAMPOLIN I

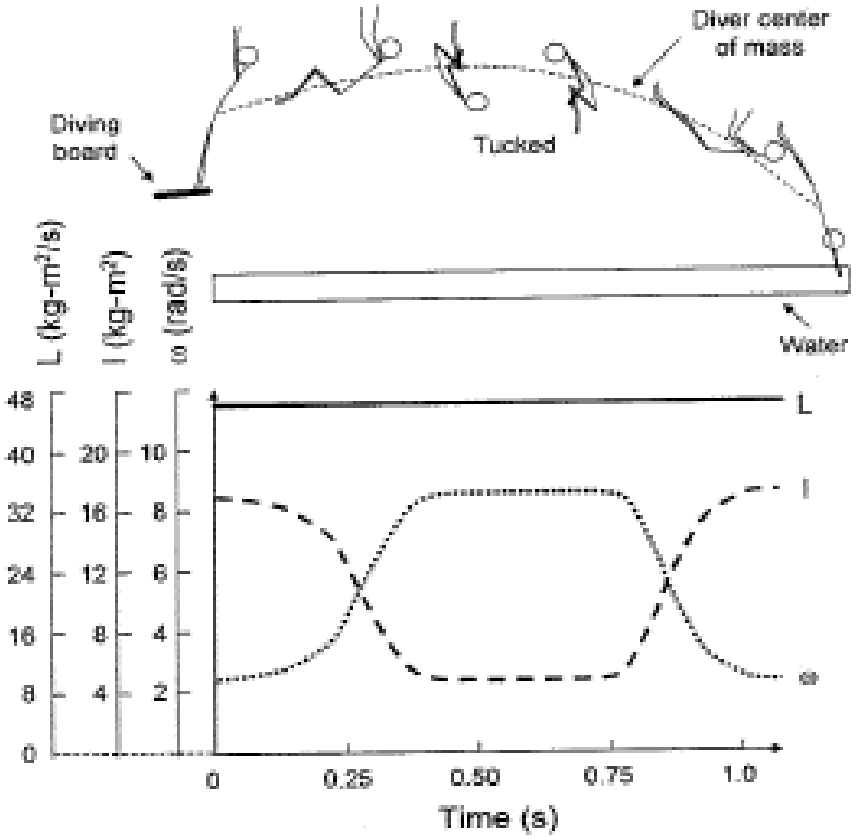


**Fig. 3.55.** Interplay between angular momentum, moment of inertia, and angular velocity during a tucked backward one-and-one half dive. In this backward dive the body is initially straight, curls up with arms around the tucked and bent legs by the knees, and becomes straight again before impact. The diver gains enough vertical momentum from the springboard to have enough time to complete this maneuver before impact. A sketch of the motion of the diver's center of mass is also shown. (Based on [127])

# ESTABILIDAD EN SALTOS DESDE TRAMPOLIN II

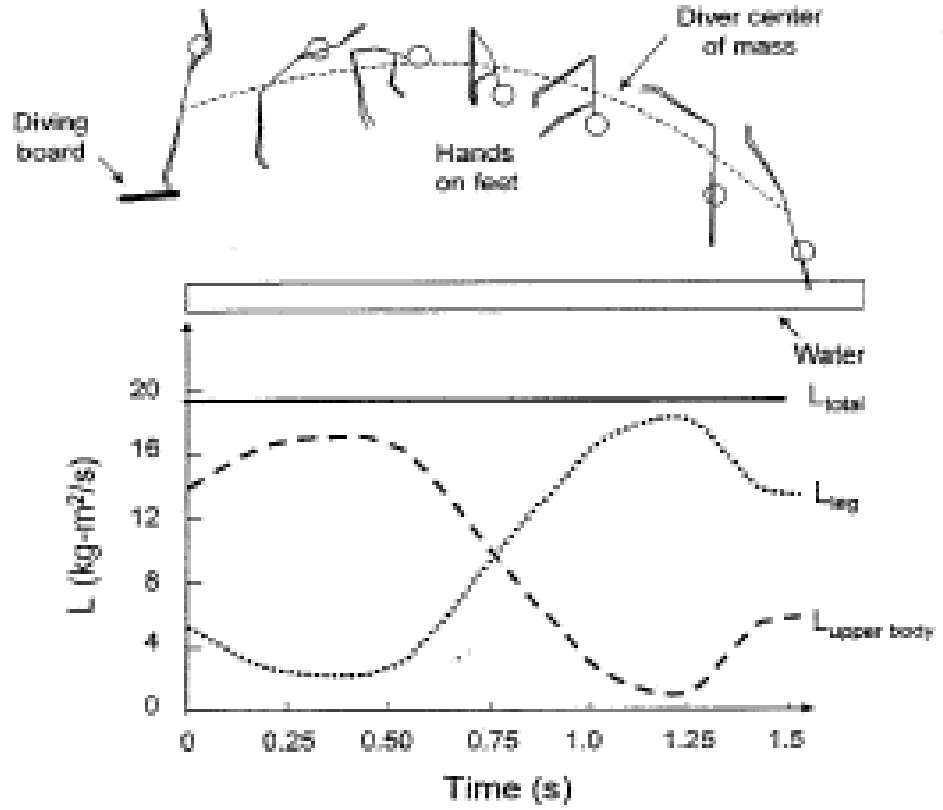


**Fig. 3.56.** Interplay between angular momentum localized first in the upper body and then in the legs during a piked front dive. In this forward dive the body is initially straight, bends over at the waist with the hands holding on to the ankles of the straight legs, and then becomes straight again before impact. The diver gains sufficient vertical momentum from the springboard to have enough time to complete this maneuver before impact. A sketch of the motion of the diver's center of mass is also shown. (Based on [127])

# ESTABILIDAD EN SALTO EN ALTO

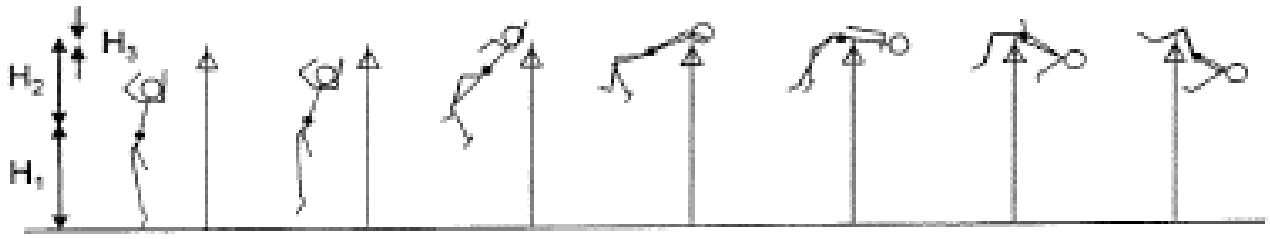


**Fig. 3.66.** Multisegment model of a high jump using the Fosbury flop method, showing that the center of mass (the *closed circle*) of the jumper is always below the bar (in this example). Heights during a high jump are also shown, with $H_1$ being the initial height of the center of mass, $H_2$ the maximum elevation of the center of mass, and $H_3$ the distance that the final center of mass is above the bar. The arrows are shown assuming the highest center of mass is above the bar, so $H_3$ would really be negative for a successful Fosbury flop. (Based on [127].) For Problems 3.34 and 3.35

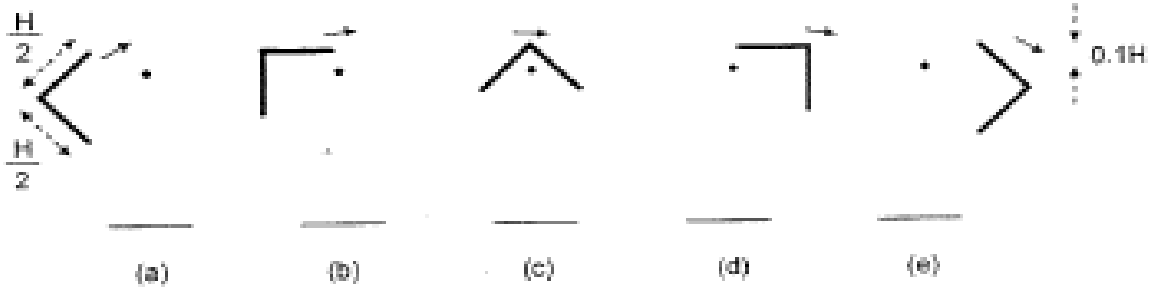


**Fig. 3.67.** Simple one-segment model of a high jump using the Fosbury flop method for a person with height $H$, with the body modeled as two segments of equal length, normal to each other. In (a)–(e), the top of the modeled body is always $0.1H$ above the bar (which is the dot). This is a reasonable assumption for (c), because the center of the person's chest is high enough for her to clear the bar. For Problems 3.36 and 3.37

# ESTABILIDAD EN SALTO EN LARGO

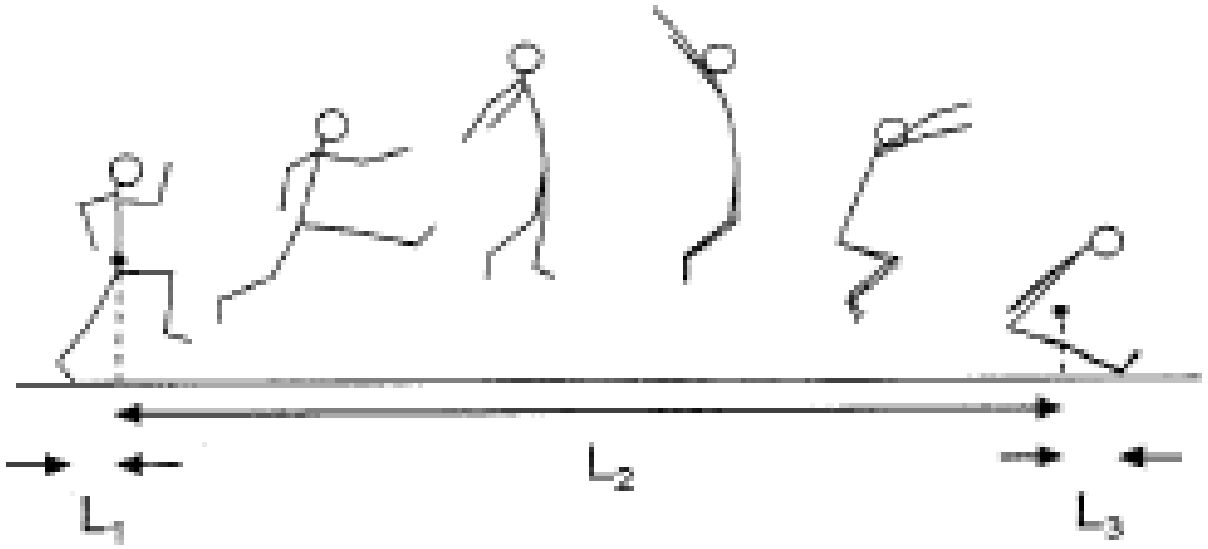


**Fig. 3.68.** Lengths during a hang-style long jump. (Based on [127].) For Problem 3.38

# Lanzamiento de pelota

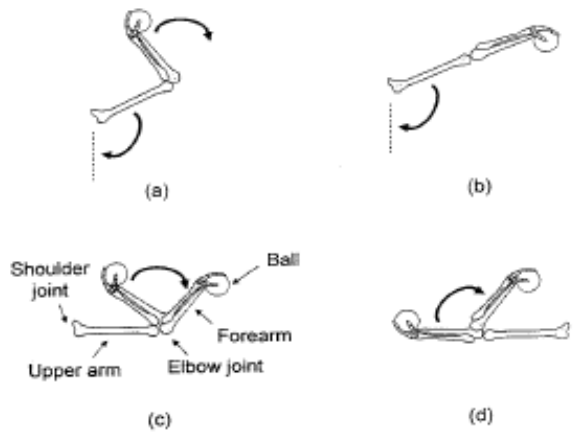


**Fig. 3.40.** Models of throwing a ball with (a) motion of the shoulder and elbow (extension), (b) motion of the shoulder only with a fixed arm, (c) extension of the elbow and a stationary shoulder, and (d) flexion of the elbow and a stationary shoulder

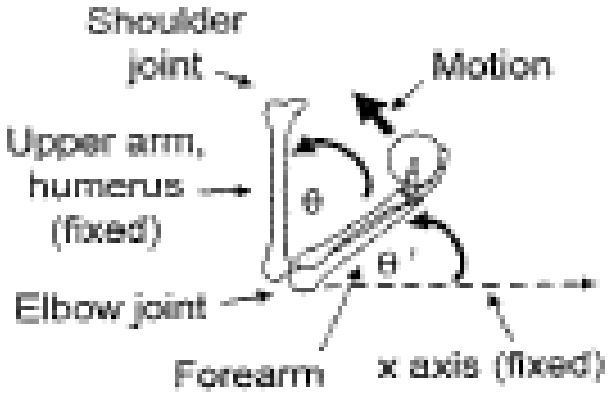


$$\sum \tau_z = M d_{\mathrm{M}} \sin\theta - W_{\mathrm{F}} d_{\mathrm{F}} \sin\theta - W_{\mathrm{B}} d_{\mathrm{B}} \sin\theta$$
$$= (M d_{\mathrm{M}} - W_{\mathrm{F}} d_{\mathrm{F}} - W_{\mathrm{B}} d_{\mathrm{B}}) \sin\theta,$$

$$\sum \tau_z = -I \frac{\mathrm{d}^2\theta}{\mathrm{d}t^2}$$

$$\sum \tau_z = (1{,}620\,\text{N-cm} - 404\,\text{N-cm}) \sin\theta = (1{,}216\,\text{N-cm}) \sin\theta$$

$$\frac{\mathrm{d}^2\theta(t)}{\mathrm{d}t^2} = -116/\mathrm{s}^2 \sin\theta(t),$$

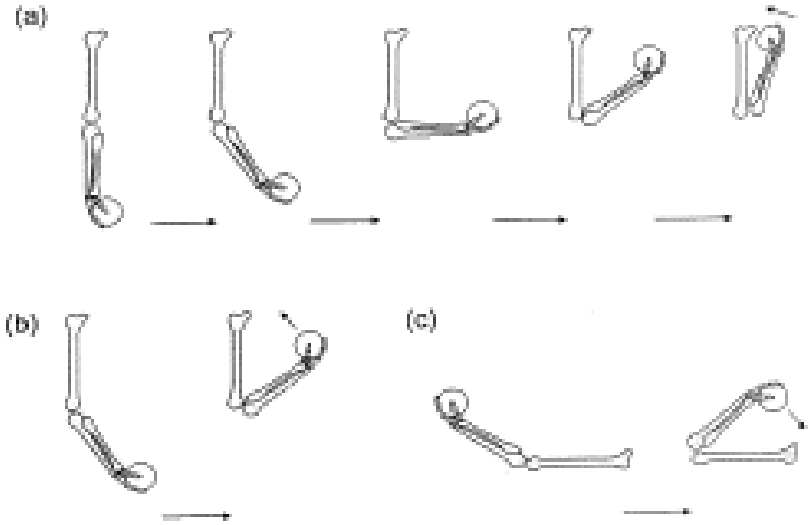


Fig. 3.43. Throwing models with (a) 180° rotation, (b) 90° rotation for vertical upper arm, and (c) 90° rotation for horizontal upper arm. The direction of the velocity vector of the released ball is shown in the last segment of each. Clearly, in this simple model a different position of the upper arm is needed to release the ball horizontally

$$\frac{d^2\theta}{dt^2} = -116/s^2\langle \sin\theta \rangle = -81.7/s^2 = -\alpha.$$

$$\frac{d\theta}{dt} = -\alpha t.$$

# BASEBALL

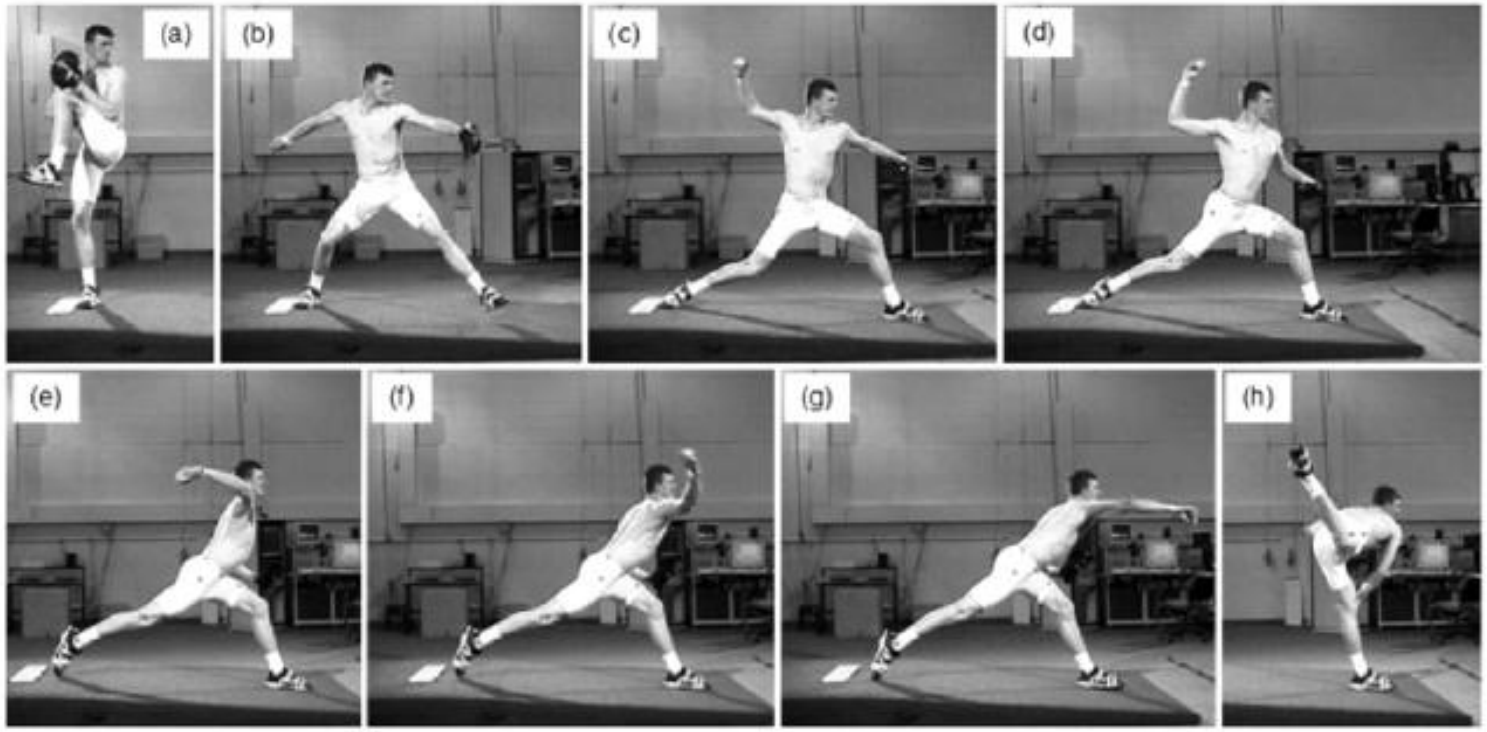


**Fig. 3.45.** The mechanics of the pitching motion. The six phases of baseball pitching are shown from windup (**a**) to stride (**b**), arm cocking (**c**), arm acceleration (**d**–**f**), arm deceleration (**g**), and follow-through (**h**). (This photo was provided by the American Sports Medicine Institute)

**Figura 1**

**Fases y eventos claves del pitcheo en baseball**

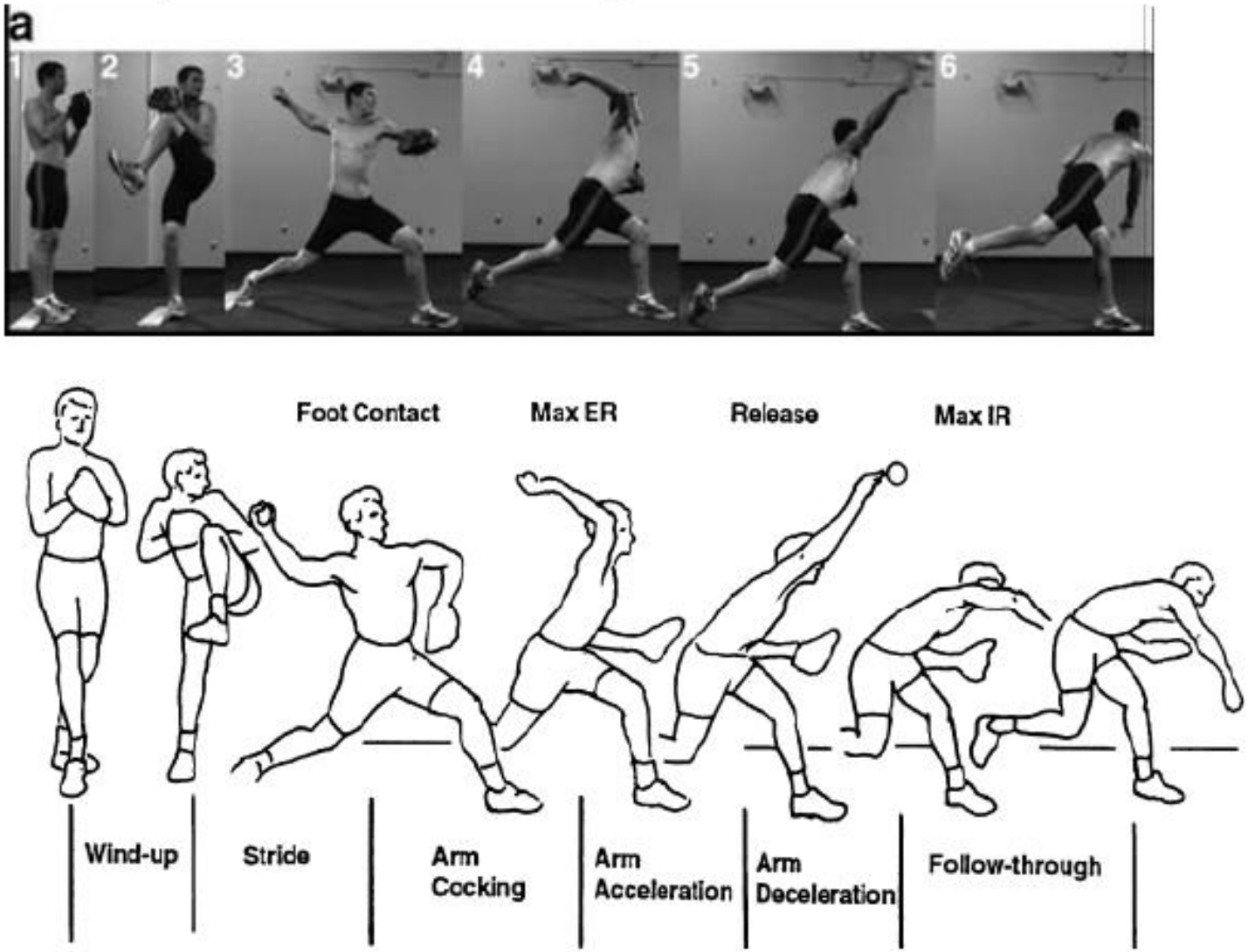


Fuente: Modificado de Dunn et al.(2008) y Fleisig et al. (1999).

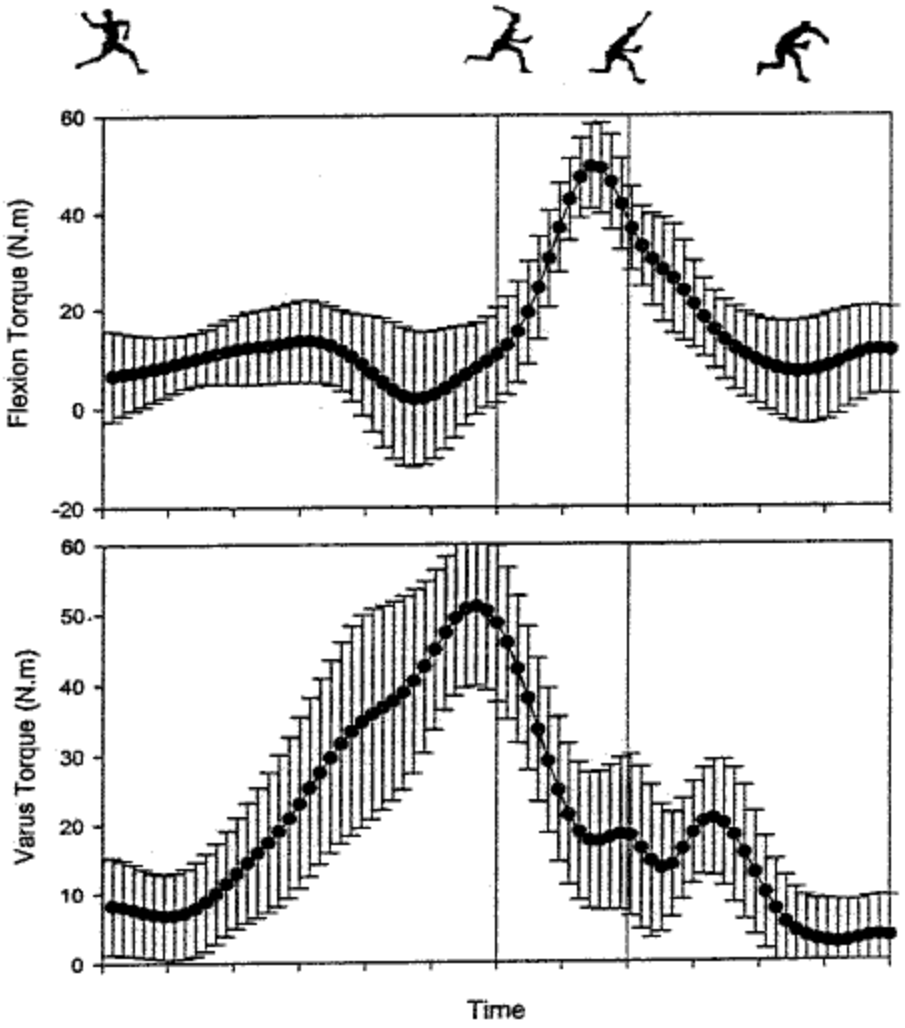


**Fig. 3.46.** Torques applied to the forearm at the elbow during a baseball pitch, with the time scale relative to the duration of the pitch. (From [176]. With the kind permission of Springer Science and Business Media)

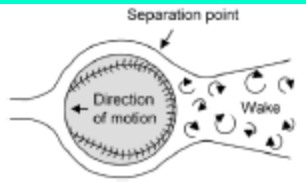


Fig. 3.48. In the rest frame of the ball (i.e., moving along in a frame with the ball), the flow of air around a baseball. The ball is moving to the left, so the air is moving to the right in the drawing. The air flows along the ball and detaches at the separation point to form a wake of chaotic, swirling flow. (Based on [173])

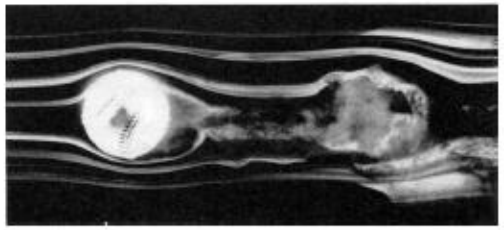

Fig. 3.49. A baseball rotating clockwise in a wind tunnel, with air moving to the right. (Smoke has been added to make the air motion visible.) The streamline detaches later on the top – where the upper surface of the ball moves in the same direction as the streaming air – leading to a downward wake and a net upward force on the ball. (From F.N.M. Brown, courtesy of the University of Notre Dame Hessert Laboratory)

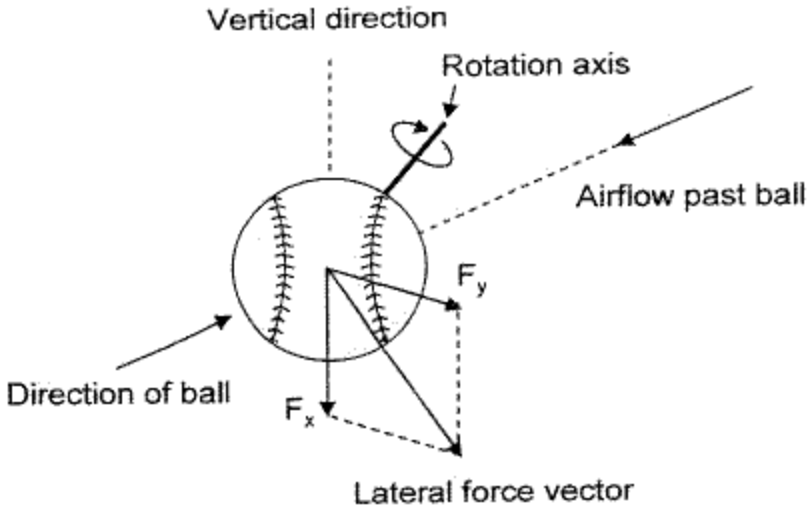


**Fig. 3.50.** Direction of the Magnus force. (Based on [173])

# BIOFISICA

## CAPITULO 3

## Impactos y Colisiones

# IMPACTOS I

**Table 3.7.** Coefficient of restitution ($e$) for balls. (Using data from [97, 127, 171, 173])

| ball | surface | $e$ | speeds |
|---|---|---|---|
| "super ball" | hardwood floor | 0.89 | slow |
| golf | floor | 0.83–0.89 | slow |
| tennis | racket | 0.76–0.88 | slow |
| racket | floor | 0.74–0.88 | slow |
| basketball | hardwood floor | 0.76 | slow |
| volleyball | hardwood floor | 0.74 | slow |
| soccer | floor | 0.69–0.80 | slow |
| squash | plywood | 0.48–0.60 | slow |
| baseball | ash boards on concrete | 0.563 | 58 mph |
| | wood | 0.588 | 25 mph |
| | wood | 0.584 | 18 mph |
| | wood | 0.46 | 89 mph |
| | typical wood bat | 0.55 | typical pitch |
| softball | hardwood floor | 0.31 | slow |

# IMPACTOS II

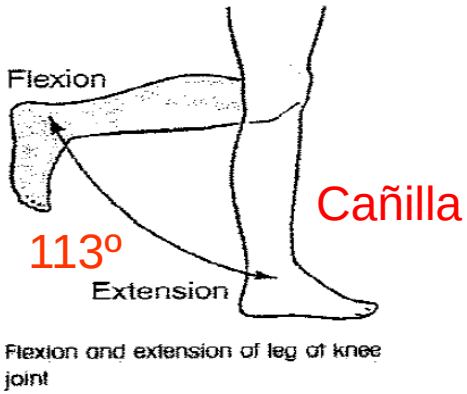


Flexion and extension of leg at knee joint

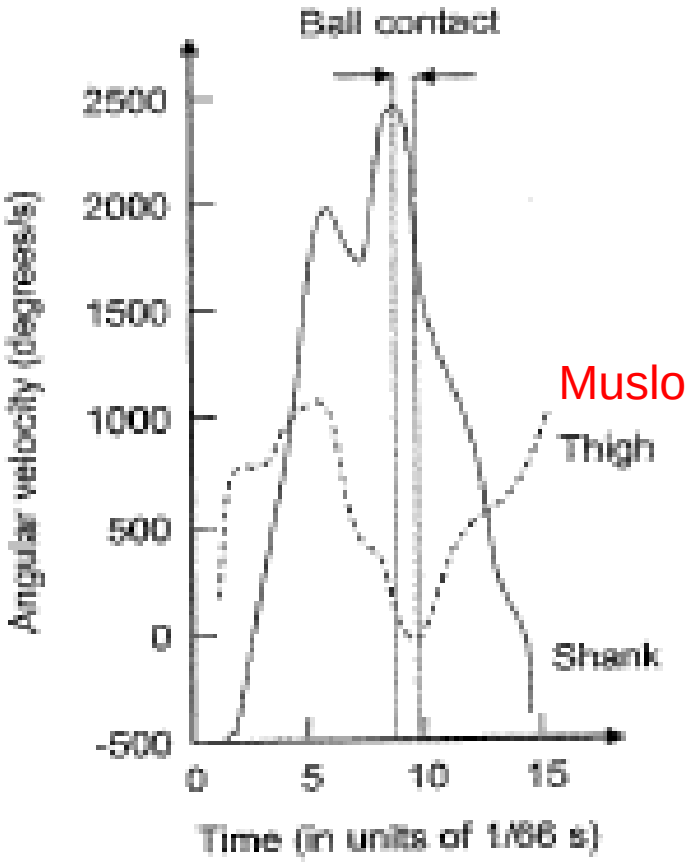


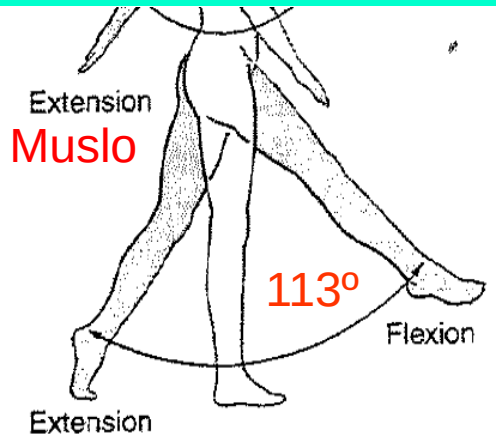


Flexion and extension of upper limb at shoulder joint and lower limb at hip joint

**Fig. 3.70.** The angular speed of the hip joint (thigh) and knee (shank) during kicking of a soccer ball. (The unusual units of 1/66 s are from the 66/s frame rate of the photographs taken by [164].) (Based on [164] and [149].) For Problem 3.93

# CAIDA DE PIE DESDE h = 1 m I

La velocidad de impacto es:

$$v_{impacto} = \sqrt{2gh} \cong 4,43 m/s$$

y la desaceleración hasta el reposo se calcula teniendo en cuenta:

$v_{final} = 0$ y $\Delta t = t_{impacto}$ con lo que:

$$a_{impacto} = \frac{\Delta v}{\Delta t} = \frac{v_{final} - v_{impacto}}{t_{impacto}} = -\frac{v_{impacto}}{t_{impacto}} \quad \text{y} \quad t_{impacto} = -\frac{v_{impacto}}{a_{impacto}}$$

Luego, si los músculos y adiposidades de la planta del pie se comprimen $\Delta x = 0,01 m$ se puede escribir:

$$\Delta x = v_{impacto} t_{impacto} + \frac{1}{2} a_{impacto} t_{impacto}^2 = v_{impacto} t_{impacto} + \frac{1}{2}\left(-\frac{v_{impacto}}{t_{impacto}}\right) t_{impacto}^2 =$$

$$= \frac{1}{2} v_{impacto} t_{impacto} = -\frac{1}{2}\frac{v_{impacto}^2}{a_{impacto}}$$

# CAIDA DE PIE DESDE h = 1 m II

$$a_{impacto} = -a_{frenado} = \frac{v_{impacto}^2}{2\Delta x} \approx 980\, m/s^2 = 100\, g$$

Si la persona que cae de pie tiene una masa corporal de: $m_b = 70kg$

la fuerza con que impactará será de: $F = 70kg \times 980\, m/s^2 = 68600N$

La tibia cerca del tobillo tiene un radio aproximado de: $r \cong 1cm$ con un área de:

$A \cong 3,14cm^2$ de modo que el esfuerzo que debe soportar es de:

$$\frac{F}{A} \cong 218,5\, N/mm^2 \cong 200MPa$$

Y como la tibia sólo puede soportar:

$$\left(\frac{F}{A}\right)_{tibia} \cong 170MPa$$ ¡Se quiebra!

# IMPACTOS III

192 km/h =

# 12 m/s

6 m/s

4,5 m/s

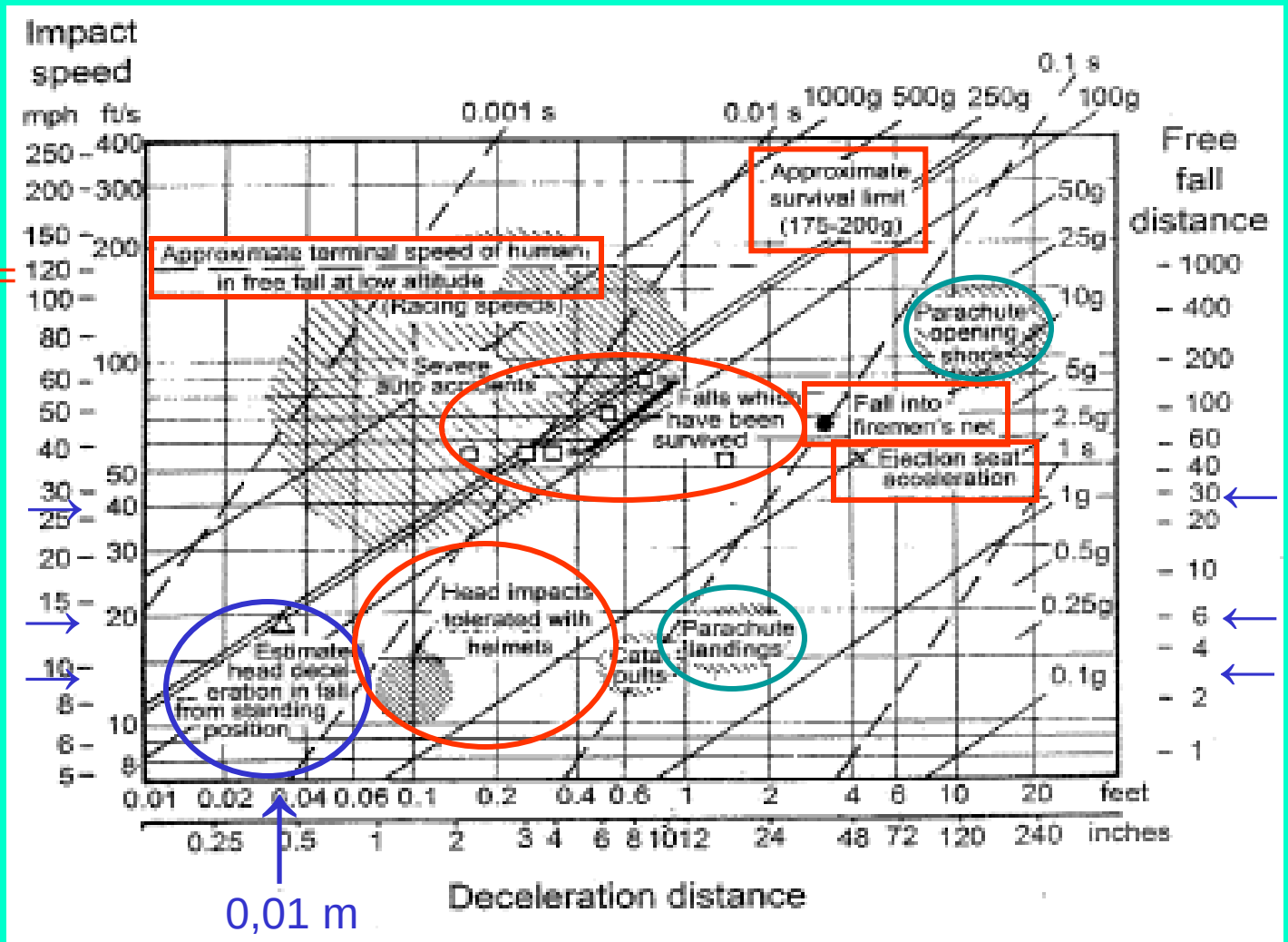


9,00 m

1,80 m

1,00 m

0,01 m

**Fig. 3.57.** Survivability of collisions. The free fall distance is that for the indicated impact speed, with allowance made for air resistance of the human body near sea level. The band shown for 175–200*g* separates the approximate survival and nonsurvival regions. (From [169])

# Caída de pie sobre concreto

# IMPACTOS IV

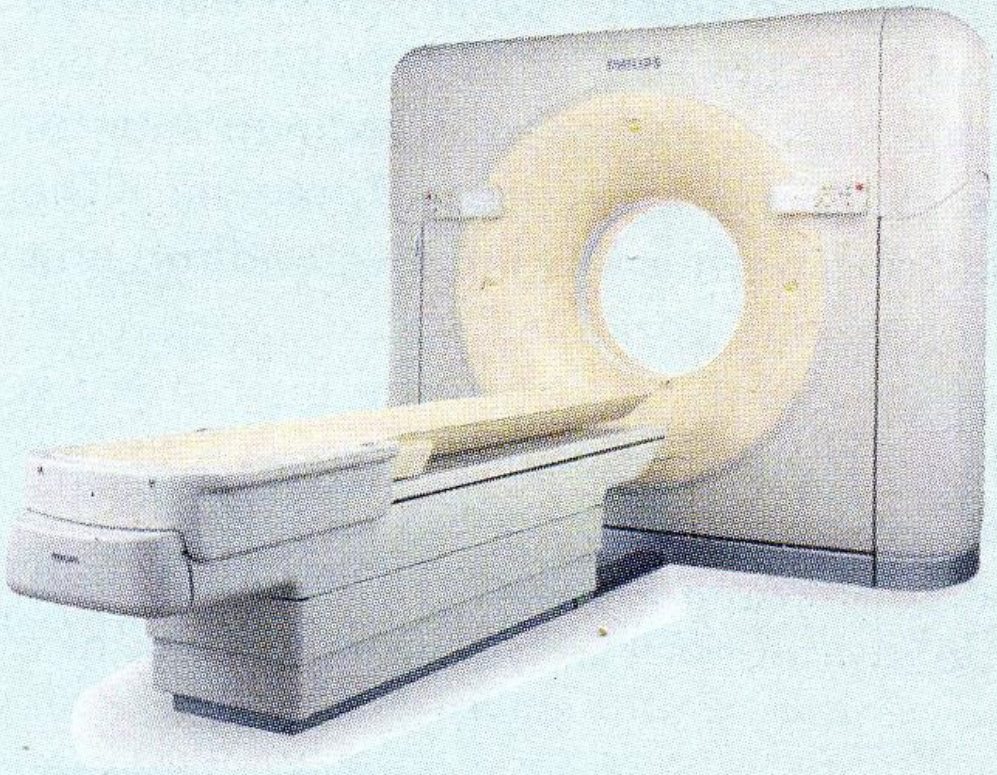

CT scanning can be used not only to diagnose diseases but also to identify bodies. Courtesy of the Radiological Society of North America.

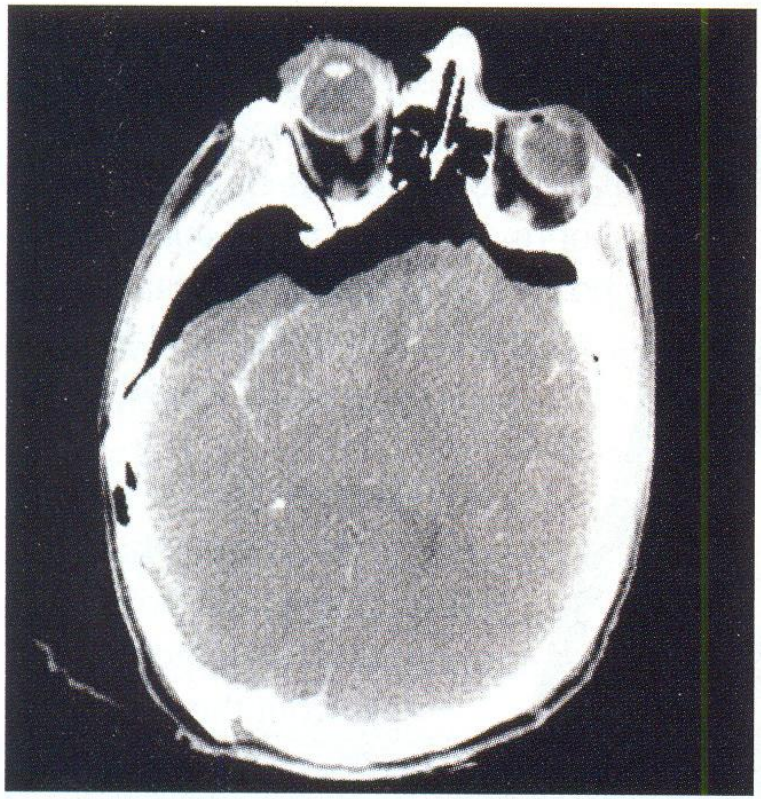

A CT image from a virtual autopsy depicts internal damage to the brain with diffuse cerebral injury. Blood is present in the right sylvian fissure. Air has entered the skull because of the skull fractures. Courtesy of the Radiological Society of North America.

# IMPACTOS V

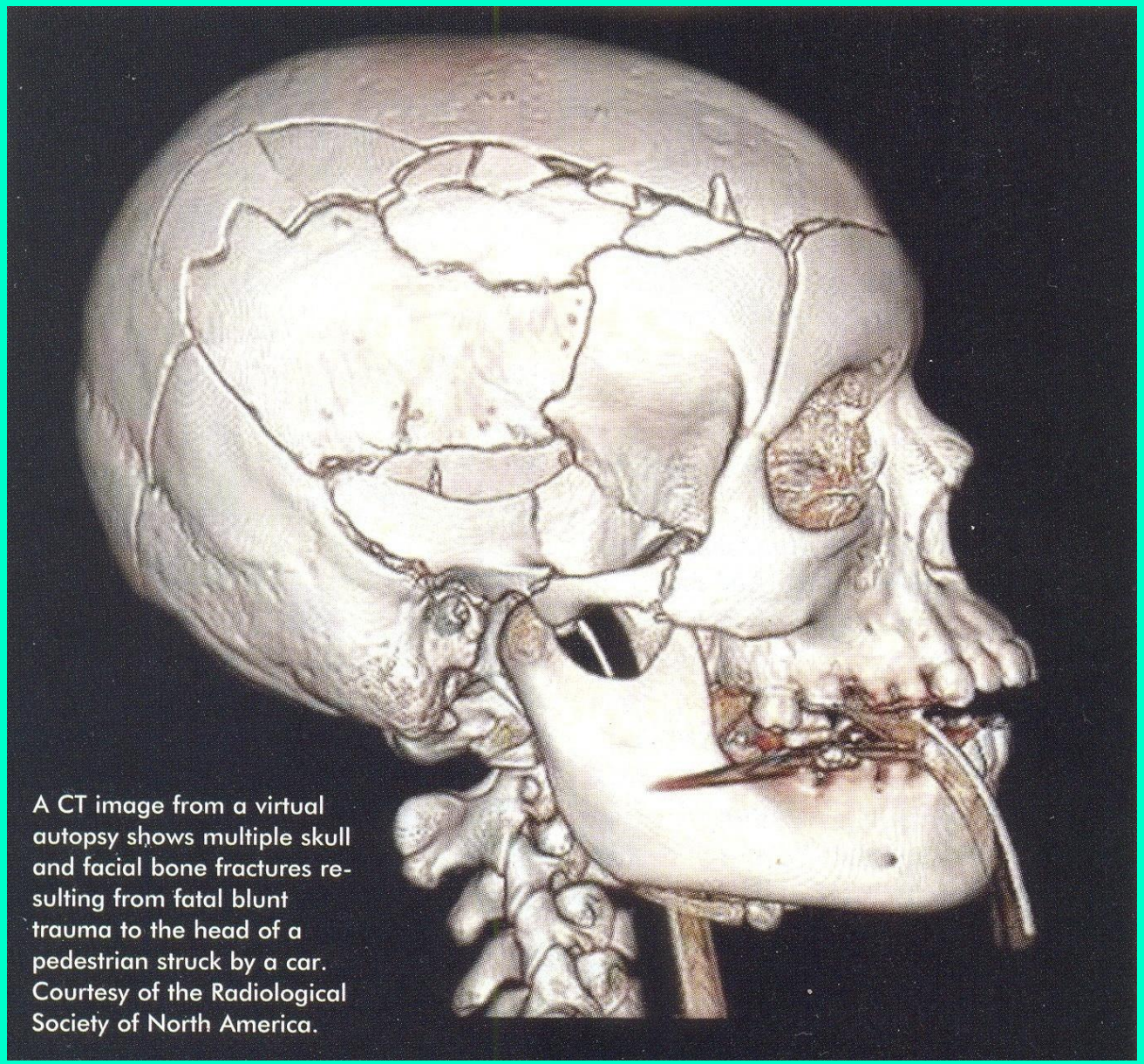

A CT image from a virtual autopsy shows multiple skull and facial bone fractures resulting from fatal blunt trauma to the head of a pedestrian struck by a car. Courtesy of the Radiological Society of North America.

# IMPACTOS VI

Se simula por una
Campana de Gauss

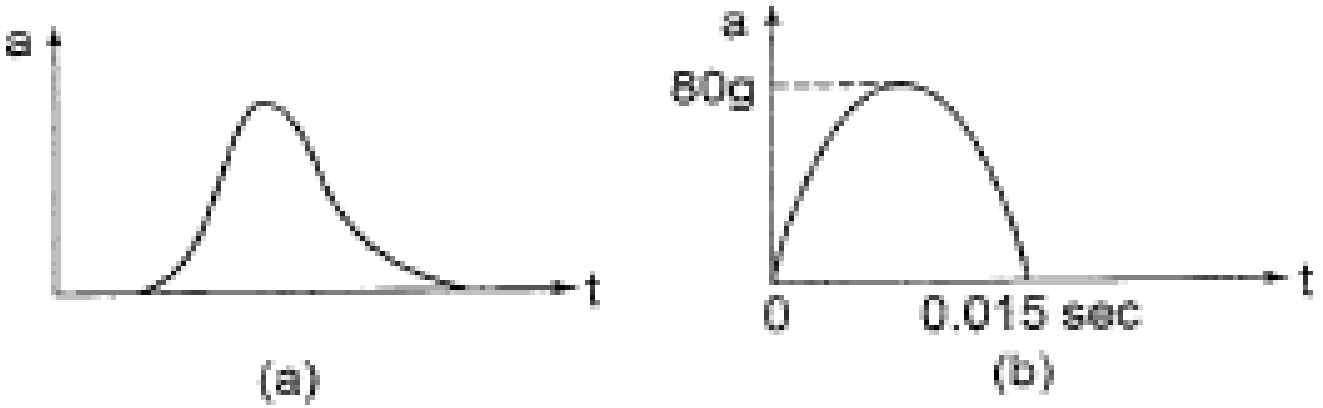


Fig. 3.58. Acceleration vs. time in a collision, (a) in general, (b) of the head of a dummy hit by a heavyweight boxer. (From [105])

*(a) Forma típica de a(t) correspondiente a un golpe frontal en la cabeza.*

*(b) Trompada de un boxeador de peso pesado en la cabeza de un modelo.*

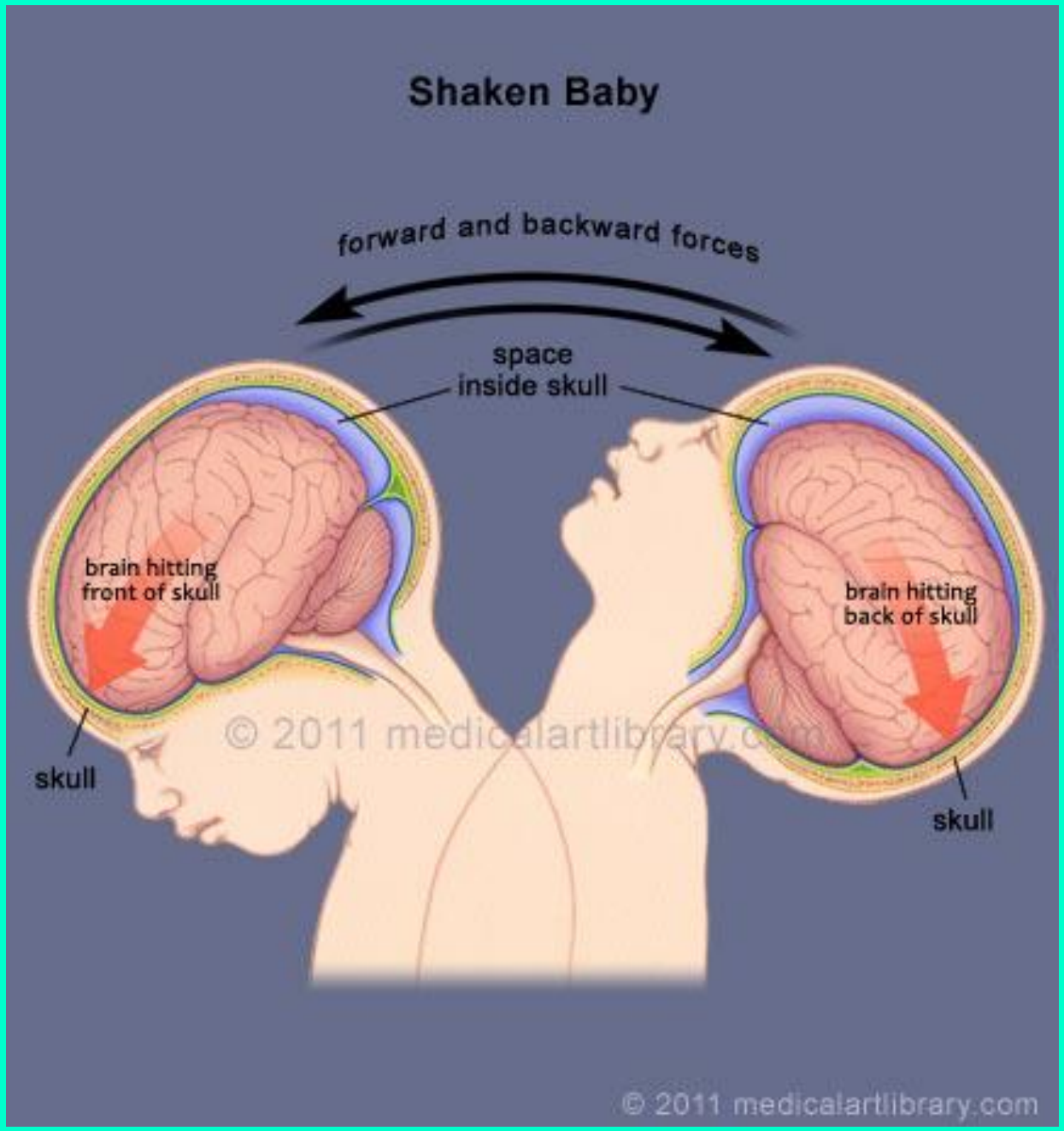
Shaken Baby
forward and backward forces
space
inside skull
brain hitting
front of skull
brain hitting
back of skull
skull
skull
© 2011 medicalartlibrary.com

# IMPACTOS VII

C. W. Gadd en experiencias con animales y cadáveres humanos frescos logró definir un índice de riesgo frente a fuertes impactos en la cabeza, conocido como **Gadd Severity Index** (**GSI**), según la expresión:

$$GSI = \int \left( \frac{a_{decel}}{g} \right)^{2,5} dt$$

Si la desaceleración o aceleración de frenado es $\mathbf{a_{decel}}$ durante el curso de la colisión, la que tiene una duración $\mathbf{t_{col}}$, entonces el **GSI** se expresa:

$$GSI = \left( \frac{\Delta v}{g \times t_{col}} \right)^{2,5} t_{col}$$

Si **GSI** ≈ 1000 (en unidades de segundos) existe 50% de riesgo de muerte, por arriba de 1000 la colisión es habitualmente fatal. Por debajo de 1000 se producen severas lesiones y en una caída (~ 400) se puede producir pérdida de conocimiento.

# IMPACTOS VIII

J. Versace reformuló la definición del **GSI** como **Criterio de Daño Craneal** (**Head Injury Criterion – HIC**) expresándolo según:

$$HIC = máx\left\{\left[\frac{1}{t_2 - t_1}\int_{t_1}^{t_2}\left(\frac{a_{decel}}{g}\right)dt\right]^{2,5}\left(t_2 - t_1\right)\right\}$$

en la que su máximo valor se obtiene para un intervalo durante el impacto $t_2 – t_1 = 36$ ms. Recientementen dicho intervalo se acortó a 15 ms; es la versión HIC-15.

Además, se definió el riesgo R de serias lesiones cerebrales (AIS ≥ 4) para HIC-15 como la integral sobre la Campana de Gauss:

$$R = \left(\frac{430}{\pi}\right)^{1/2}\int_0^{HIC-15}\exp\left\{-\left[\left(x - 1434\right)/430\right]^2\right\}dx$$

representada en la figura siguiente.

# IMPACTOS IX

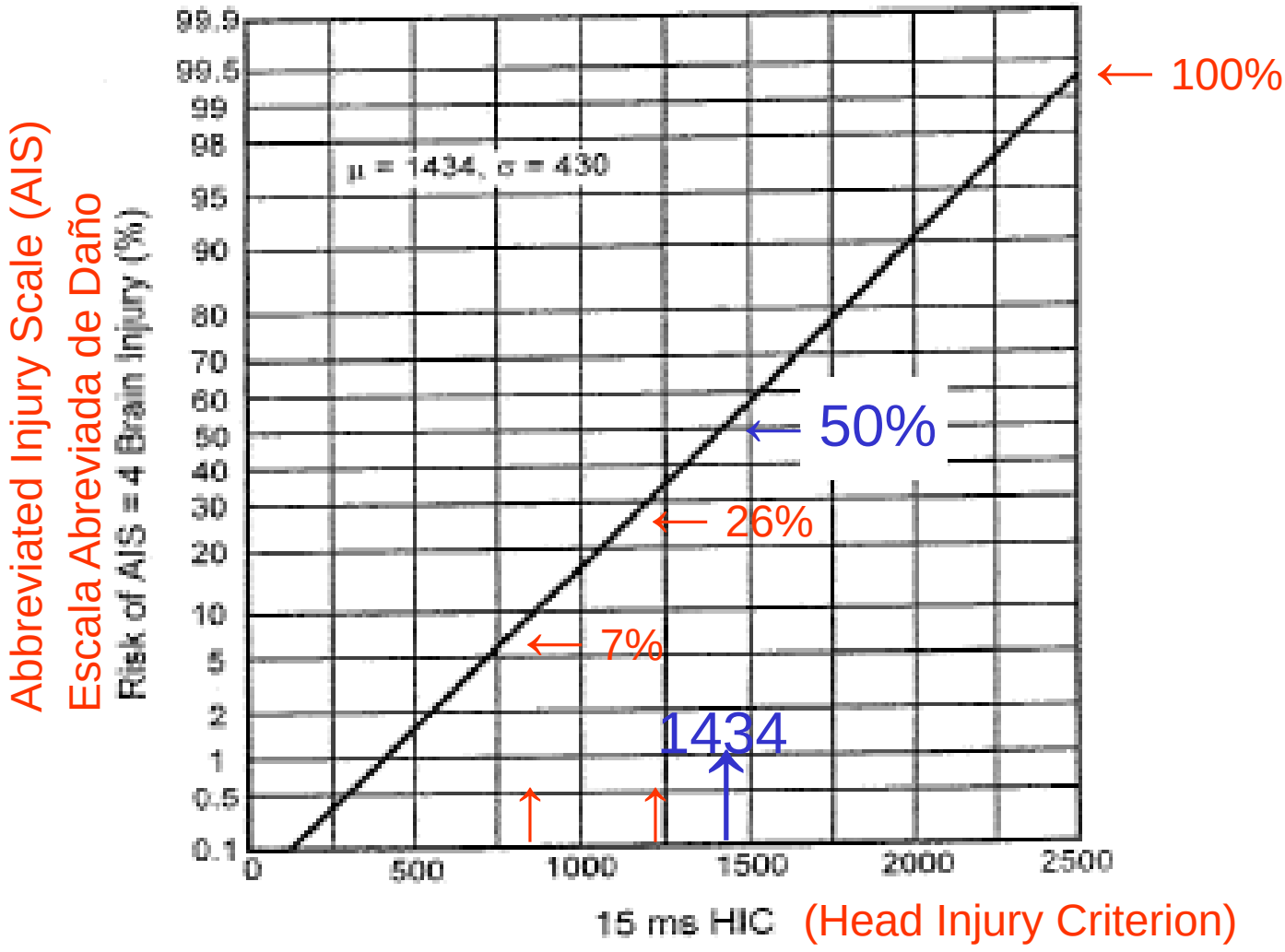


**Fig. 3.59.** Risk of AIS $\geq$ 4 brain injury as a function of 15-ms HIC for forehead impacts. (From [147])

# IMPACTOS X

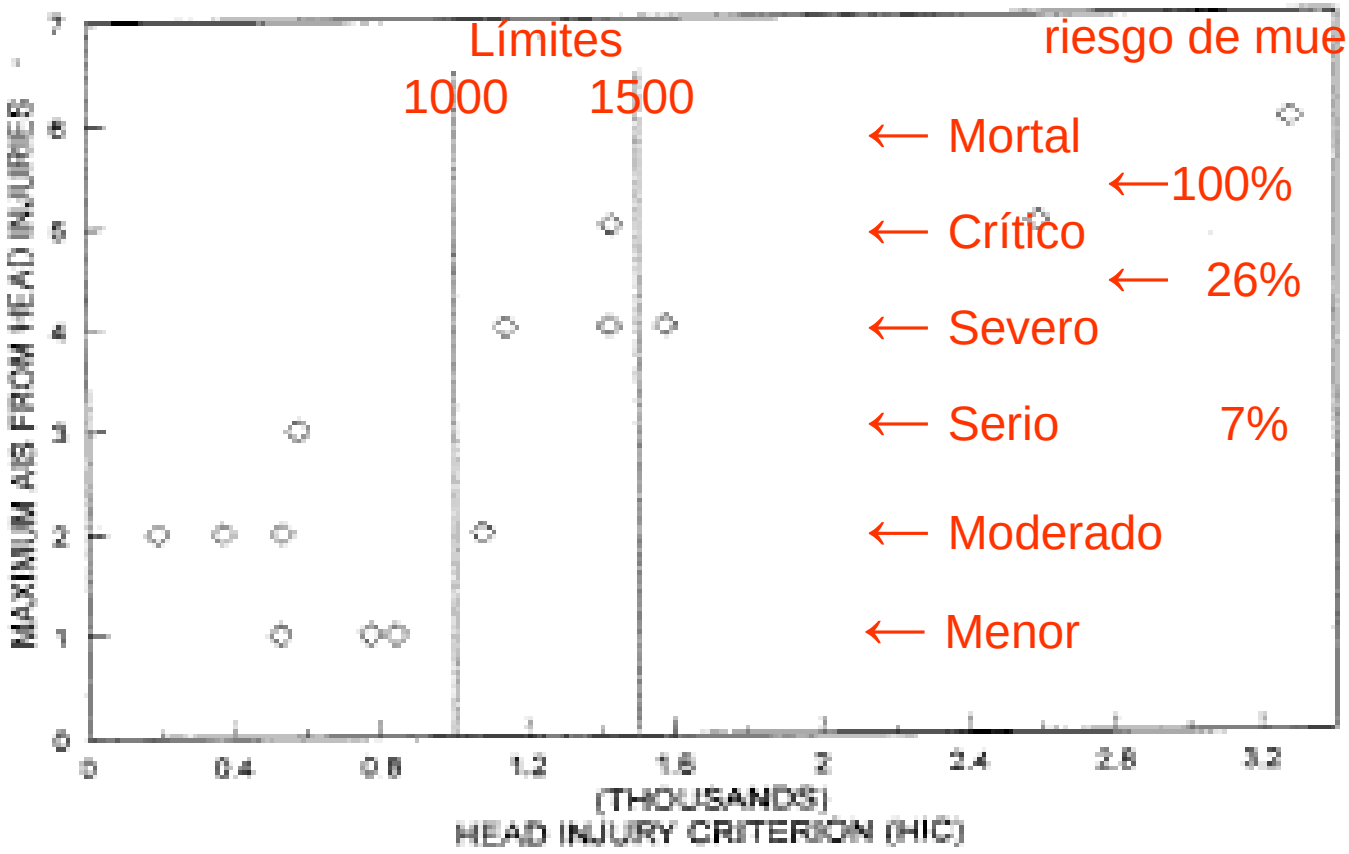


**Fig. 3.60.** Classification of case-studies of collisions leading to head injury, plotted as the maximum head injury (using the AIS scale) vs. the collision condition as quantified by the HIC. (From [167], as from [130])

# IMPACTOS XI

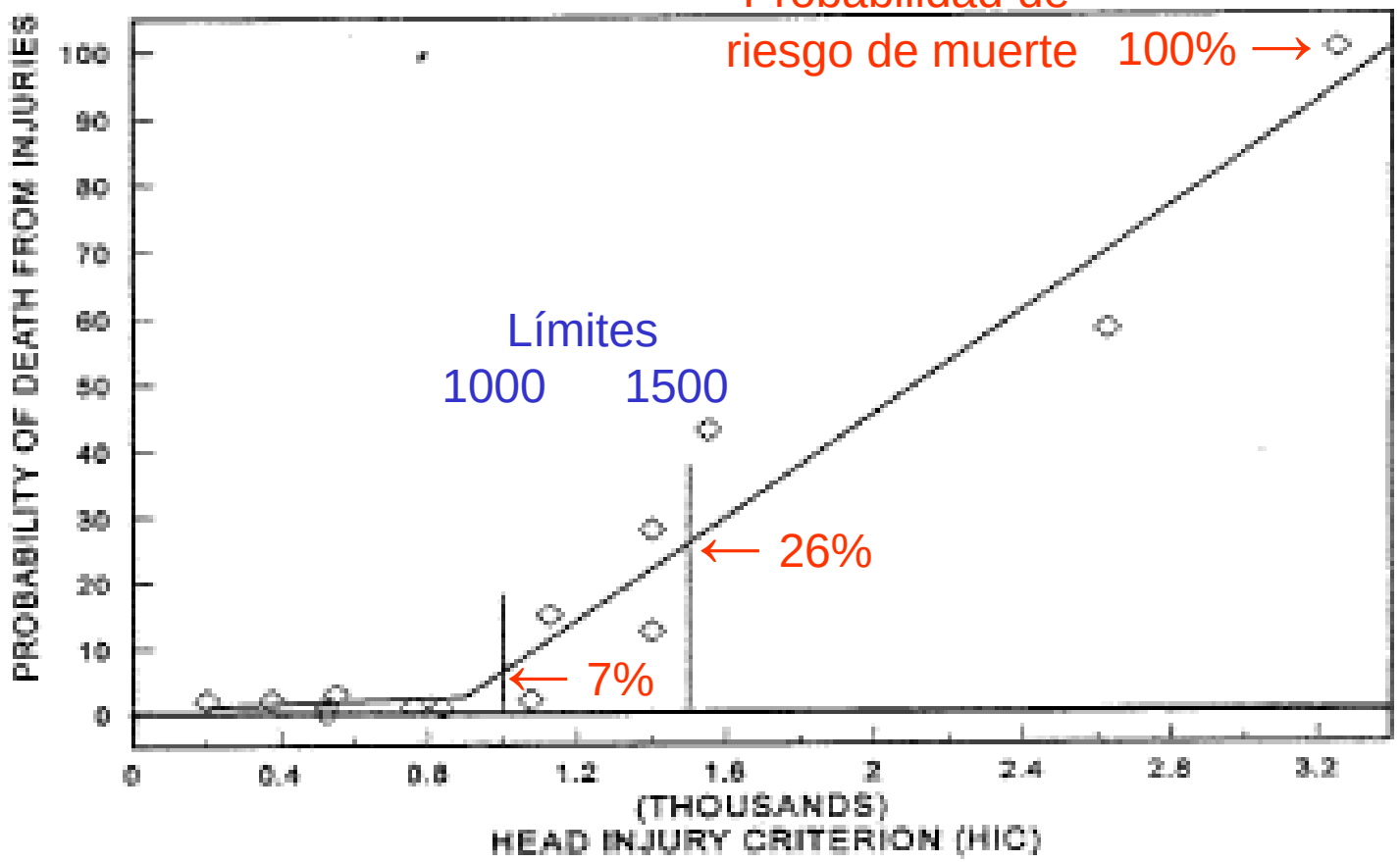


**Fig. 3.61.** Classification of case studies of collisions leading to death, plotted as the probability of death vs. the collision condition as quantified by the HIC. (From [167], as from [130])

# IMPACTOS XII

$$GSI = \left( \frac{\Delta v}{g \times t_{col}} \right)^{2,5} t_{col}$$

Expresión del GSI para desaceleración constante

En el caso del choque de un auto, si la cabeza de un ocupante golpea contra algo duro y rebota **elásticamente**, resulta $v_f = -v_i$, y el GSI se expresa como:

$$GSI_e = \left( \frac{2v_i}{g \times t_{col}} \right)^{2,5} t_{col}$$

Mientras que si la colisión de la cabeza es **inelástica**, se expresa como:

$$GSI_i = \left( \frac{v_i}{g \times t_{col}} \right)^{2,5} t_{col}$$

Si $v_i$ = 80 km/h y $t_{col}$= 10 ms, resulta $GSI_e$ = 44 000 y $GSI_i$ = 7 800, lo que de cualquier modo resultan ser mortales.

# Boxeo

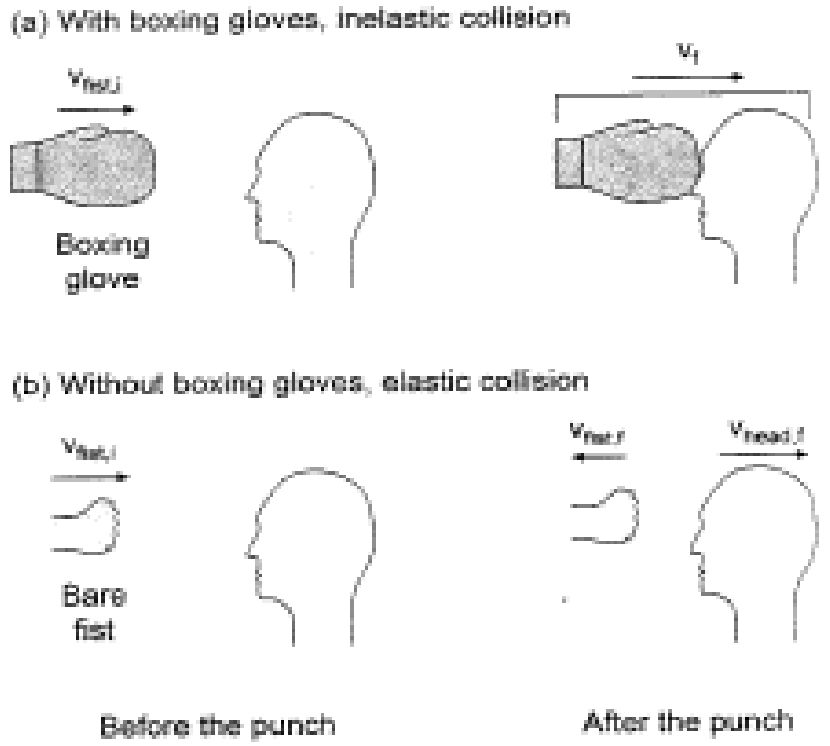


Fig. 3.63. Models of boxing, with (a) boxing gloves, leading to an inelastic collision with the head, and (b) bare fist, leading to an elastic collision with the head

$$P = \frac{|F|}{A} = \frac{m|\Delta v/\Delta t|}{A} = \frac{mv_i}{At_{coll}}.$$

$\Delta v = 2v_i$

La fuerza por unidad de área es el doble también!

# Golpear una pelota: Bateo

$$v'_{\text{ball}} = \frac{(m_{\text{ball}} - em_{\text{bat}})v_{\text{ball}} + (m_{\text{bat}} + em_{\text{bat}})v_{\text{bat}}}{m_{\text{ball}} + m_{\text{bat}}}.$$

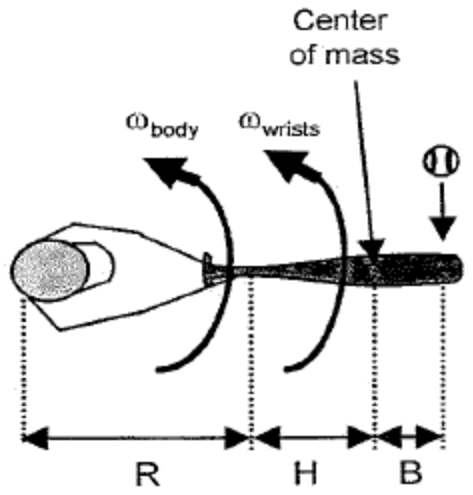


**Fig. 3.64.** Model of batting a ball. (Based on [173])

$$\frac{W_{\text{bat,ideal}}}{W_{\text{ball}}} = \frac{v'_{\text{ball}} - v_{\text{ball}}}{v'_{\text{ball}} + ev_{\text{ball}}}.$$

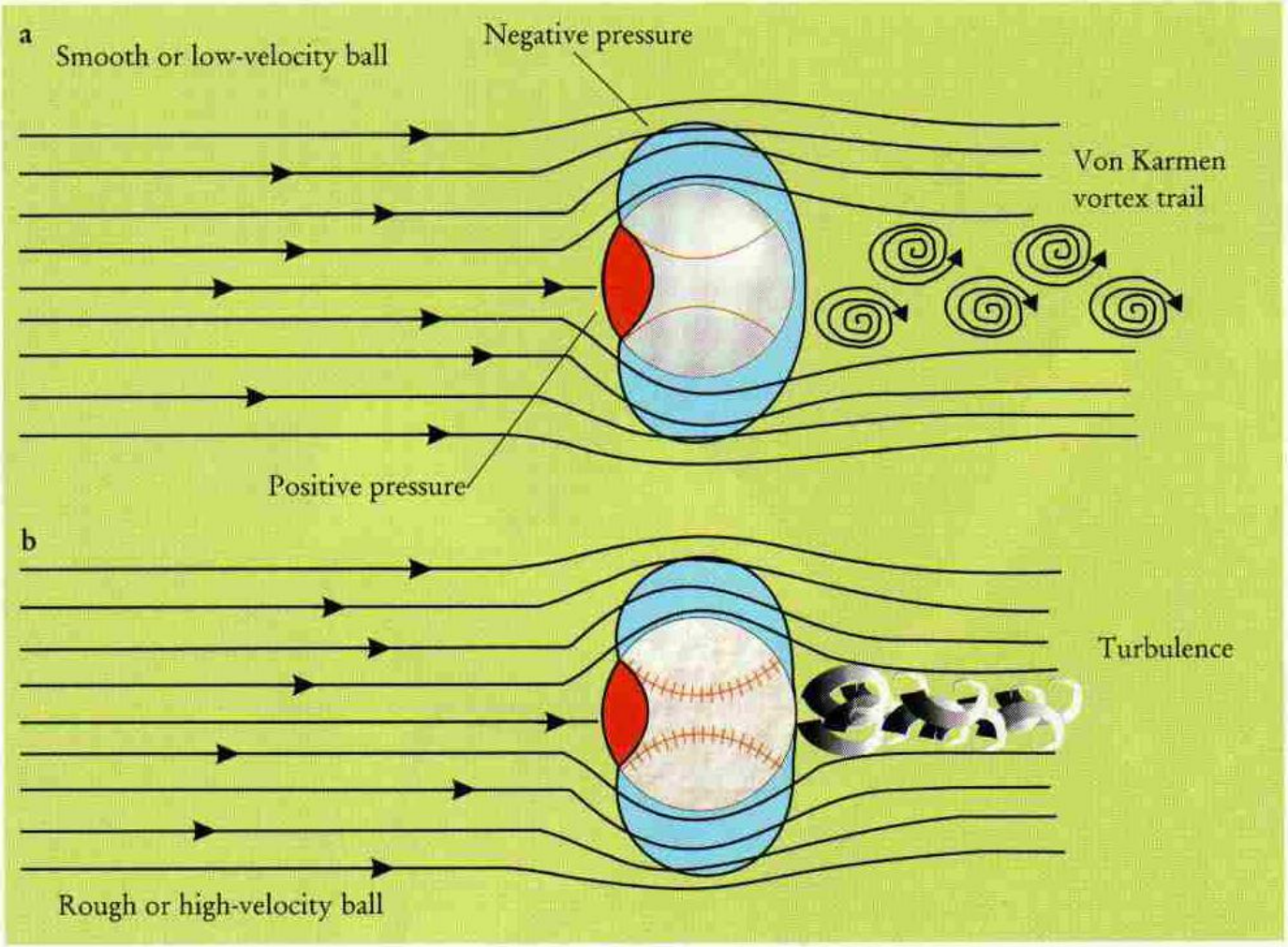


**AERODYNAMIC FORCES** on a ball moving through air depend on both the ball's velocity and its surface roughness. **a:** Low-velocity balls, regardless of surface roughness, pass smoothly through the air, generating an area of positive pressure in front of them and an area of negative pressure along their surfaces as the air speeds up to go around the ball. This area of negative pressure extends to the rear of the ball, generating a significant drag force. In the ball's wake, the air swirls in classical von Kármán vortices. **b:** At some velocity, whose value decreases as the ball's surface roughness increases, the flow of air around the ball becomes turbulent. Such flow still generates a positive pressure at the front of the ball. However, the area of negative pressure at the sides and rear of the ball is reduced. Thus, counterintuitively, the drag force is less for a rough ball than for a smooth ball. **FIGURE 2**

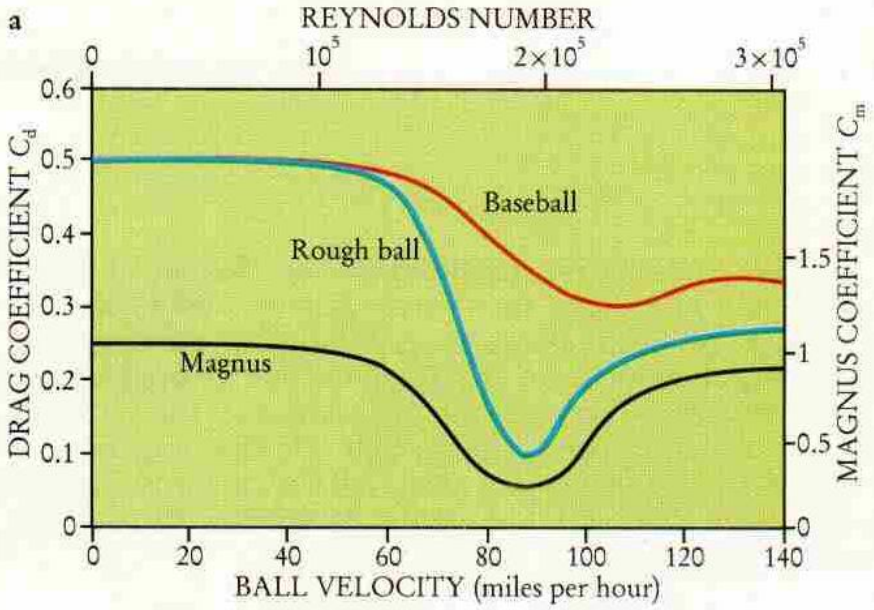


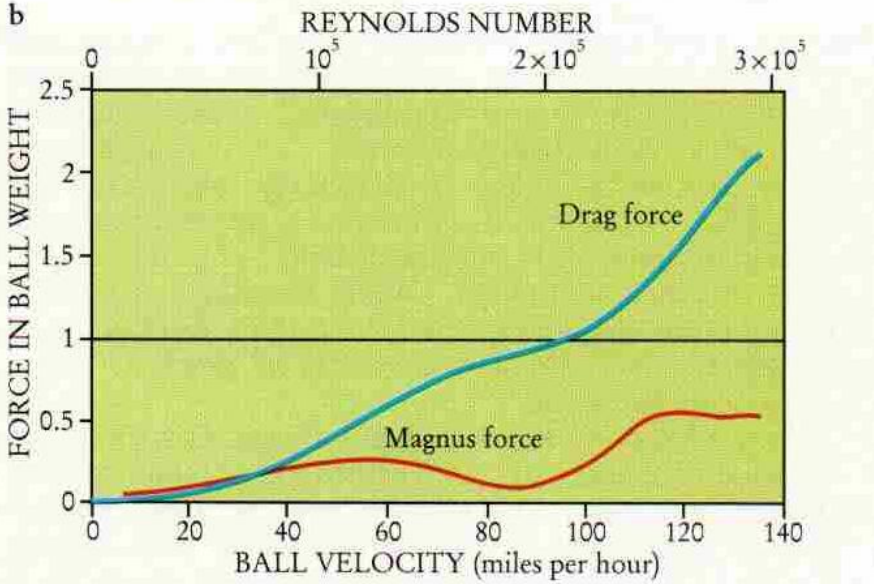


**DRAG ON A BASEBALL.** The drag force on a uniformly rough ball of cross-sectional area $A$ moving with velocity $v$ through air of density $\rho$ is approximately $(C_d/2)A\rho v^2$. **a:** Baseball velocities are typically between 60 and 120 miles per hour, where the transition to turbulent flow—or "drag crisis"—causes $C_d$ to vary rapidly with velocity. A rotating baseball is neither uniformly smooth nor rough, since it presents both its smooth cover and raised stitching to the air. This smooths the transition somewhat. However, a ball of radius $r$ spinning with angular velocity $\omega$ interacts with air of density $\rho$ through which it passes, generating a Magnus force equal to $C_m\rho A\omega rv/2$ perpendicular to the direction of motion and the axis of the spin. This is the force that makes a curveball curve. Below 60 mph the Magnus coefficient $C_m$ is effectively constant with a value of about 1. The values are not well known at higher velocities; hence the results shown on the graph should be considered as sensible estimates. **b:** The drag force (calculated using the coefficients from **a**) increases monotonically and becomes equal to the force of gravity at about 95 mph. The Magnus force for $\omega = 1800$ rpm is always less than the force due to gravity but is still significant. **FIGURE 3**

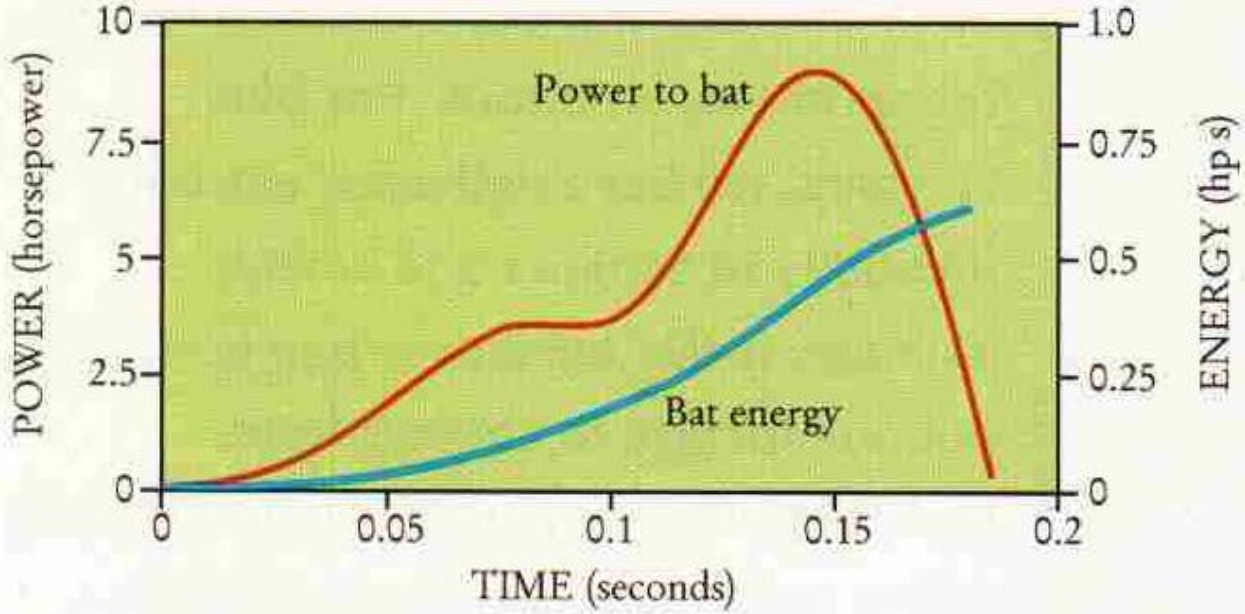


**BATTING POWER.** A batter's swing typically lasts 0.2 seconds, during which time the rate of energy transferred to the bat increases from 0 to about 9 horsepower during the first 0.15 seconds and then decreases to 0 as the bat crosses the plate. Because muscle can generate only about 1 horsepower per 10 pounds, the majority of the swing's power must come from the large muscles of the legs and thorax rather than from the hands and wrists. Even assuming a major contribution by these large muscles, the power of the swing can be explained only if the batter stores translational and rotational kinetic energy early in the swing and transfers that energy to the bat late in the swing. **FIGURE 4**

# Golpear una pelota: Tenis

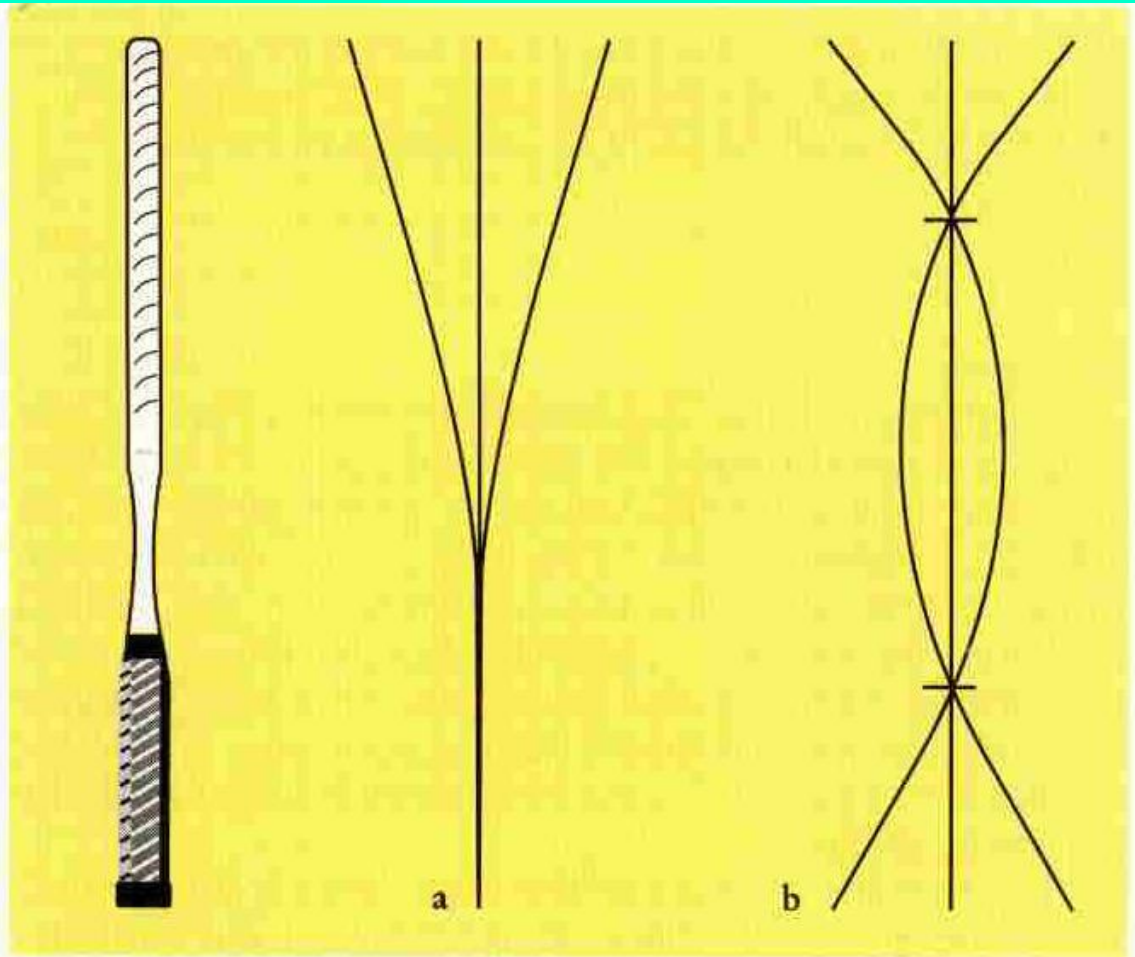


VIBRATION MODES of a tennis racket (a) with the handle clamped and (b) with both ends free. FIGURE 3

$$v' = -ev + (1+e)V$$

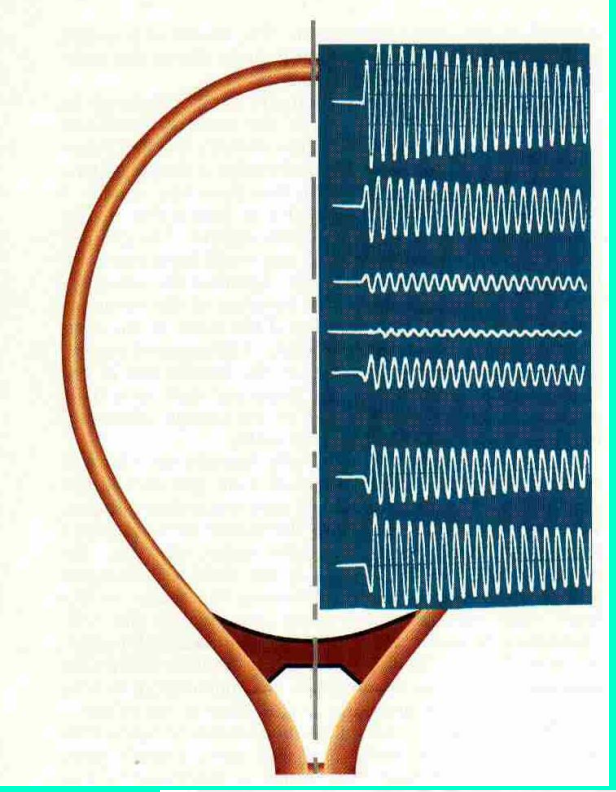

VIBRATION AMPLITUDE TRACES for a freely suspended tennis racket struck at various locations on its longitudinal axis. At the node the phase of the oscillation is reversed. FIGURE 4

POWER SPOT FOR SERVING a tennis ball is higher on the racket than for a ground stroke, because the effective pivot point of the service motion is very close to the butt end of the racket. For a very stiff, head-heavy racket (right) the power point is higher than it is for a more flexible, neutral-balance racket (left). Successive contours going outward from the optimal power point (red) indicate loci for 99%, 95% and 90% of maximum ball speed. FIGURE 6